ADDIS ABABA UNIVERSITY

SCHOOL OF GRADUATE STUDIES

INSTITUTE OF TECHNOLOGY

ENERGY CENTER

Design and Development of Fast Pyrolysis Fluidized Bed Reactor for Bio-oil Production

By: Tigabu Abrha

Advisor: Dr.Ing: - Abebayehu Assefa

Co –Advisor: Sileshi Kore (Phd Student)

December, 2011

Addis Ababa, Ethiopia

ADDIS ABABA UNIVERSITY

FACULITY OF TECHNOLOGY

SCHOOL OF GRADUATE STUDIES

DEPARTMENT OF MECHANICAL ENGINEERING

Design and Development of Fast Pyrolysis Fluidized Bed Reactor for Bio-oil Production

By: Tigabu Abrha

Approved by Board of Examiners

_____	_____	_____
Chairman,		
Department Graduate Committee	**Signature**	**Date**
Abebayehu Assefa (Dr.Ing.)	_____	_____
Advisor	**Signature**	**Date**
_____	_____	_____
Internal Examiner	**Signature**	**Date**
_____	_____	_____
External Examiner	**Signature**	**Date**

DECLARATION

I, the undersigned, declare that this thesis is my original work and has not been presented for a degree in any University, and that all the source of materials used for the thesis has been duly acknowledged.

Declared by:

Name: **Tigabu Abrha Shemuye**

Signature: _____

Date: _____

Confirmed by:

Name: _____

Signature: _____

Date: _____

ACKNOWLEDGEMENTS

These all are nothing without my Lord, so my greatest and heartfelt thanks go to the almighty **GOD** who gave me not only what I asked him but also what I should have.

This work would not have been possible without the valuable assistance of many people. I would like to express and extend my heartfelt appreciation and deep gratitude to the many people who have, in one way or other, helped and supported me in my work.

Firstly, I would like to express my deepest gratitude to my thesis advisor **Dr.Ing.- Abebayehu Assefa** for his skillful guidance, encouragement, enormous patience, and willing attitude throughout of this thesis work. I also thanks **Ato Sileshi Kore** heartily, who shared me his experience and was as co-advisor in finding the research problem. I like to thanks to Ato **Masresha Wondemu** who had been engaged in the manufacturing and development process. I am also very thankful to the entire faculty and staff members of Mechanical Engineering Department for their direct-indirect help and cooperation.

I am deeply indebted to thank to my beloved parents; my father **Ato Abrha Shemuye**, my mother **W/o Werkinesh Abebe**, my brothers **Zinabu Abrha, Habtu Abrha** and **Gebeyaw Abrha** who are always behind me with full support in my entire educational carrier and for their encouragement, inspiration and patience which enabled me to finish my thesis work.

Table of Contents

LIST OF FIGURES

LIST OF TABLES

NOMENCLATURES

A_b Bed cross sectional area (m^2)

A_c Reactor cross - sectional area (m^2)

A_r Archimedes number (dimension less)

C_{Ao} Inter mediate concentration, mol/lit

C_{Ro} Final concentration, mol/lit

C_{Ai} Initial concentration, mol/lit

D Nominal screw feeder diameter (m)

D_c Cyclone diameter (m)

D_r Reactor diameter (m)

d_b Bubble diameter (m)

d_h Grid hole diameter (m)

d_{bo} Initial bubble diameter (m)

d_p Particles diameter (m):

d_p^* Dimension less particle size

f_c Cloud volume to bubble volume

f_w Wake volume to bubble volume

f_e Fraction of bed in emulsion

g Gravitational acceleration (m/s^2)

H_o Initial static bed height (m)

H_{mf} Bed height at minimum fluidization velocity

K_{bc} Inter change co-efficient between bubble and cloud

K_{ce} Inter change co-efficient between cloud and emulsion

K_{f12} Effective rate constant, s^{-1}

K_{r12}	Effective rate constant for the conversion of initial to inter mediate product, s^{-1}
K_{fAR}	Final rate constant for the process, s^{-1}
M_B	Bed weight (kg)
N_u	Nussult's Number
Q_{gas}	Gas volumetric flow rate (m^3/s)
ΔP_b	Bed pressure drop (Pa)
ΔP_d	Grid pressure drop (pa)
P_r	Prandtl Number
R	Universal gas constant (j/kgK)
R_{emf}	Reynolds number at minimum fluidization velocity
T	Temperature (K)
T_b	Bed temperature (K)
T_{wall}	Wall temperature (K)
u_{br}	Velocity of bubble rise (m/s)
U_o	Superficial gas velocity (m/s)
U_{mf}	Minimum fluidization velocity (m/s)
U_t	Terminal velocity (m/s)
U_t^*	Dimension less terminal velocity (m/s)
V_g	Gas velocity (m/s)
V_o	Initial bed volume (m^3)
τ	Reaction time, s
ε_e	Void of emulsion
ε_f	Average bed void
ε_{mf}	Void at the minimum fluidization condition

γ_d Fraction of bed in the bubble

γ_b Volume of solids dispersed in bubble / Volume of bubble

γ_c Volume of solids dispersed in cloud / Volume of bubble

γ_e Volume of solids dispersed in emulsion / Volume of bubble

ϕ_p Sphericity of the particle

λ Trough filling coefficient

ε Void fraction.

ρ_b Bulk density (kg/m^3)

ρ_g Gas density (kg/m^3)

ρ_p Particle density (kg/m^3)

μ_g Gas dynamic viscosity (kg/ms)

ABSTRACT

Fast pyrolysis of biomass is the most promising technology of converting solid biomass to liquid bio-oil as a renewable substitution of fossil resources in fuel and chemical feed stocks applications. Ethiopia with abundant biomass resources especially from coffee processing industry has the potential to provide an ideal platform for the development of this thermal conversion technology. This thesis was aimed of developing a 145 mm reactor diameter pilot scale fast pyrolysis system with coffee husk as the main feedstock.

For detail analysis of the fast pyrolysis system a two-stage fluidized bed reactor was designed based on the fluidization technology with silica sand as the heat carrier to achieve rapid heat transfer required for the reaction. The amount of silica sand required was determined from the hydrodynamics and heat transfer performances. The assembly of the system consists of five main sections. These are the feed hopper, reactor subsystems (reaction chamber, gas-preheating chamber, plenum, and gas distributor plate), cyclone separator and condensation system. Smooth process and substantial bio-oil yields could be achieved for the experiments carried out with the reaction temperature within 300 ℃ to500℃. But due to lack of appropriate fluidizing medium (lack of continuous gas supply compressor) the maximum gas temperature in the reaction chamber achieved was only 100℃.

Key Words: Biomass, Fast pyrolysis, Bio-oil

CHAPTER ONE

INTRODUCTION

1.1 Background

The challenges to overcome the depletion of fossil fuels, especially the petroleum based fuels are the critical issues of this century. It is also clear that combusting fossil fuels produces green house emissions which cause a negative environmental impact. Due to these environmental and economical problems connected with fossil fuels, there are various fuel alternative technologies which can be developed in order to mitigate both the dependence on fossil fuels and the negative impact caused by its emissions [9].

Biomass is gaining higher attention as it is one of the most available renewable energy resources that can be used to reduce the dependency on fossil resources [27]. Coffee husk and other forms of biomass are some of the main renewable energy resources available and provide the only source of renewable liquid, gaseous and solid fuels. Biomass derived energy has no net carbon dioxide (CO_2) impact on the atmosphere and is therefore advantageous in offering resistance to a climate change due to the greenhouse effect. Moreover, biomass can play a role in improving the country's energy security as part of a diversification strategy.

Utilization of biomass can be achieved through thermo-chemical conversion processes to provide energy:

- By direct combustion to provide heat for use in heating, for steam production and hence electricity generation;
- By gasification to provide a fuel gas for combustion for heat, or in an engine or turbine for electricity generation;
- By fast pyrolysis to provide a liquid fuel that can substitute for fuel oil in any static heating or electricity generation application. The liquid can also be used to produce a range of specialty and commodity chemicals

Among these technologies, fast pyrolysis of biomass has emerged as the most promising technology to make use of the waste biomass resources to produce value added products. Fast pyrolysis is a process in which biomass is rapidly heated to moderately high temperature (usually

350 ℃ to 650 ℃ which higher than carbonization, lower than gasification and combustion) in the absence of oxidizing agent [25].

In fast pyrolysis process, solid biomass is converted from solid to form char, gas and most importantly high yields of liquid products which is known as pyrolysis oil, or bio-oil. The bio-oil from fast pyrolysis consists of a complex mixture of oxygenated components and it could be processed into liquid fuel for power generation or raw material for chemical feedstock such as phenol [4].

Production of bio-oil from biomass fast pyrolysis is a promising trend of using reproducible types of energy because biomass is becoming an important source of energy for several reasons.

- Carbon dioxide (the main green house gas) formed by the pyrolysis of biomass-derived fuels is recycled. That is biomass plants uses carbon dioxide (CO_2) from the atmosphere to grow and releases as much CO_2 is consumed.
- The energy production costs for biomass derived energy are becoming economically competitive because of the high oil price.
- Political instabilities in many oil producing countries drive the need to seek for alternative sources of energy.

Short time of heating a biomass particle in the reactor provides a high yield of the liquid product requires and, a short residence time of gaseous and condensable pyrolysis products in the high-temperature reactor zone needed to prevent their destruction.

1.2 Objectives

The general objective of this work is designing and development of a laboratory model fast pyrolysis fluidized bed reactor for bio-oil production, where coffee husk is used as a feed stock material.

The specific objectives are:

- To identifying basic concepts in biomass to bio-oil conversions that may lead to higher overall energy efficiency and lower costs on longer terms.
- To design and develops of the system components; reaction chamber, feed stock feeding sub system (hopper), feeding screw, cyclone separator, heating system, condenser and bio-oil storage and test.
- Numerical modeling of the particle behavior in the bed.

1.3 Methodology

The methodology is primarily based on the appropriate design of the system components which represents the actual activities. The models are produced in the workshop. The methods to be employed to achieve the objectives of the research are:

- Literature review: Background and theory of the thesis.
- A technological assessment on various types of fast pyrolysis reactors.
- Designing and detail drawing of the system components using Auto CAD.
- A workshop, used for the development and testing of the components.
- A computer program MATLAB is to be used for simulation of the particle behavior in the bed.

1.4 Outline of the Work

This thesis consists of eight chapters and relevant appendices. Chapter Two presents the literature reviews on previous works on fast pyrolysis process. Chapter Three discusses the hydrodynamics, heat transfer and particle dynamics of the bed. The hydrodynamics defines different particle velocities of the bed mathematically by analyzing the dynamics of the bed; a numerical model of the heat transfer process in the bed is explained. Chapter Four discuses the designs work of the fluidized bed reactor. The design process is analyzed in detail in this chapter. In Chapter Five the manufacturing procedures of each parts and production cost are discussed. Chapter Six discusses the experimental setup and procedures of the system. Chapter Seven presents and discuses the experimental results obtained. Chapter Eight concludes with a summary and recommendations for future work.

CHAPTER TWO

LITERATURES REVIEW

Contrary to this work, a lot of researches have been done in bio-oil production from fast pyrolysis fluidized bed reactor using biomass as a feed stock material. All these reviews are used as basic inputs for this work. The main literature parts covered in this work are,

- Biomass as a source of renewable energy
- Energy conversion of biomass
- Principle of fast pyrolysis
- Fast pyrolysis process
- Fast pyrolysis rectors technologies and reactor design considerations
- Applications of fast pyrolysis products

2.1 Biomass as a Source of Renewable Energy

Biomass, one of the renewable resources, is a material of recent biological origin exploited by mankind which is abundant and available in most parts of the world. It is the most abundant organic resources as well as the only renewable source for fixed carbon [2]. A report from International Energy Agency (IEA) in 2003 has distinguished biomass from other renewable resources in that of its production from agriculture and forestry industry as byproduct which provides various feed stocks to power generation and energy conversion.

The supply of energy from biomass plays an increasing role in the debate on renewable energies. The relative large amount of biomass has already used for energy generation that reflects mainly the use of wood and traditional fuels in the developing countries [13] [29]. The energetic and industrial usage of biomass is becoming more and more technologically and economically attractive. The use of biomass offers the advantages, such as biomass is available in every country in various forms.

Thus, assures a secure supply of raw material to the energy system. From environmental benefits, the utilization of biomass for energy is an alternative for decreasing current environment problems such an increase of CO_2 in the atmosphere caused by the use of fossil fuels [21]. Plant biomass is essentially a composite material constructed from oxygen-containing organic polymers.

The major constituents consist of cellulose (a polymer glucosan), hemicelluloses (also called polyose), lignin, organic extractives, and inorganic minerals.

Ligno-cellulosic biomass normally consists of three major components which are cellulose, hemicelluloses and lignin. Some minor components such as ash, soluble phenolics and fatty acids extractives also exist in much smaller amount. Generally, these lignocellulosic biomass materials are complex and heterogeneous, the structures and composition of the major components vary for different parts and species of the plants.

- Cellulose is a high molecular-weight forms long chains that are bonded to each other by a long network of hydrogen bonds. When cellulose is pyrolyzed at a heating rate of 12 °C/min under helium gas, an endothermic is observed at 335 °C (temperature of maximum weight loss). The reaction is completed at 360 °C.

- Hemicelluloses exhibit lower molecular weights than cellulose. The onset of hemicelluloses thermal decomposition occurs at lower temperatures than crystalline cellulose. The loss of hemicellulose occurs in slow pyrolysis of wood in the temperature range of 130-194 °C, with most of this loss occurring above 180 °C. However, the relevance of this more rapid decomposition of hemicellulose versus cellulose is not known during fast pyrolysis, which is completed in few seconds at a rapid heating rate [22].

- Lignin is the most abundant polymeric aromatic organic in the plant world. It occurs together with cellulose and other polysaccharides in the cell walls of the plants. Lignin decomposes when heated at 280-500 ºC. Lignin pyrolysis yields phenols through the cleavage of ether and carbon-carbon linkages. Lignin pyrolysis produces more residual char than does the pyrolysis of cellulose [26].

2.2 Energy Conversion of Biomass

A research on biomass energy conversion is gaining more attention due to the escalating fossil fuel prices and green house emissions. Ligno-cellulosic biomass is natural resources conventionally to agricultural wastes. However, biomass can be converted to energy and value added products through thermo chemical, biological, physical, and liquefaction conversion processes. These conversion processes provide much greater commercial potentials than conventional applications of biomass.

The main routes of biomass energy conversion can be categorized as shown in Figure 2.1.

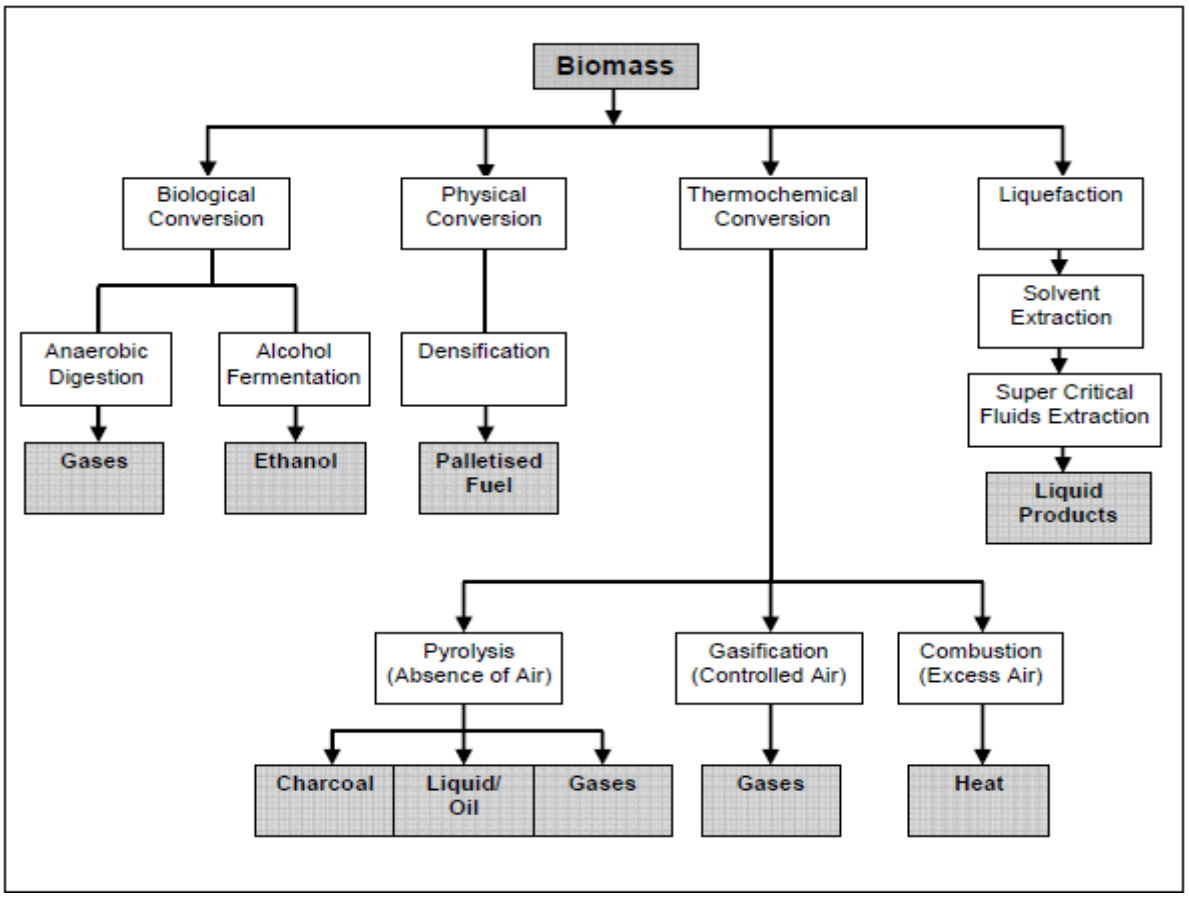

Fig 2.1 Main processes of biomass energy conversion [1]

There are two general types of biological conversion processes:

- Anaerobic digestion and
- Alcohol fermentation.

Anaerobic digestion: - is usually applicable to humid biomass such as sludge, effluence and landfill wastes. The wet material is converted to gaseous product by bacteria reaction with the absence of oxygen, usually in an enclosed reactor called digester. The gaseous product is known as biogas and contains mainly methane, carbon dioxide and acidic components [20] [21].

Alcohol fermentation: - is a process to ferment the sugar in simple glucose form using micro-organism to produce ethanol. The sugar is usually extracted from high sugar content crops, such as sugar cane and corn. This technology has gained overwhelming success in Brazil where ethanol is

commercially produced from sugar cane. It is being used as a blended fuel nationally with up to 22% ethanol mixed in the ethanol or gasoline blends, while it can also be used as pure fuel [20].

Densification: - Biomass can also be utilized through physical method known as densification, which is a relatively straight forward process. The biomass raw material usually in loose forms is densified with mechanical pressure to produce briquette fuel, pelletized fuel or fuel logs. This process usually incorporates with carbonization or partial carbonization of briquette to improve the combustion properties [1].

Liquefaction: - is also categorized as thermo-chemical conversion. However, it differs with other thermal processes as,

- ✓ It always integrates with hydrogenation to produce liquid products from organic materials.
- ✓ With high pressure (10 MPa-30 MPa) and moderate temperature (300 ℃ - 400℃), the decomposition processes employ reactive hydrogen or carbon monoxide carrier gases to produce hydrogenated liquid fuel.
- ✓ Super-critical fluids technology is one of the applied liquefactions, where the lingo-cellulosic materials are broken down in super-critical fluid with the present of solvent. The carbohydrates (celluloses and hemicelluloses) derived components are resolved in water while lignin derived components are resolved in solvent after the reactions.
- ✓ In this process, sugar can be extract from cellulose and hemicelluloses in fermentable portions. The lignin compounds can be recovered for other applications [15] [21].

2.2.1 Thermo-Chemical Conversion of Biomass

Thermo-chemical conversion is widely accepted as the most favorable conversion route compare to the other conversion processes. This is because,

- o Developments of biological conversion and physical conversion are limited.
- o Slow processing time, high initial cost, low efficiency is among the main reasons limiting the large scale commercial application.
- o Moreover, the biological and physical conversions usually produce a single or specific product for each process.

There are several advantages of thermo-chemical conversion over the other conversion routes. In the most significant aspect [2] [5],

- The thermo-chemical conversions are rapid processes in which very short processing times are required.
- Furthermore, diversify, complex and valuable products can be generated from these rapid processes with high conversion efficiencies

There are three main thermo-chemical processes available for converting biomass to a more useful energy forms:

- o Combustion
- o Gasification and
- o Pyrolysis.

In thermo-chemical conversion of biomass, biomass is heated under hot flowing gas stream. However, they are distinguished from each other by the amount of air supplied, residence time, temperature, the heat transfer rate in the process and the range of their products.

Different products as shown in Figure 2.2 can be obtained by fully making use of the relation of oxygen and heat in the thermo-chemical conversion processes [5].

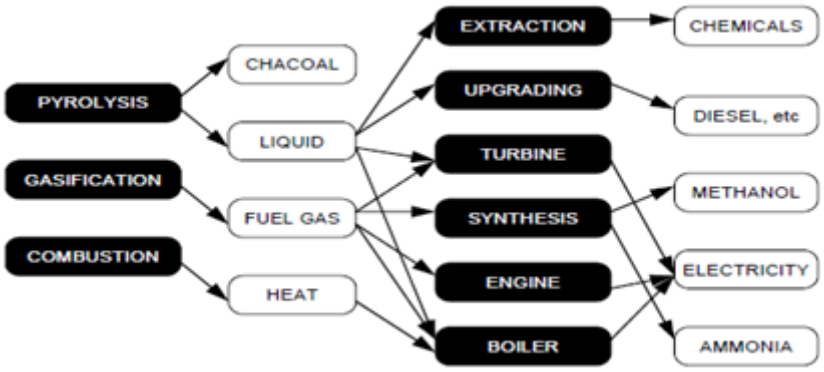

Fig 2.2 Biomass thermo-chemical processes and products [5]

2.2.1.1 Combustion

In combustion the biomass is directly burnt in the presence of air and completely transformed to heat, which must then be used for power generation immediately because storage is not a viable option. In most of the cases it requires some pre-treatment like drying, chopping, grinding, etc. Biomass combustion is more complex than either pyrolysis or gasification since the biomass must first pyrolyze, then be partially combusted (gasified) before it is fully combusted [6].

2.2.1.2 Gasification

Biomass gasification is a complex thermal process conversion of biomass in to the mixture of combustible and non-combustible gases by partial oxidation at high temperature around 800℃ - 900℃ in the presence of a gasifying medium such as air, oxygen or steam. The synthesis gas from biomass a mixture of carbon mono oxide (CO), carbon dioxide (CO_2), hydrogen (H_2), water (H_2O) and a small amount of methane (CH_4) .

Biomass gasification has vast potential to be used to produce heat, steam, chemicals and electricity. The development of this technology has benefited from the well established coal gasification technology [9]. However, these two technologies are not directly comparable due to the differences of feed stocks.

In ideal gasification, the process only produces non-condensable gas and generates ash as residue. However, in practical operation, incomplete gasification and pyrolysis always occurs along the biomass gasification process, produces gas containing contaminants such as particulates, tars, alkali metals and fuel-bound nitrogen compounds. Specific downstream equipments are req

uired for the gas filtration before it can be used in gas turbines and internal combustion engines. Although development of biomass gasification has reached the demonstration on large scale, some technical and non-technical barriers such as expensive cost and gas storage difficulties slowed down its penetration to energy markets [7] [9].

2.2.1.3 Pyrolysis

Biomass pyrolysis is the thermal decomposition of the organic matrix in the absence of oxygen to obtain gaseous, liquid and solid products that can be used as improved fuels or intermediate energy carriers. It is always the first step of biomass thermal conversion process. Essentially the method consists of heating the biomass in an inert atmosphere up to a certain desired temperature. The products from biomass pyrolysis include water, charcoal (a carbonaceous solid), oils and permanent gases including methane,(CH_4), hydrogen(H_2),carbon monoxide(CO) and carbon dioxide(CO_2) [7].

A large part of the produced vapors can be condensed to a brown liquid leaving the non-condensable gases as a combustible fuel for immediate use. It is attractive because solid biomass and wastes, which are difficult and costly to manage, can be readily converted to liquid products.

These liquids have advantages in transport, storage, combustion, retrofitting and flexibility in production and marketing [20].

2.3 Principles of Pyrolysis

Pyrolysis can be classified as slow, intermediate or fast pyrolysis. These differ from each other in terms of chemistry, overall yields and quality of products [10].

2.3.1 Slow Pyrolysis

It has been practiced for thousands of years and its product, charcoal was one of the most important heating sources before the exploration of petroleum fuels. In slow pyrolysis [4],

- Biomass is typically heated to ~ 500 ºC.
- The vapor residence time varies from 5 min to 30 min.
- Vapors do not escape as rapidly as they do in fast pyrolysis.
- The heating rate in slow pyrolysis is typically much slower than that used in fast pyrolysis.
- A feedstock can be held at constant temperature or slowly heated; vapor can be continuously removed as they are formed.
- Slow pyrolysis processes produce 18-30 wt% of liquid bio-oil, 20-35-wt% of solid char, and 30-40-wt% of gases, depending on the feedstock used.

2.3.2 Fast Pyrolysis

In contrast, fast pyrolysis is a relatively new re-discover from slow pyrolysis process developed to focus with high yield of liquid production. Studies in to pyrolysis mechanisms have shown that the proportions of gas, liquid and solids products can be controlled by changing the heating rate, reaction temperature and residence time [4]. Extensive development of fast pyrolysis was initiated only since 1970s, when the shortage of petroleum fuels and the escalating energy prices revived interest in alternative energy resources.

Comprehensive research works carried out by Scott and co-researchers in early 1980s can be credited with the foundation of modern fast pyrolysis establishing for maximum liquid yields it was recognized only in the 1980s that fast pyrolysis is a good alternative for the expensive hydro-cracking technology. The potential to convert lignocellulosic biomass to liquid chemicals and fuels gained great responses followed with rapid research and development, even though depressed oil

prices in 1990s to early of this decade do not provide much incentive for converting biomass to bio-oils [4] [25].

Fast pyrolysis is a high temperature process in which biomass is rapidly heated in the absence of oxygen. As a result it decomposes to generate mostly vapors and aerosols and some charcoal. Liquid production requires very low vapor residence time to minimize secondary reactions of typically 1 s, although acceptable yields can be obtained at residence times of up to 5 s, if the vapor temperature is kept below 400°C.

After cooling and condensation, a dark brown mobile liquid is formed which has a heating value about half that of conventional fuel oil. [2] [7].

The essential features of a fast pyrolysis process are:

- Very high heating and heat transfer rates, which usually requires a finely ground biomass feed;
- Carefully controlled pyrolysis reaction temperature of around 500 °C in the vapor phase, with short vapor residence times of typically less than 2 s;
- Rapid cooling of the pyrolysis vapours to give the bio-oil product.

Table: 2.1 Comparison of fast pyrolysis characteristics to other pyrolysis technologies [2]

Pyrolysis Technology	Heating rate	Temperature	Residence Time	Main products
Fast Pyrolysis	Very high >1000 °C/s	< 600 °C/s	0.5 – 5 seconds	Bio-oil, gas, char
Slow Pyrolysis	Low ,2 °C/s	< 600 °C/s	5 – 30 minutes	Charcoal, tar, gas

A simplification of biomass global pyrolysis reaction is widely accepted to explain the decomposition pathways of whole biomass in fast pyrolysis reaction. Lower reaction temperature and longer vapor residence time favor the production of solid char as the energy provided is not sufficient for breaking down most of the active material to primary vapor. However, higher temperature and longer residence time provide excess energy for secondary reaction to break down the primary products to secondary gas and tar products.

Therefore, the fast pyrolysis process requires accurate control of moderate temperature and short vapor residence time to obtain maximum liquid production [10].

Bio-oil is sensitive to the elevated temperatures when it undergoes chemical change so it cannot be distilled. The bio-oil has a distinctive odor of acid smoky smell causes by the low molecular weight aldehydes and acids, which can irritate the eyes and noses. Extra care should be taken during the storage and handling due to the wide range of the chemical compounds [4].

2.3.2.1 Fast Pyrolysis Process

Fast pyrolysis is a series of rapid thermal processes that carried out in an integration of subsystems designed for different stages of process flow. A typical fast pyrolysis system consists of an integrated series of operations starting with material feeding is shown in Fig.2.3.

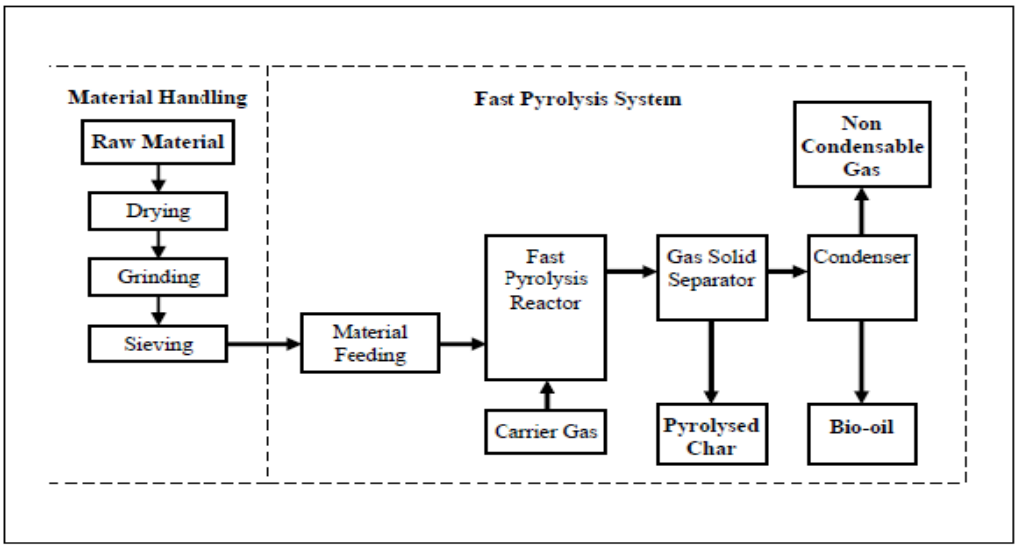

Fig. 2.3 Basic Principles of Fast Pyrolysis Process [20]

- **Material Handling**

The raw materials are usually needed to be processed before they can be fed into the fast pyrolysis reactor. In laboratory, the material can be easily processed with several simple equipments to reduce the moisture content and particle size. However, in commercial operation, the pre-treatment of the some raw materials is more complicated and costlier than the fast pyrolysis process. Raw biomass feed stocks are usually received in various forms such as chips, logs, straws, fibers, bunches and shells. Each kind of feed stocks has different methods of handling but all require large space for reception and storage.

Unless the biomass feedstock is a naturally dry material such as straw, most materials consist of considerable high amount of moisture content and hence need to be dried. Many factors contribute to the excessive moisture content in the biomass including atmosphere humidity and the storage

conditions. Thus, drying is an essential process to reduce the moisture content especially in the region with high humidity such as Ethiopia. Most of the fast pyrolysis systems require feed stocks with less than 10% of moisture content to eliminate the excessive dehydration reaction in the reactor which will require extra heat, reduce the heating rate to the biomass and result in excess aqueous fraction in bio-oil [3].

Different reactor configurations have different requirements on the feedstock particle sizes, mainly based on each heat transfers and hydrodynamics considerations. The feed specifications range from less than 200 μm for the rotating cone to less than 2 mm for bubbling fluidized bed and less than 6 mm for transported bed or circulating fluid bed. Cost of size reduction could become expensive as it requires more complicated cracking and shredding machineries to produce smaller particles. Reactors using larger particles have advantages in this respect [8] [10].

- **Material Feeding**

Material feeding is a critical feature in fast pyrolysis system for smooth and continuous operation. Feeding of biomass feedstock at accurately controllable feeding rate can be achieved either mechanically or pneumatically. Mechanical feeding with screw conveyor is a common practice in biomass application for the proven reliability and lower operational cost required of this established method. Most of the commercial and pilot scale operations employ screw conveyor as the major feeding device. Even in some models using the pneumatic feeding as major feeding device, screw conveyor is still applied as auxiliary transport mechanism to convey biomass from hopper to the feeding points.

In pneumatic feeding, the biomass is blown into the reactor by higher pressure from steam or inert gas. Pneumatic feeding is also applied in some laboratory models. However, in large scale operation, this method is not favored as increasing amount of inert gas or steam is required. Generation of inert gas and steam for feeding involves extra devices, which increases production cost of bio-oil.

- **Fast Pyrolysis Reactor**

The reactor is always considered as the heart of the fast pyrolysis system to provide the appropriate conditions for rapid thermal decomposition of biomass particles. There are three essential features of a fast pyrolysis reactor to achieve the conditions required, which are,

- Very high heating rate and heat transfer rate to rapidly decompose biomass particles

- Moderate and controllable reaction temperature to accommodate pyrolysis temperature of different feedstock, and
- Absence of oxidizing agent to eliminate the oxidation or combustion of biomass.

Wide ranges of reactor configurations have been investigated with considerably diversify and innovative methods developed to meet the basic requirements of fast pyrolysis reaction. Each configuration has its pros and cons while the best method that unanimously recognized by the industry is not yet established.

- **Heat Supply**

The high heat transfer rate that is necessary to heat the particles sufficiently quickly imposes a major design requirement on achieving the high heat fluxes required to match the high heating rates and endothermic pyrolysis reactions. Reed et al. (1990) originally suggested that to achieve true fast pyrolysis conditions, heat fluxes of 50 W/cm2 would be required, but to achieve this in a commercial process is not practicable or necessary.

Each mode of heat transfer imposes certain limitations on the reactor operation and may increase its complexity. The two dominant modes of heat transfer in fast pyrolysis technologies are,

- conductive and
- convective

Each one can be maximized or a contribution can be made from both depending on the reactor configuration.

- **Char Separation**

Separation of solid char from product vapors is difficult. However, hot char is known to be catalytically active. It contributes to secondary cracking of organic vapors to secondary char, water and gas. The secondary cracking reaction can occur as quickly as the char presences during primary vapors formation and in the reactor environment. Rapid and complete char separation is desirable to minimize the contact with pyrolysis product.

The fine char escape from the separation devices will be carried over to the condensation trains, and eventually be collected with the liquid product. Carryover of char is not favorable as the char may stick on the condenser wall reducing the heat transfer coefficient. Char settled in the liquid is

difficult to be separated and can only be removed by liquid filtration. Furthermore, the presence of char in the liquid will disturb the chemical stability and affect the storage quality.

- **Vapors Condensation and Liquid Collection**

Primary pyrolysis vapors are chemically active, where the secondary cracking reaction can occur under the influence of high temperature. The longer the vapors exposed at high temperatures, the greater is the extent of cracking. Thus, the temperature of the primary vapours must be immediately brought down to the temperature below the boiling points of the organic hydrocarbons, usually below 50℃ , to cover the liquid components in the vapours Secondary reactions are significantly slowed down at temperature below 350℃, however some secondary reactions will still continue down to room temperature which will results in the instability of the bio-oil [11].

The time and temperature profile from the formation of pyrolysis vapors to the condensation of liquid components influences the chemical composition and the quality of bio-oil. The time-temperature envelope that the pyrolysis vapours endure will affect the oil quality. Longer vapors residences time result in significant reductions in organic yields from cracking reactions.

The collection of liquid condensed can be difficult in the operation of fast pyrolysis processes if the liquid has high aerosol content. Mixing of the cooled liquid and placing the liquid collector in chilled water bath are both effective methods in order to maintain liquid products at low temperature. The process vessels, especially condensing trains and liquid collection apparatus should be made in stainless steel or corrosion free material in order to avoid erosion by the acid components in the primary vapors and bio-oil.

2.4 Fast Pyrolysis Reactor Technologies

During the last twenty-five years, a variety of reactor configurations have been developed to achieve rapid heat transfer and controllable moderate temperature at oxygen free basis for the conditions required in fast pyrolysis reactions. Heat transfer mechanisms are the most distinctive factor in the reactor developments. Biomass has very poor thermal conductivity, estimated at 0.1 W/mK along the grain, or approximately 0.05 W/mK across the grain. Reliance on heat transfer medium in the reactor to achieve rapid heating is therefore significant [25].

In most reactor configurations, heat is first supplied from the heating sources to the heat transfer medium and then to the biomass particles [2]. The development of fast pyrolysis reactor has received enormous creativity and innovative producing a wide range of design in configurations.

These configurations can be generally classified into three major categories based on the different concepts in heat transfer and reaction mechanism, which are,

- Fluidized bed reactors,
- Rotating cone reactor,
- Ablative pyrolysis reactor

2.4.1 Fluidized Bed Reactors

In fluidized bed pyrolysis, rapid heating is achieved by a mix of conductive and convective heat transfer mechanism. Heat is first transferred from hot gas to the fluidized sand particles where the heat can significantly be retained before transferred to biomass particles. In this case, hot gas is the heating source and fluidized sand is the heating medium. Fluidized bed pyrolysis utilizes the inherently good solids mixing to transfer approximately 90% of heat to the biomass by solid-solid conductive heat transfer with a probable small contribution from gas-solid convective heat transfer of up to 10%.

2.4.1.1 Bubbling Fluidized Bed Reactor

Bubbling fluidized bed reactor is the first and the most commonly applied reactor model for fast pyrolysis application. It is currently the most promising model among various pyrolysis reactor configurations with several pilot plants and commercial plants in operation. This reactor is characterized by [2],

- Small feedstock particle sizes are needed (< 2-3 mm) to ensure that the high heat rate requirement is fulfilled. The particle heating rate is the major factor limiting the rate of the pyrolysis reaction
- have good gas-to-solids contact, good heat transfer rate, good temperature control
- good scale up potential with high specific capacity, easily started and stopped, greater tolerance to particle size range and,
- There is some carbon loss with ash and a large heat storage capacity [1] [8]. \

Some design considerations in bubbling fluidized bed systems are [16]:

- Heat can be applied to the fluid bed in a number of different ways that offer flexibility for a given process.
- Vapor residence time is controlled by the carrier gas flow rate
- Biomass feed particles need to be less than 2-3 mm in size
- Char can catalyze vapor cracking reactions so it needs to be removed from the bed quickly
- Char can accumulate on top of the bed if the biomass feed is not sized properly, provisions for removing this char may be necessary

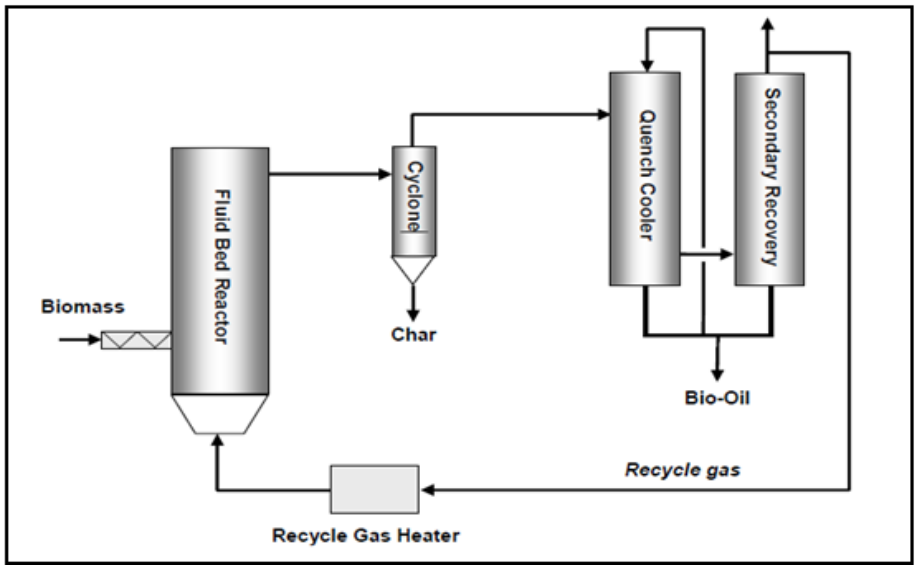

Fig 2.4 Flow diagram of bubbling fluidized bed pyrolysis system [7]

In a bubbling fluidized bed reactor, a heated sand medium in a zero-oxygen environment quickly heats the feedstock to 500℃, where it is decomposed into solid char, gas, vapors and aerosols which exit the reactor by the conveying fluidizing gas stream. After exiting the reactor zone, the charcoal can be removed by a cyclone separator and stored.

The scrubbed gases, vapors and aerosols enter a direct quenching system where they are rapidly cooled (< 50℃) directly with a liquid immiscible in bio-oil or indirectly using chillers (heat exchanger). The condensed bio-oil is collected and stored, and the non-condensable gas may be recycled or used as a fuel to heat the reactor [7] [14].

2.4.1.2 Circulating Fluidized Bed Reactors

This type of solids transport reactor technology has also been practiced for many years in refinery catalytic cracking units. This reactor design also is characterized as,

- Having high heat transfer rates and short vapor residence times which makes it another good candidate for fast pyrolysis of biomass.
- It is somewhat more complicated by virtue of having to move large quantities of sand (or other fluidizing media) around and into different vessels.
- Particles in the 1-2 mm are the desired size range.
- Feed particles sized for a circulating bed system must be even smaller than those used in bubbling beds.
- In this type of reactor the particle will only have 0.5-1.0 second (s) residence time in the high heat transfer pyrolysis zone before it is entrained over to the char combustion section in contrast to the bubbling bed where the average particle residence time is 2 to 3 second.

A schematic of this type of pyrolysis system is shown below in Figure 2.5

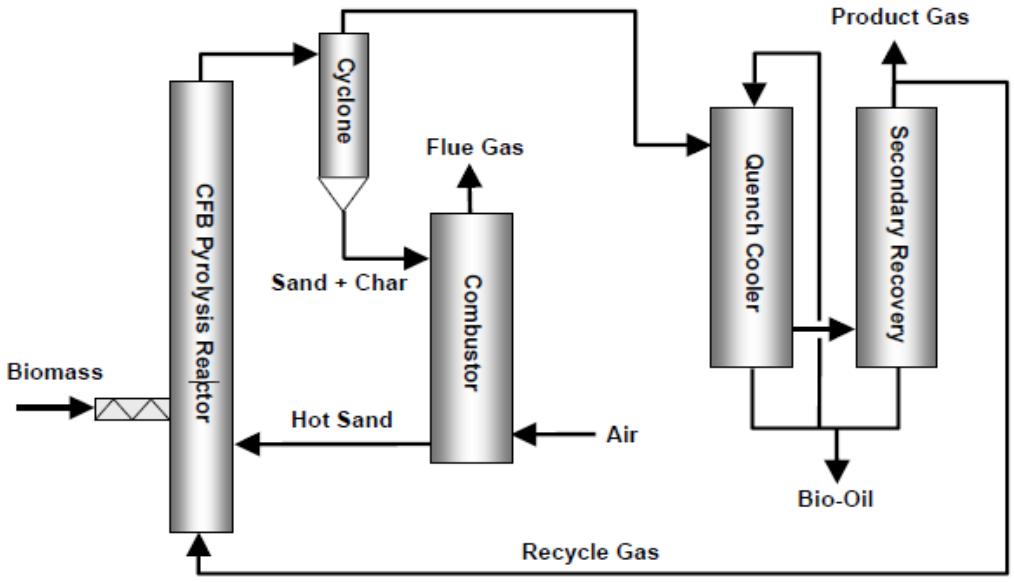

Fig 2.5 Process schematic for a circulating fluidized bed pyrolysis system [7]

For relatively large particles this would not be enough time to transport heat to the interior of the particles. This is especially true as a char layer develops on the outside surface, which acts as an insulating layer preventing further penetration of heat. The movement of sand and particles through the system causes abrasion of this char layer but mostly at the elbows and bends where there is more forceful interaction between the particles and sand. The incompletely pyrolyzed larger particles will end up in the char combustor where they will simply be burned. Consequently, if larger feed particles are used, the oil yield will be reduced due to combustion of incompletely pyrolyzed particles. The circulating fluidized bed systems have similar technical advantages

compared to the systems based on bubbling fluidized bed, such as good temperature control and rapid heating rate.

Moreover, circulating fluidized bed reactor can be fed with larger biomass particle of up to 6 mm with a char residence time almost similar with the product vapors. However, there are some drawbacks come along with the advantages [7], such as

- ✓ Large amount of gas flow required, and complexity in hydrodynamics.
- ✓ Some operational problems required further improvement are choking, back-mixing of product vapors and bed expansion above the optimal heat transfer considerations.

2.4.2 Rotating Cone Reactor

The rotating cone is also known as interconnecting fluidized bed, consists of two inverted cone connected through an orifice as exhibited in Figure 2.7. Fluidization of the inner cone is achieved through the rotation of the cone and thus reduces the carrier gas required.

In rotating cone, heat is transferred from hot sand that is mechanically circulated by an inverted cone spinning on its axis to the finely ground biomass. The heated sand is introduced near the bottom of the cone along with biomass particles. These particles are sucked up due to the centrifugal forces generated by the cone rotation and move spirally upwards along the hot cone wall from the bottom to top. These particles are eventually driven outward and fall over the edge into the second fluidized bed which is the combustion bed around the rotating cone.

Fast pyrolysis of biomass is completed along the spirally paths on the hot cone wall, and the product vapors escape from the top of the inverted cone. The remained char particles drop into the combustion bed together with sand are burned and the energy is used for heating the reactor and the sand. In between the two fluidizing beds is a connection through orifices where the hot sand can be again transported back to the inner cone bed.

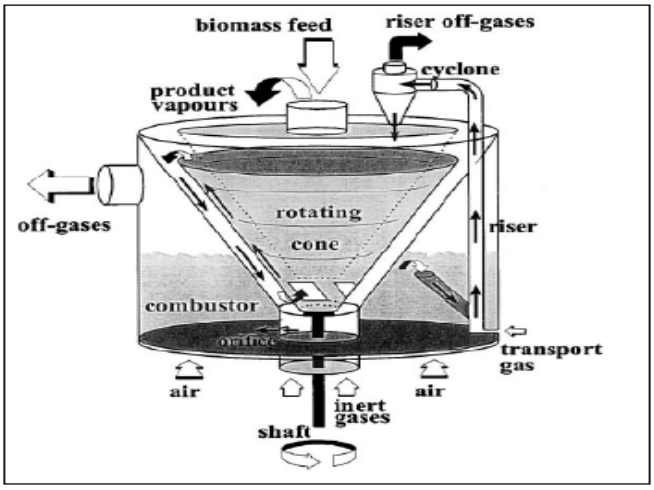

Fig. 2.6: Rotating cone with interconnecting fluidized bed reactor [7]

The advantages of this system are,

- ✓ Cost reduction due to less carrier gas required
- ✓ The throughput capacity for solids and biomass is very high.
- ✓ The requirement of very fine biomass particle, approximately less than 200 μm, which may increase the material handling cost.

The disadvantages of this reactor are the complicated mechanism and complexity of integrated operations.

2.4.3 Ablative Pyrolysis Reactor

The concept of ablative reactor is to achieve high rate of conductive heat transfer through pressing the biomass against a heated surface with mechanical or centrifugal forces. In an ablative reactor, the pressed biomass is rapidly moved during which the biomass particle melts at the heated surface and leaves an oil film behind which evaporates as vapors.

The idea was brought about as a solution to counter the pre-treatment cost of the input material where the pre-treatment cost of some biomass species is costlier than the process.

2.5 Application of Fast Pyrolysis Products

2.5.1 Application of Bio-oils

Fast pyrolysis of lignocellulosic biomass produces similar products in different compositions regardless of the technology applied. Bio-oils are mixtures of a vast number of components derived

from decomposition of cellulose, hemicellulose and lignin, the three major components in biomass. Physically, bio-oils are dark brown in colors, with distinctive smoky odors result from the chemical components of the oil [13].

Fig 2.7: Bio-oils from biomass

Pyrolysis liquids are formed by rapidly and simultaneously depolymerizing and fragmenting cellulose, hemicellulose, and lignin with a rapid increase in temperature. Rapid quenching then "freezes in" the intermediate products of the fast degradation of hemicellulose, cellulose, and lignin. Presently, more than 300 compounds have been identified in chemical analysis. The major groups of compounds identified include phenolic, carbonyl, carboxyl, hydroxyl, aldehyde, cresols, levoglucosan and organic acids [10].

Therefore, the bio-oil has considerable advantage as potential resource of a wide variety of valuable chemical compounds. Recovery of pure compounds from this complex mixture is technically feasible but economically unattractive for some compounds because of the low yield of some specific compound. However, it is definitely economically viable to extract some compounds which are available in bio-oil abundantly.

2.5.2 Application of Char Products

Char is black intermediate solid residue, which is formed in the fast pyrolysis from fixed carbon content of the carbonaceous biomass after its volatile content is vaporized. In most of the fast pyrolysis systems, char is separated immediately after the biomass is pyrolyzed, because char can act as a vapors cracking catalyst. Thus, rapid and effective separation of char from the pyrolysis products vapour is essential for high bio-oil yield [7].

The particle size of char formed is highly dependent upon the particle size of the feeding material used. This is due to the char becomes highly porous material without much reduction of size upon the completion of pyrolysis reaction. When most of the moisture and volatile matter content in the biomass are pyrolyzed into products vapor, the solid separated have left with very high fixed carbon content [10].

The solid char can be used as [16],

- A fuel in the form of briquettes or as a char-oil, char-water slurry; alternatively the char can be upgraded to activated carbon and used in purification processes.
- The pyrolyzed char is flammable and it can be considered as an excellent solid energy resource, similar to pulverized coal.
- Char can be readily used as solid fuel as in some pyrolysis system integrated with the combustion system to recover the heating energy in char.

2.5.3 Application of Gaseous Products

The third main product from fast pyrolysis of biomass is gas. Typically the gas was intermittently trapped in a gas bottle or gasbag, and then was analyzed using gas chromatography (GC). The gas component mainly consisted of H_2, CO_2, CO, and CH_4 together with traces of C_2H_4 and C_2H_6, CO_2 and CO evolved out at lower temperature, while H_2 released at higher temperature. [13].

Some of the applications of gas product from fast pyrolysis are [1] [20],

- ✓ Used for feedstock drying, process heating, power generation,
- ✓ Can be use as synthesis gas with extensive reforming and shifting to form the desired gas composition.

CHAPTER THREE

HYDRO DYNAMICS AND HEAT TRANSFER PROCESS

3.1 Fundamentals of Fluidization

Fluidization is the process by which solid particles (either homogeneous or heterogeneous) are transformed in to a fluid like state through suspension in a gas. To help characterize particles of fluidization behavior, Geldart created four particle classifications or "Geldart Groups" [12].

- Geldart A particles have small diameters (20 - 100 μm), low densities (< 1400 kg/m^3), are easily fluidized, expand significantly and are representatives of most granular catalysts.
- Geldart B particles typically have larger diameters (40 - 500 μm), medium densities (1400 - 4500 kg/m^3), are easily fluidize, readily form bubbles and are representative of sand-like granular materials.
- Geldart C particles typically have very small diameters (20 - 30 μm) and are difficult to fluidize due to large cohesive forces produced within the bed.
- Geldart D particles typically have very large diameters (> 600 μm), and are representative of the spouting granular materials

A fluidized bed is formed by passing a fluid upwards through a bed of particles supported by a distributor. The fluidized bed is known as a gas-solid fluidized bed or liquid-solid fluidized bed based on the state of the fluid flowing through. This work focuses on gas-solid fluidization in which the gas phase is assumed to behave as an ideal gas in thermodynamic equilibrium. In a gas-solid fluidized bed, the solid particles are transformed into fluid like state through the suspension in a gas. A stirring action is generated when the gas passes through the bed as bubbles or gas voids. This action continually moves the particles around, shearing and exposing it to the gas.

The good mixing of the bed particles therefore gives high rates of heat transfer and isothermal conditions from gas to particles and from particles to particles. Fine solid particles have a very large specific surface area which is essential for rapid thermal and chemical reaction, depending upon the appropriate methods employed.

A bed of solid particles passes through several fluidization regimes corresponding to the increase of gas flow rate are shown in Figure 3.1.

- ✓ At low flow rate, the gas merely percolates through the void spaces between the stationery particles, this condition is known as a 'fixed bed', where the flow rate is too low to overcome the weight of solid particles. The bed becomes an 'expanded bed' with the increase of the flow rate where the particles move apart and vibrate in restricted regions.

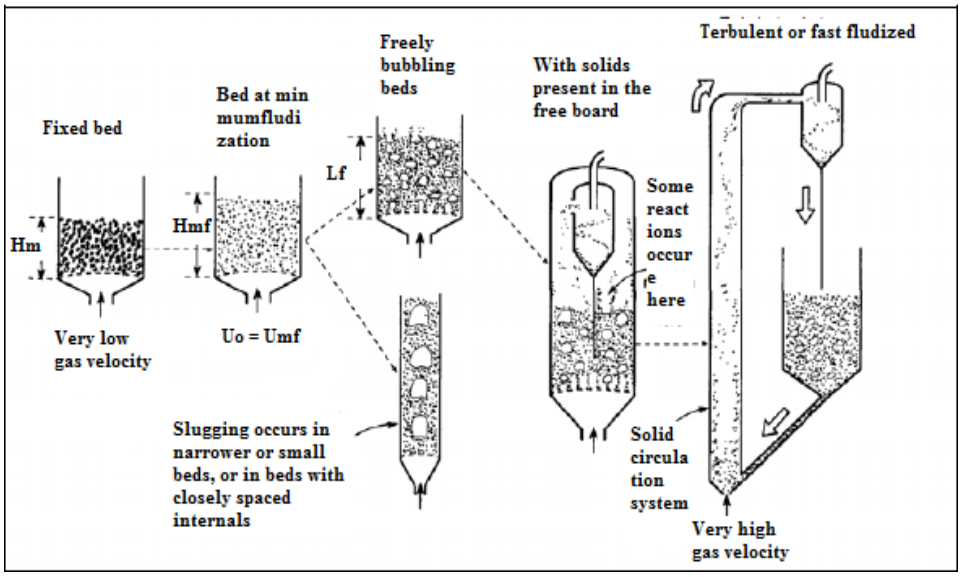

Figure 3.1: Gas/solid fluidizing regimes depending on the gas velocity and bed geometry [19]

- ✓ At a certain high gas velocity, a point is reached where all the particles are just suspended by the upward-flowing gas. The expansion of the bed is hardly observed at this point as the frictional force between solid particles and gas is just enough to counterbalance the weight of solid particles. At this condition, the bed is considered as just fluidized, or reaches its 'minimum fluidization'.
- ✓ As the flow rate is increased further above minimum fluidization, agitation of solid particles becomes violent and their movements become more vigorous. The bubble-like behavior of the gas channeling through the bed indicates the expansion of the solid particle bed. This is known as the 'bubbling fluidized bed', which is one of the preferred fluidizing conditions.

An upper layer upon the expanded bed surface clearly separates the fluidized bed into two phases: I) a 'dense phase' dominated by highly concentrated fluidized solid particles, and, II) a 'lean phase' or 'freeboard' with only very fine particles thrown up by the gas flow over the bed expansion limit. This upper layer of the bed surface disappears when the solid particles are fluidized at a sufficiently high gas flow rate that exceeding the 'terminal velocity' of the solids. Solids entrainment becomes appreciable and a turbulent motion of solid clusters and irregular shapes of gas voids can be observed instead of gas bubbles. This regime is identified as the 'turbulent fluidized bed' or 'lean

phase fluidization' where solids are removed from the bed with the gas flow higher than terminal velocity.

- ✓ If the gas flow rate is further increased beyond this point, pneumatic transport of solid particles can be achieved with large amounts of particles entrain at this regime, which is recognized as 'fast fluidization'. The entrained solid particles can be collected with a cyclone collector outside the bed.

3.2 Hydrodynamic of Bubbling Fluidized Bed: Theory and Analysis

Understanding the hydrodynamics of fluidized bed reactors is essential for choosing the correct operating parameters for the appropriate fluidization regime, proper design and efficient operation. The hydro dynamical parameters of the fluidized bed such as: void fraction, minimum fluidization velocity, superficial gas velocity and terminal settling velocity have a great influence in the practical design of the reactor subsystems.

The key design parameters assumed for the numerical calculations of the hydrodynamics and react component design are given in Appendix A.

3.2.1 Calculation of Minimum Fluidization Velocity, U_{mf}

The minimum fluidizing velocity is one of the most important parameters frequently used to indicate in what condition a bed of solid particles can be fluidized. It is the velocity at which fluidization starts and determines the lower limit of the operating gas velocity for any fixed particle. A bed of solid particles behaves as a static packed bed at low temperature and begins to exhibit the fluid-like behaviors as the state of minimum fluidization is achieved [20].

Minimum fluidizing velocity of a solid particle, U_{mf}, can be estimated by relating the pressure drop through a packed bed. When gas is passed through a packed bed unrestrained at its upper surface, the bed pressure drop, ΔP_b, increases almost linearly with gas velocity until the drag on an individual particle exceeds the force exerted by the gravity. The particle is then suspended due to the frictional force between particle and gas to overcome the particle weight. Relationships have been developed to predict fluidization characteristics for a single-component bed, such as pressure drop through the bed and minimum fluidization velocity. Pressure drop, ΔP_b, is derived from a force balance for a bed of particles assuming negligible cohesive forces.

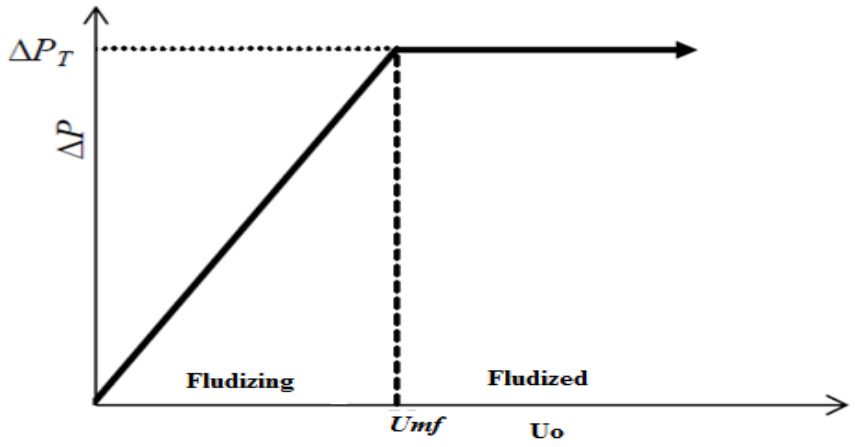

Fig 3.2: Relationship between pressure drop and gas inlet velocity [19]

The pressure drop ΔP_b, across a fluidized bed is the only parameter which can be accurately predicted given by:

$$\Delta P_b = \frac{M_{Bed}\, g}{A_r} \tag{3.1}$$

, for a bed material of mass M_{Bed}, reactor cross sectional area, A_r, and gravity g. Assuming gas density to be negligible in comparison to particles density it is possible to express pressure drop as:

$$\Delta P_b = \rho_b g H_{Bed} \tag{3.2}$$

Where the initial bed height is, H_{Bed} , and the bulk density is, $\rho_b = M_{Bed} / V_o$ for an initial bed volume, V_o. Bulk density can also be related to the particles volume fraction, ε_p, and particles density, ρ_p:

$$\rho_b = \varepsilon_p \rho_p \tag{3.3}$$

$$\text{Where, } \varepsilon_p = \left(\frac{0.071}{\phi_p}\right)^{1/3} \tag{3.4}$$

To establish the appropriate fluidization regime for any given application, one needs to calculate the minimum fluidization velocity and the terminal velocity of the bed particles. The superficial velocity of the gas for minimum fluidization (U_{mf}) can be calculated by solving the following equation for R_{emf} : The minimum fluidization velocity can be found theoretically from the pressure drop for known void fraction at minimum fluidization velocity using the equation below [23].

$$U_{mf} = \frac{(\phi_p d_p)^2}{150\mu_g}\left[g(\rho_p - \rho_g)\right] \times \left(\frac{\varepsilon_{mf}{}^3}{1-\varepsilon_{mf}}\right) \tag{3.5}$$

But, for unknown ϕ_p and ε_{mf} are not known for Eq. (1), an estimate of the minimum fluidization velocity can be obtained by the equation of [28]:

$$U_{mf} = \frac{R_{emf}\mu_g}{d_p\rho_g} \tag{3.6}$$

Where R_{emf}, is the Reynolds is number at minimum fluidization velocity and is given by the equation:

$$R_{emf} = \left[1140 + 0.0408A_r\right]^{1/2} - 33.7 \tag{3.7}$$

The estimated Reynolds number at minimum fluidizing velocity can be worked out by first determining the motion of solid particle due to the density differences. The expression of this motion is represented by a dimensionless group of parameters, which is known as Archimedes number, A_r, calculated as:

$$A_r = \frac{\rho_g g {d_p}^3 \left(\rho_p - \rho_g\right)}{{\mu_g}^2} \tag{3.8}$$

$$A_r = \frac{2.596 \times 9.81 \times (2.2\times10^{-3})^3 \times (1500 - 2.596)}{(3.599\times10^{-5})^2}$$

$$A_r = 296760$$

Where:

μ_g = Dynamic viscosity of the fluidizing gas (kg /s)

ρ_p = Density of the fluidizing gas (kg /m^3)

d_p = Mean particle size of the bed material (μm)

ρ_p = Density of solid particles (kg /m^3)

g = Acceleration due to gravity (m/s^2)

Substituting equations (3.7) and (3.8) in equation (3.6), the minimum fluidizing velocity, U_{mf} of sand particles is thus can be calculated as:

$$U_{mf} = \frac{\mu_g}{\rho_g d_p}\{(1135.7 + 0.0408 A_r)^{1/2} - 33.7\} \quad (3.9)$$

$$U_{mf} = \frac{3.599 \times 10^{-5}}{2.596 \times 2.2 \times 10^{-3}}\{(1135.7 + 0.0408 \times 296760)^{1/2} - 33.7\}$$

$$U_{mf} = 0.522 m/s$$

3.2.2 Calculation of Terminal Velocity, U_t

The fluidized bed experiences transition from bubbling fluidization to turbulent fluidization and then fast fluidization when it is operated above the terminal velocity, U_t of the bed particles. In this regime, entrainment and elutriation of bed materials become severe. Solid circulating device is required to retain certain amount of bed material in the reactor. Therefore, in bubbling fluidized bed, fluidizing gas velocity must be controlled in between minimum fluidizing velocity, U_{mf} and terminal velocity, U_t of the bed material in order to avoid or reduce entrainment of particles from the fluidized bed.

The terminal velocity, U_t, is a fluid mechanics expression of the terminal free fall velocity when a size of solid particle falls through an upward moving fluid. In a correlation described by Kunni and Levenspiel (1991), estimation of the terminal velocity can be obtained by evaluating dimensionless particle size, d_p*, and dimensionless terminal velocity, U_t *. Haider and Levenspiel determine direct evaluation of terminal velocity from physical properties of solid and gas using these dimensionless parameters.

The dimensionless particle size is expressed as:

$$d_p^* = d_p\left[\frac{\rho_g(\rho_p - \rho_g)g}{\mu_g^2}\right]^{1/3} \quad (3.10)$$

$$d_p^* = A_r^{1/3}$$

$$d_p^* = (2682.89)^{1/3}$$

$$d_p^* = 13.89$$

Whereas the dimensionless terminal velocity for particle with higher sphericity can be expressed as:

$$U_t^* = \left[\frac{18}{(d_p^*)^2} + \frac{2.335 - 1.744\phi_p}{(d_p^*)^{0.5}} \right]^{-1}, 0.5 < \phi_p < 1 \quad (3.11)$$

Where: ϕ_p = Sphericity of sand particle (0.8 for silica sand)

$$U_t^* = \left[\frac{18}{(13.89)^2} + \frac{2.335 - 1.744 \times 0.8}{(13.89)^{0.5}} \right]^{-1}$$

$$U_t^* = 8.401 m/s$$

Therefore, the terminal velocity for a selected size of particle can be determined by solving Equation (3.11),

$$U_t = U_t^* \left[\frac{\mu_g (\rho_p - \rho_g) g}{\rho_g^2} \right]^{1/3} \quad (3.12)$$

$$U_t = 8.401 \times \left[\frac{3.599 \times 10^{-5} (1500 - 2.596) \times 9.81}{2.596^2} \right]^{1/3}$$

$$\underline{U_t = 3.629 m/s}$$

3.2.3 Calculation of the Fluidization (Superficial) Gas Velocity, U_o

The superficial gas velocity, U_o, can be found by balancing the volumetric flow rate entering the plenum, Q_{gas}, with the volumetric flow rate entering the reactor chamber after passing through the distributor plate. The distributor plate is assumed to produce a uniform velocity profile, U_o, across the entire reactor cross sectional area. Therefore, the superficial or inlet gas velocity can be expressed as:

$$U_o = \frac{Q_{gas}}{A_c} \quad (3.13)$$

Above the bed of granular material is the freeboard, which is considered to contain only gas phase. The outlet of the reactor is located above the freeboard and typically exits to atmospheric pressure.

3.2.4 Bubbles in Fluidized Beds

Knowledge of the general behavior of a fluidized bed is insufficient for some purposes, e.g. reaction kinetics and heat transfer depends on details of the gas-solids interaction in the bed. Hence, a satisfactory treatment of these phenomena requires a reasonable model representing the gas flow through the bed and its interaction with bed material. As a consequence, the bubble size, rise velocity, shape, distribution, frequency and flow patterns are of key interest.

Bubble size is non-uniform throughout the bed and bubbles grow as they rise through the bed, which makes the determination of the bubble size difficult. Various empirical and semi-empirical correlations have been proposed to determine the mean bubble size for bubbles in freely bubbling beds. However, as discussed by Davidson (1985), these correlations are based on particular data from relatively small beds, which means they do not include all parameters affecting the variables to model. Based on experimental bubble observation in fluidized beds, the following correlation was presented by Clift and Grace (1985) for the bubble rise velocity and is often used for bubbles in any kind of fluidized bed:

The velocity of mass transport in the bed is a function of bubble size. In general, velocity of transfer between different phases (bubble, cloud, wake, and emulsion) has an important effect on the performance of fluidized bed reactor. So far, various equations have been proposed for describing variations of bubble diameter through coalescence as a function of apparent gas velocity, design of distributor, and bed height. These equations include linear and exponential functions of bed height (H). One of the widely used correlations was proposed by Geldart (1972) taking into account the effect of bed diameter and distributor type on bubble diameter as follows:

$$d_b = 2.05(U_o - U_{mf})^{0.94} H_{mf} + d_{bo} \tag{3.14}$$

Where, the initial bubble diameter, d_{bo} is given by:

$$d_{bo} = 0.376(U_o - U_{mf})^2 \text{ , for porous plates} \tag{3.15}$$

$$d_{bo} = 0.8716\left(\frac{A_b(U_o - U_{mf})}{ND}\right)^{0.4}$$, for perforated plates and ND is the number of orifice openings.

The velocity of bubble rise u_{br} in a bubbling fluidized bed reactor is greatly affected by the bubbles size d_b, and on the basis of simple two phase theory, Davidson and Harrison [36] proposed the following bubble rise velocity for only a single bubble:

$$u_{br} = 0.711(gd_b)^{1/2} \tag{3.16}$$

Davidson and Harrison [6] showed theoretically that the average absolute velocity of aggregated bubbles in the fluidized bed is

$$u_{bo} = U_o - U_{mf} + u_{br} \tag{3.17}$$

Similarly for velocity of bubbles in bubbling beds of different sizes of solids, Werther [37] had been proposed the following expressions:

- For Geldart A solids with $D_r \leq 1$m

$$u_b = 1.55\{(U_o - U_{mf}) + 14.1(d_b + 0.005)\}D_r^{1.35} + u_{br} \tag{3.18}$$

- For Geldart B solids with $D_r \leq 1$m

$$u_b = 1.6\{(U_o - U_{mf}) + 1.13d_b^{0.5}\}D_r^{1.35} + u_{br} \tag{3.19}$$

Then the volume fraction of the bed in the bubbles 'δ' and the average bed voidage 'ε_f' are then related to the voidage of emulsion 'ε_e' by:

$$\varepsilon_f = (1-\delta)(1-\varepsilon_e) \tag{3.20}$$

In vigorously bubbling beds, where $U_o \gg U_{mf}$, we may take as an approximation

$$\delta = \frac{U_o}{U_{mf}} \tag{3.21}$$

The distribution of solids in the various regions given by [38]:

$$\gamma_b, \gamma_c, \gamma_e = \frac{\text{Volume of Solids dispressed in,b,c,and e respectively}}{\text{Volume of bubbles}} \tag{3.22}$$

With δ as the volume fraction of the bed consisting of bubbles, the γ values are related by the expression:

$$\delta(\gamma_b + \gamma_c + \gamma_e) = 1 - \varepsilon_f = (1-\varepsilon_{mf})(1-\delta) \tag{3.23}$$

From which,

$$\gamma_e = \frac{(1-\varepsilon_{mf})(1-\delta)}{\delta} - \gamma_b - \gamma_c \tag{3.24}$$

With the wake included in the cloud region,

$$\gamma_c = (1-\varepsilon_{mf})(f_c + f_w) = (1-\varepsilon_{mf})\left[\frac{3}{u_{br}\varepsilon_{mf}/(U_{mf}-1)} + f_w\right] \tag{3.25}$$

And γ_b is about 10^{-2} to 10^{-3} by [38]

Cloud volume to bubble volume:

$$f_c = \frac{3}{u_{br}\varepsilon_{mf}/(U_{mf}-1)} \tag{3.26}$$

Fraction of bed in emulsion (*not counting bubble wakes*)

$$f_e = 1-\delta-f_w\delta \tag{3.27}$$

The mass transfer coefficient between bubbles and cloud, between cloud and emulsion interfaces were determined by considering the reaction as a first order reaction. Harson derived the following expression for the mass transfer co-efficient between bubbles and cloud.

$$K_{bc} = 4.5\left(\frac{U_{mf}}{d_b}\right) + 5.85\left(\frac{D^{1/2}g^{1/4}}{d_b{}^{5/4}}\right) \tag{3.28}$$

The fundamental governing diffusion through the cloud-emulsion interfaces were solved by Chiba and Kobayashi [39] as:

$$K_{ce} = 6.77\left(\frac{D_{emf}(0.711)(gd_b)^{1/2}}{d_b{}^3}\right)^{1/2} \tag{3.29}$$

Now the effective rate constant can be obtained from the given equation:

$$K_{f12} = \left[\gamma_b K_{r12} + \frac{1}{\frac{1}{K_{bc,A}} + \frac{1}{\gamma_c K_{r12} + \frac{1}{\frac{1}{K_{ce,A}} + \frac{1}{\gamma_e K_{r12}}}}}\right]\frac{\delta}{1-\varepsilon_f} \tag{3.30}$$

The concentration of reaction components leaving the bed denoted by subscript 'o' as

$$\frac{C_{Ao}}{C_{Ai}} = \exp(-K_{f12}\tau) \tag{3.31}$$

$$\frac{C_{Ro}}{C_{Ai}} = \frac{K_{f12}}{K_{f34} - K_{f12}}\left[\exp(-K_{f12}\tau) - \exp(-K_{f34}\tau)\right] \tag{3.32}$$

Where ; $K_{fAR} = \frac{K_{r1}}{K_{r2}} K_{f12}$

Hence the selectivity, S_R and the residence time τ were given as follows;

$$S_R = \frac{C_R / C_{Ai}}{X_A} \tag{3.33}$$

$$\tau = \frac{H_O(1-\varepsilon_f)}{U_o} \tag{3.34}$$

3.2.5 Numerical Modeling of the Particles Behavior in the Bed

To optimize the design process and to predict design parameters for a broad range of operating conditions, it is necessary mathematically, to model particle behavior in the reactor. Particle velocity in the bed depends upon many parameters, such as particle diameter and sphercity, gas velocity, particle density, gas density and viscosity, and gas temperature. To simulate particle velocity behavior in the bed, numerical models were developed by balancing the forces acting on a particle. These models were developed based on numerous assumptions including ignoring the pressure drop and the frictional losses. These programs are included in the appendices. Particle minimum fluidization velocity and terminal settling velocity behavior was analyzed as a function of the particle diameter and gas temperature.

3.2.5.1 Effects of Minimum Fluidization Velocity and Terminal Settling Velocity

- **Effect of Particles Diameter**

It can be noticed from Equations (3.6) and (3.7) that the minimum fluidizing velocity depends on the properties of solid particle (density and particle size) as well as fluidizing medium (density and viscosity). Assuming particle density, gas density and viscosity, and gas temperature are constant, minimum fluidization velocities and terminal settling velocities for different particle diameters were calculated by the model.

The behavior of the minimum fluidization and terminal settling velocity is shown graphically in Figure 3.3 and 3.4 respectively. Fig 3.3 shows that with the same fluidizing gas velocity, larger silica sand particles are more difficult to be fluidized. In order to achieve minimum fluidization, a higher velocity is required to overcome the particles weight and inter particle forces when larger particles are used. In contrast, the very small particles can easily be fluidized.

By comparing Fig 3.3 and 3.4 it can be said that velocity profile of terminal settling velocity and minimum fluidizing velocity are identical..The fast pyrolysis reactor can serve as a solid classifier when appropriate sizes of silica sand particle are selected.

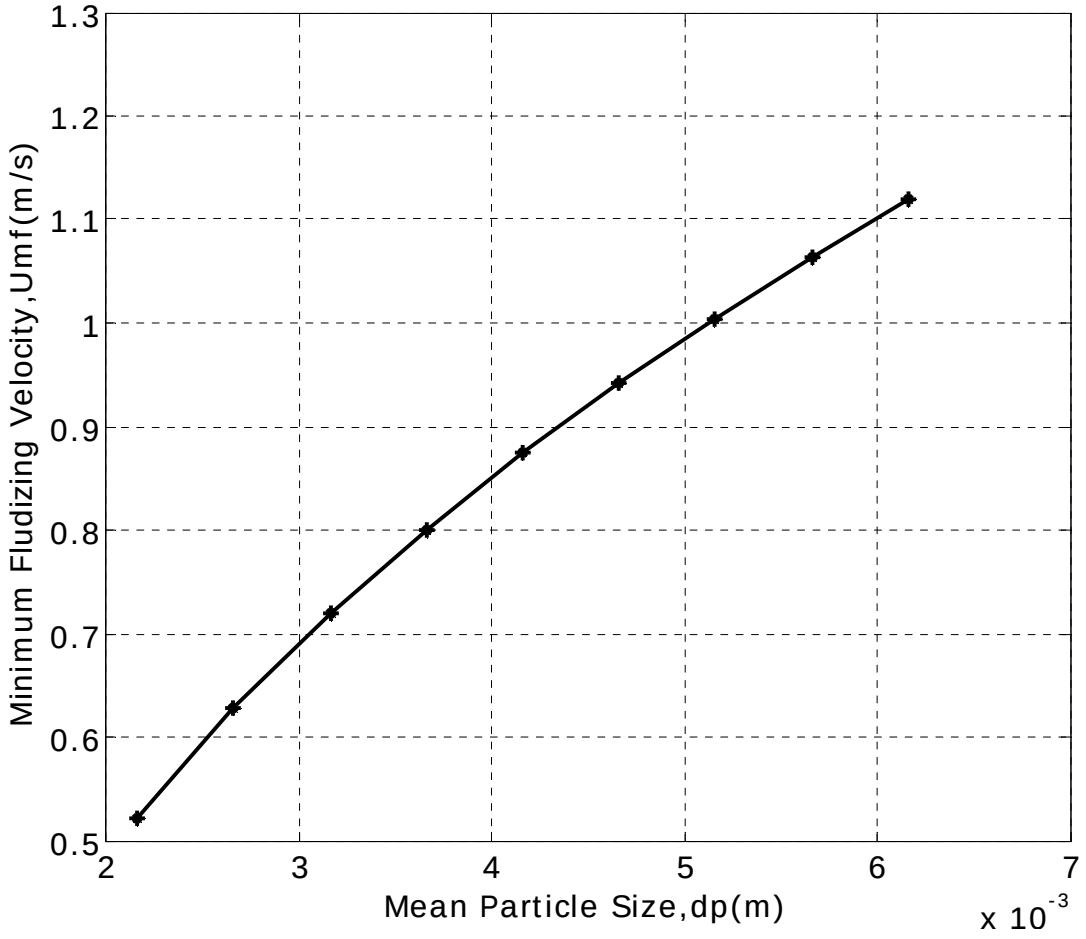

Fig. 3.3: Effect of particle sizes, d_p, to minimum fluidizing velocity

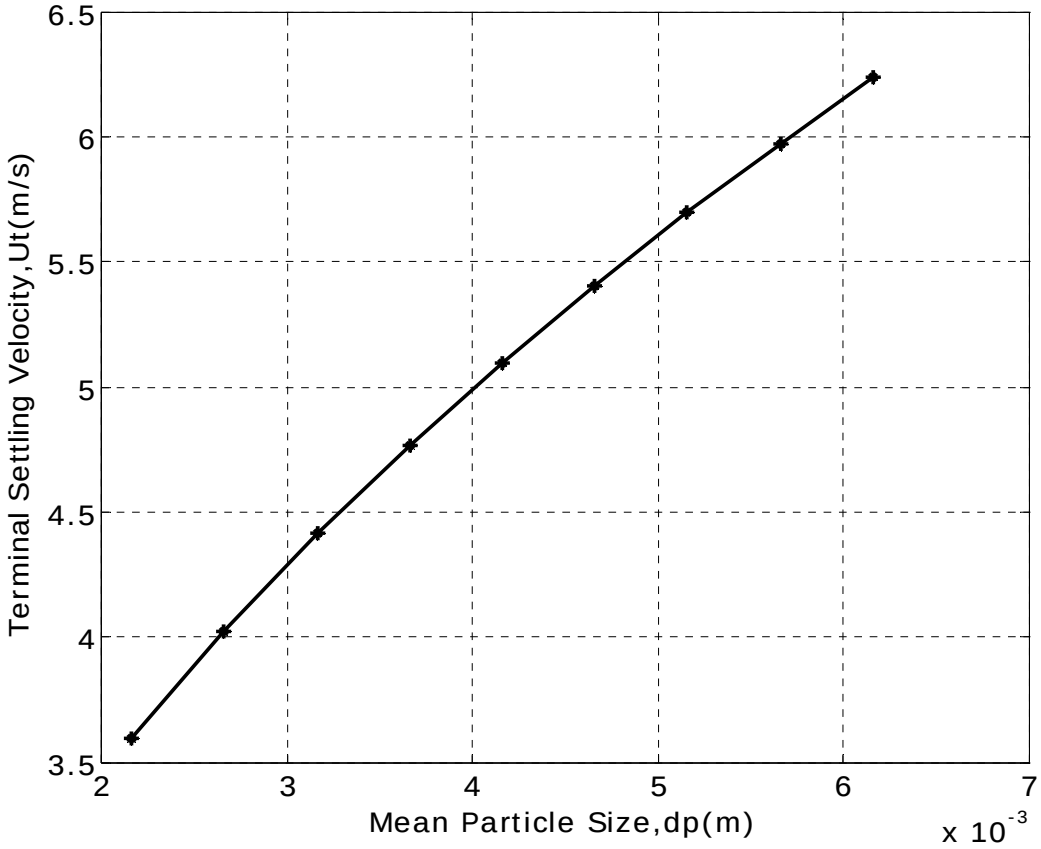

Fig. 3.4: Influence of particle sizes, d_p, to Terminal Settling Velocity

Effect of Gas Temperature

The Temperature of the fluidizing gas has an adverse effect on minimum fluidization velocity, U_{mf}, since the density of a gas is inversely proportional to its absolute temperature. Gas density will decrease with increasing temperature; the viscosity of a gas on the other hand increases with increasing temperature. Generally, gas expands and moves more vigorously with the elevated temperature. Since the gas movement is more vigorous at higher temperature, the inter particle forces are easier to overcome. Consequently, the silica sand particles fluidize more easily. As shown in Figure 3.4, according to Geldart's correlations among the three mean particle sizes, *dp*.

The general trend of minimum fluidizing velocity that it will increase if operated at higher gas temperature. The minimum fluidizing velocity of silica sand with mean particle size, d_p= 0.00216 has increased from 0.4107 m/s at 50 ^{0}C to 0.522 m/s at 500°C. The smaller particles decrease with a greater rate over the same temperature range, where sand particles with d_p = 0.003 m and d_p= 0.0045 m experience the increase of 27.05% and 30.97 % from 50 ^{0}C to 500°C respectively.

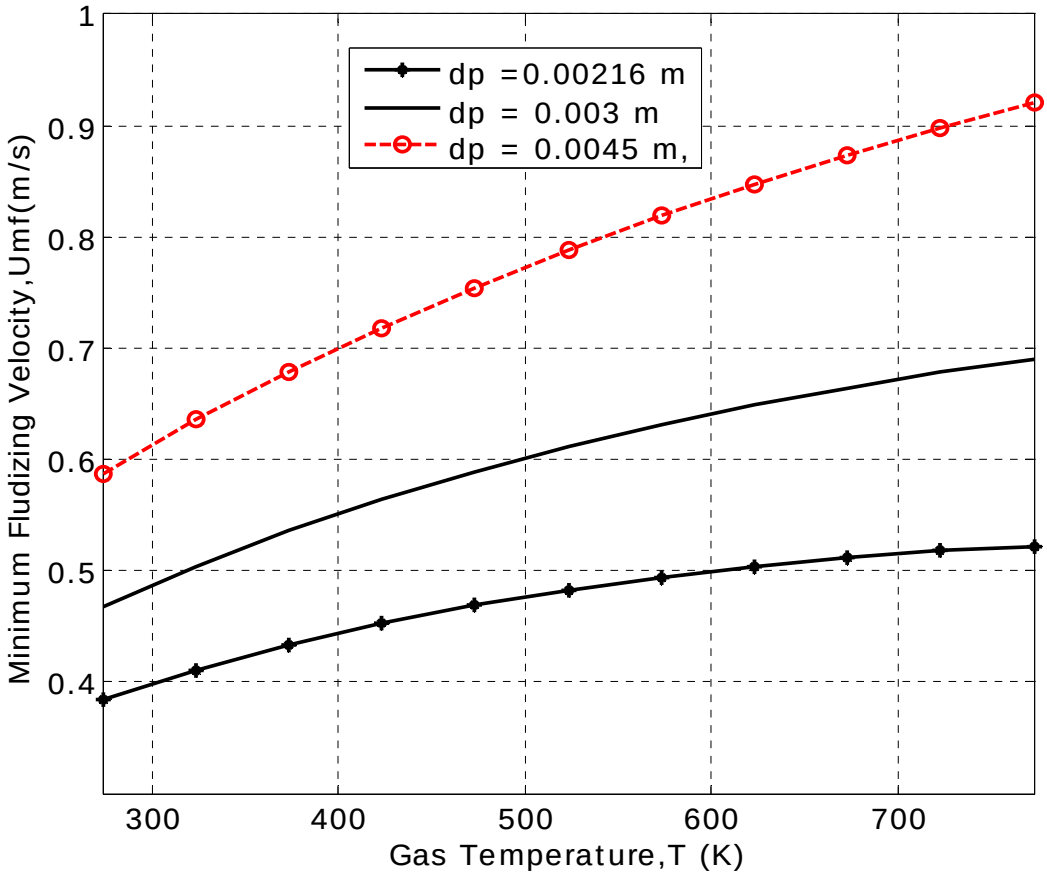

Fig 3.5: Effect of Gas Temperature to Minimum Fluidization Velocity

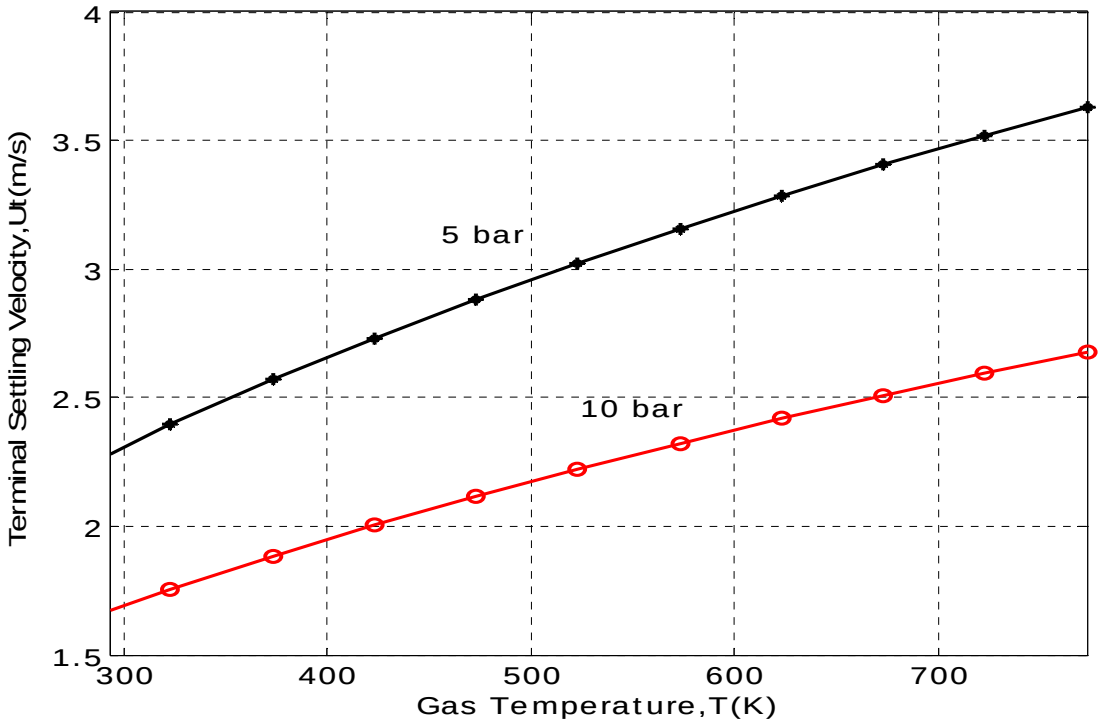

Fig 3.6: Effect of gas temperature to terminal falling velocity of the particles

Effect of Gas Pressure

As it was described in chapter three, the fluidizing gas used in this work is a pressurized air. Therefore, it is necessary to see the adverse effects of increasing pressure on minimum and terminal settling velocity of the particles. Fig. 3.7 and 3.8 shows the effect of increasing pressure (1-10) bar to minimum fluidization and terminal velocities respectively. As shown from the figures, a slightly increasing in pressure decreases particles velocity. This is because gas density increases while gas viscosity decreases as pressure increases and the velocity increases.

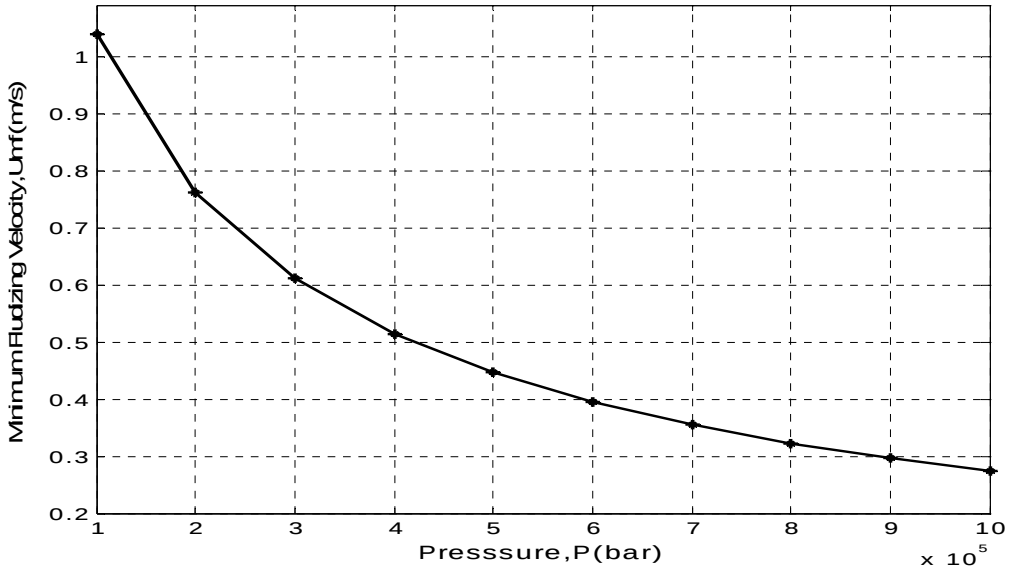

Fig 3.7: Effect of pressure on minimum fluidization velocity

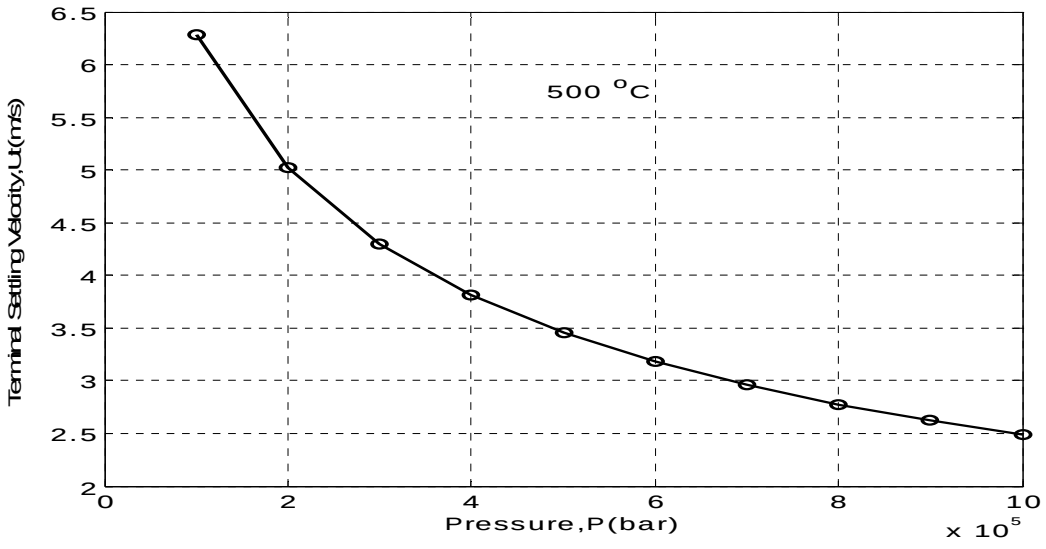

Fig 3.8: Effect of pressure on terminal falling velocity of the particle

3.3 Heat Transfer Process

Understanding the heat-transfer mechanism in a fluidized bed reactor is important due to its influence on the required bed surface area, bed height, and biomass feed rate. The prediction of the particles temperature is needed to calculate the burning rate of the feed material and the production rate of the gases, condensable vapors and chars. Even though considerable analytical and experimental researches have been conducted, few of them represent the local heat-transfer of a single solid particle accounting for effect of direct environment [16].

3.3.1 Heat Transfer Process in Fluidized Bed Reactor

The heat-transfer in a fluidized bed is an extremely complex phenomenon due to the wide variety of conditions and regimes. In a bubbling fluidized bed reactor, heat transfer involves,

- Interaction of conduction in and between particles
- Convection in moving gas, and
- Radiation between wall and particles.

The relative significance of these modes of the heat-transfer process depend on the combination of gas temperature, flow pattern of the gas and solids, surface area of the particles, wall surface area of the reactor and concentration, and size distribution of particles suspended in the gas.

In gas–solid fluidized beds, radiation may be neglected when the bed temperature is below 400℃. The relative effect of particle convection to gas convection on heat transfer depends appreciably on the types of particles used in fluidization.

- Particle convection is the dominant mechanism for small particles (dp < 400 μm), such as Group A particles.
- Gas convection becomes dominant for large particles (dp > 1500 μm), such as Group D particles (Maskaev and Baskakov, 1974) and for high-pressure or high velocity fluidization.

When the solid coffee husk particles enter the hot bed of sands, they are subject to fast pyrolysis. The rate of temperature increase in the coffee husk particles is important in calculating the final yield of different products. In the range of particle sizes of this study (less than 1 mm) the internal heat transfer limitation is negligible. Moreover, the yield of the different products in gasification of biomass in fluidized bed has been shown to be independent of particle size in the range of 4 μm to

2 mm. This eliminates the possibility of secondary reactions between the evolving vapor products and tar with char and the consequent thermal impact (endothermic or exothermic) of those reactions on particle temperature.

In this condition, the heat balance for a single particle can be expressed as follow:

$$\left(\rho_p * C_p * V_p\right)\frac{dT}{dt} = h_{conv} * A * \left(T_b - T_p\right) + \left(\sigma_{rad} * \varepsilon_{rad} * A * \left(T_b{}^4 - T_p{}^4\right)\right) \quad (3.35)$$

The convection heat transfer coefficient is calculated by the Ranz–Marshall correlation and given as follows.

$$\frac{h_{conv} * d_p}{k_g} = \left(2 + 0.6 * \mathrm{Re}^{0.5} * \mathrm{Pr}^{0.33}\right) \quad (3.36)$$

The effective emissivity in the condition of fluidized bed is calculated according to the correlation developed by Linjewile:

$$\varepsilon_{rad} = \frac{1}{\varepsilon_p} + \frac{1}{\varphi\left(\frac{1}{\varepsilon_{fb}} - 1\right)} \qquad \text{And } \varphi = \left(1 + np\frac{di}{da}\right)^2 \quad (3.37)$$

Table 3.7 Input data's for the determination of heat transfer

Parameters	***Value***
Coffee husk specific heat	Cp =1112.0 + 4.85(T - 273)J/(kg K)
Density of the coffee husk	136, kg/m^3
ε_p for wood particles	0.90
Effective emissivity, ε_{fb}	0.78
Parameter in Eq. 52, n_p	5.0
Stephan–Boltzmann constant, σ	5.67 *10^{-8} W m^{-2} K^{-4}

Where ε_p is the emissivity; ε_{fb} is the effective emissivity of the fluidized bed; and *di* and *da* are the diameters of the inert (sand) and feed stock respectively.

3.3.2 Heating Value of Feed Stock

HHV of the biomass was calculated by Dulong and Petit's Formula given in eqn. *(3.45)* using results from ultimate analysis.

$$HHV_{biomass} = \left(33823 * C + 144249 * \left(\frac{8 * H - O}{8}\right) + 9418 * S\right) \text{ kJ / kg} \qquad (3.38)$$

Where: C, H, O and S are the carbon, hydrogen, oxygen and sulfur content of biomass in dry basis, and are given in table 6.1.

The reaction chamber is maintained at a fixed temperature level (800 - 900 °C). The fuel particle was initially at a uniform room temperature, T, and suddenly exposed to the bed temperature, T_b. If the particle enters the bed at t=0, the temperature of the solid particle will increase. For t>0 until it reaches the bed temperature, T_b. Heat is transferred by convection by the flowing hot gas at the particle surface-gas interface, and by radiation between wall and particles.

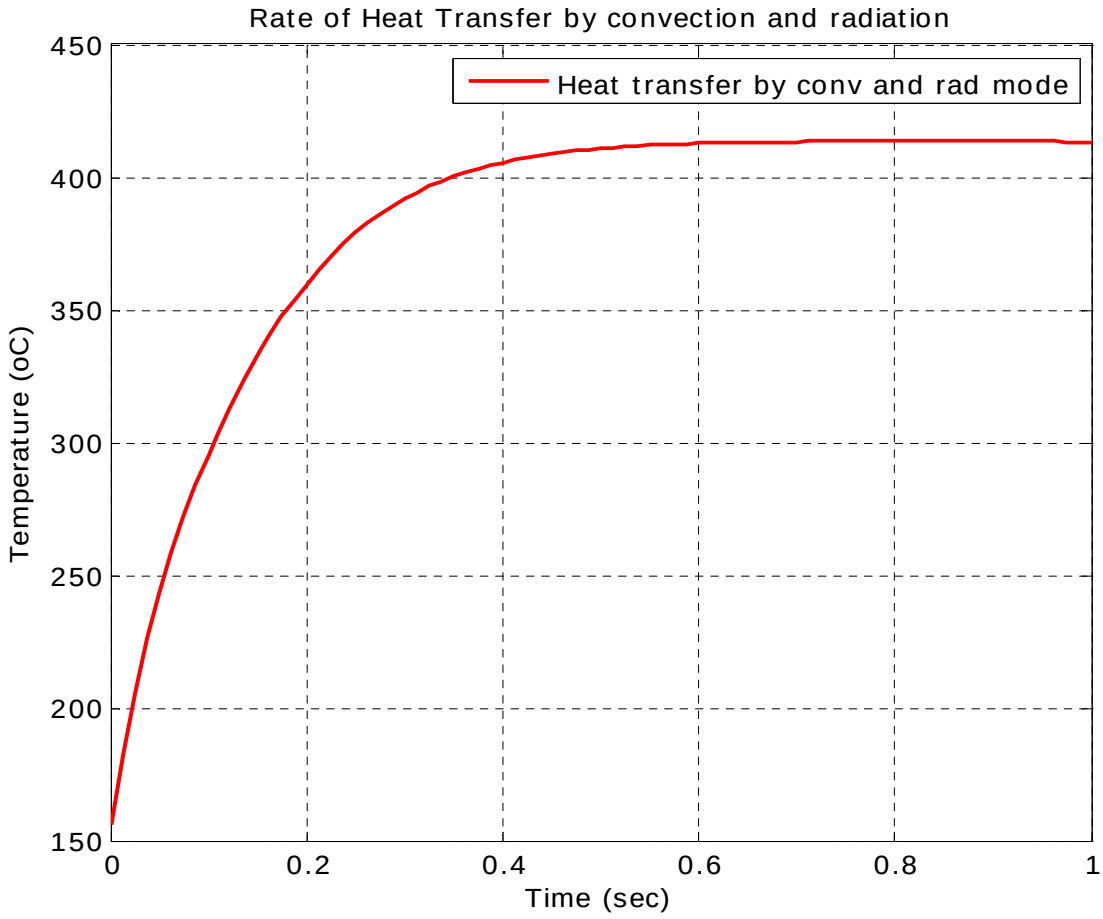

Fig 3.9: Heat transfer by convection and radiation mode

CHAPTER FOUR

BASIC DESIGN ANALYSIS OF FLUDIZED BED REACTOR

Pyrolysis is defined as a thermo chemical conversion process whereby biomass is heated in a absence of oxygen to produce liquids, gaseous fuel and vapours. There are various types of reactors and the design is specified by the feedstock type, preparation and end□use of product gas. For instance, fluidized bed gasification is originally developed to overcome the operational problems with fixed bed gasification of fuels with high ash content, but is very suitable for the larger capacities (larger than 10 MWT) in general. The fuel is fed into a hot (sand) bed which is in a state of bubbling. The bed behaves more or less like a fluid and is characterized by high turbulence. Fuel particles mix very quickly with the bed material, resulting in a fast pyrolysis and a relatively large amount of pyrolysis gases.

For this study, the fluidized bed reactor is selected due to:

- The characteristic of the feedstock and the ease of control in terms of handling of feedstock in the reactor.
- Uniform particle mixing**:** due to the intrinsic fluid-like behavior of the solid material, fluidized beds do not experience poor mixing as in packed beds. This complete mixing allows for a uniform product that can often be hard to achieve in other reactor designs. The elimination of radial and axial concentration gradients also allows for better fluid-solid contact, which is essential for reaction efficiency and quality.
- Uniform temperature gradients: many chemical reactions require the addition or removal of heat. Local hot or cold spots within the reaction bed, often a problem in packed beds, are avoided in a fluidized situation such as an FBR. In other reactor types, these local temperature differences, especially hotspots, can result in product degradation. Thus FBRs are well suited to exothermic reactions. Researchers have also learned that the bed-to-surface heat transfer coefficients for FBRs are high.
- Ability to operate reactor in continuous state: the fluidized bed nature of these reactors allows for the ability to continuously withdraw product and introduce new reactants into the reaction vessel. Operating at a continuous process state allows manufacturers to produce their various products more efficiently due to the removal of startup conditions in batch processes.

Bubbling fluidized beds have a wide range of applications and comes in many sizes and shapes. They are cylindrical configurations with an internal reactor diameter, D_r, height, H_r, and cross sectional area A_r. The material used for the vessel must have high melting point and low thermal conductivity to minimize heat loss. An additional layer can be added to the inner side of the reaction chamber vessel, which in turn acts as an erosion resistance layer.

4.1 Reactor Design Considerations

There are several factors to consider in designing a biomass pyrolysis reactor. Important factors to consider in selecting gas–solid reactors include gas–solid contact schemes, nature of the reactions temperature, and pressure among many other factors. Of particular pertinence in determining desirable reactor performance can be proper selection of particles, flow regime, material selection and system configurations.

- **Particle Selection**

Particles are the bed material employed in fluidized bed reactors and can be reactants (e.g., coal and limestone), products (e.g., polyethylene), catalysts, or inert materials (eg. silica sand). The choice of particle size, in general, affects the hydrodynamics, transport processes, and hence the extent of reactor conversion. Particles experience particle–particle collisions, friction between particles and walls or internals, and cyclones.

- **Flow Regime Relevancy**

The factors considered for choosing a fluidization/flow regime include,

- Gas–solid contact pattern and interphase mass transfer
- Back-mixing characteristics for both gas and particle phases
- Hydrodynamic parameters of the reactor
- Heat transfer
- Residence time and reactor height/diameter
- Insulation for the reactor

Contact schemes of gas–solid systems in fluidized beds are classified by the state of gas and solids motion. With an increase in gas velocity, particles move apart and become suspended; the bed has entered the fluidization state. Further increase of gas velocity subjects the flow to a series of transitions from a bubbling fluidization regime at low velocities to a dilute transport regime at high

velocities accompanied by significant variations in gas–solid contact behavior. The basic design parameters assumed are presented in Appendix A.

- **Material Selection**

The size and especially the thickness of the materials need also to be considered in the design and manufacturing of a reactor. The cost and the life span of the reactor unit are basically affected by the size of the material. Thin metal sheets are difficult to weld using an electric arc welding and require the use of oxy acetylene gas welding in order to fix them.

To simplify, the following assumptions are made for construction of biomass reactor:

- Insulating materials (i.e. material with very low thermal conductivity) can be used to reduce heat losses.
- Gas temperature is constant (about 300 - 500℃).
- Densities of the bed material, heat capacity, and thermal conductivity are considered.
- Only part of the convection and radiation is considered as useful in heating, the thermal conductivity of the material.
- Material composition, temperature, pressure, flow, and so on to ensure good quality control and to enable easy manufacture.

All the joints in the casing are either riveted or folded and welding, soldering or brazing is required. The minimum recommended thickness of mild steel used for reactor is 2.0 mm. If material thinner than 0.5 mm is used in the main casing, the folded joint around the waist will crack and separate after a short time. If a material thicker than 2 mm is used, making the folds and the waist joint will be awkward and difficult (Allen.H, 1991).

4.2 Reactor Sizing

The reactor is the core of fast pyrolysis system where the first step of a series of rapid thermal process occurs. It is essential to provide very high heating rate with closely controlled moderate temperature to enable the rapid thermal decomposition of biomass to primary vapors. Subsequently, the primary vapors must be rapidly removed from the reactor and cooled down in order to freeze the secondary reactions that will further decompose the vapors and produce lower molecular weight products, which are less valuable. Inert carrier gas is therefore important for controlling vapors residence time and eliminating the presence of oxidizing agent in the reactor atmosphere.

The reactor was designed to be tall, shell-type component with an inner erosion resistant layer that can facilitate less friction. On the other hand, the reactor shell and the friction layer must be able to withstand high temperature and should not lose a lot thermal energy. In this cylindrical vessel with a diameter of 145 mm, the static bed height required to accommodate 0.5 kg to 1.5 kg of the silica sand particles is less than 80 mm or 55% of the diameter. Sizing of the reactor includes determining of the overall height of the reaction chamber, height of feeding point, maximum expanded bed height and free board height.

Maximum Expanded Bed Height, H_{exp}: - is the height at which the bed expands when heat is supplied to the reactor.

Free Board Height, H_f :-is the measure of the free space above the boundary between the dense phase and the lean phase. A fluidized bed usually has two regions or phases: dense bubbling phase and lean dispersed phase.

The Transport Disengagement Height, TDH:- The TDH is the height at which the kinetic energies of particles due to the collisions in the bed has been expended against gravity potential, and the coarse particles whose terminal velocities are greater than the superficial velocity are able to fall back down to the bed. Transport Disengagement Height, TDH, depends upon the gas superficial velocity and the particle properties. The fine particles, whose terminal velocities are less than the superficial velocity, continue to be entrained out of the column. When $H_f > TDH;$ then the holdup and entrainment rates is close to their minimums. If $H_f < TDH,$ then the coarse particles will be carry out of the column. Usually H_f equal to *TDH* is the most economical design height for the fluidized bed. The Zens and Weil empirical plot based on the superficial gas velocity and reactor diameter is widely used to *TDH* calculation.

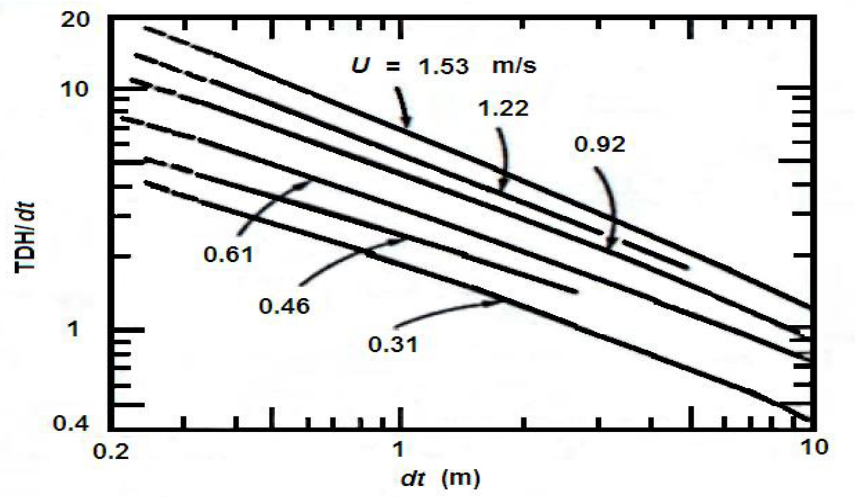

Fig 4.1: Zen's and Weil Graphical Correlation to TDH Calculation

According to Kunni and Levenspiel (1991), the overall height of the reactor, H_t is the sum of the maximum expanded bed height, $H_{b,exp}$ and the Transport Disengagement Height, TDH.

$$H_t = H_f + H_{B,\exp} \tag{4.1}$$

The bed height at minimum fluidization, H_{mf}

$$H_{mf} = \frac{M_{Bed}}{A_r(1-\varepsilon_{mf})\rho_p} \tag{4.2}$$

Where:

$$M_{Bed} = \rho_b \times V_{Bed} \tag{4.3}$$

Substitute the expression for, ρ_b from equation (3.4)

$$M_{Bed} = \varepsilon_p \times \rho_p \times A_{bed} \times H_B$$

$$M_{Bed} = 0.5 \times 1500 \times 0.01651 \times 0.10$$

$$M_{Bed} = 1.2kg$$

Substitute the value of M_{Bed}, in equation (5.2)

$$H_{mf} = \frac{1.2}{0.01651 \times (1-0.5) \times 1500}$$

$$H_{mf} = 0.10\,\text{m}$$

The maximum expanded bed height, $H_{b,exp}$

$$H_{B,\exp} = 1.3 \times H_{mf} \tag{4.4}$$

$$H_{B,\exp} = 1.3 \times 0.10\,\text{m}$$

$$H_{B,\exp} = 0.13m$$

The Transport Disengagement Height, TDH was estimated from Horio (1983) who has represented Zens and Weil empirical plot (Fig 4.1) by the correlation as follows:

$$\frac{TDH}{D_r} = (2.7D_r^{-0.36} - 0.7)\exp(0.74U_o \times D_r^{-0.23}) \quad (4.5)$$

At gas superficial velocity U_o of 0.66 m/s and reactor diameter of 0.145 m, TDH could be;

$$\frac{TDH}{D_r} = (2.7 \times 0.145^{-0.36} - 0.7)\exp(0.74 \times 0.219 \times 0.145^{-0.23})$$

$$TDH = 0.879\ \text{m}$$

From equation (5.1) the Overall Height H_t,

$$H_t = 0.88m + 0.13m$$

$$H_t = 1.01m$$

Height of the biomass feed point H_{feed}:

$$H_{feed} = \frac{1}{2}H_o \quad (4.6)$$

$$H_{feed} = \frac{1}{2} \times 0.10m$$

$$H_{feed} = 0.05m$$

4.3 Designing the Gas Distributor Plate

The purpose of the distributor plate is to introduce the fluidizing gas evenly through the bed cross section by keeping the solid particles in constant motion and preventing the formation of de-fluidization zones within the bed. From the gas distribution point of view, the essential requirement is to design a gas distributor in order to create sufficiently high pressure drop when the fluidizing gas is passing through. Additionally, the distributor is required to withstand the gas pressure and bed weight during the operation and shutdown, as well as to prevent the bed solid particles from falling into the plenum.

The design of the gas distributor plate can be as simple as a perforated plate, which can be made from a metal sheet drilled or punched with regular array of orifices or slots. The distributor is normally constructed from metal plate with a number of perforations in a definite geometric pattern. The perforations may be located in simple nozzles or nozzles with bubble caps, which serve to prevent solid particles from flowing back into the space below the distributor. The quality of bubbling fluidization is strongly influenced by the type of gas distributor used.

Gas distributors should be properly selected and designed. In this work, I have selected a single perforated distributor plate because it is,

- Easy to fabricate
- Inexpensive
- Easy to modify hole size and easy to scale up

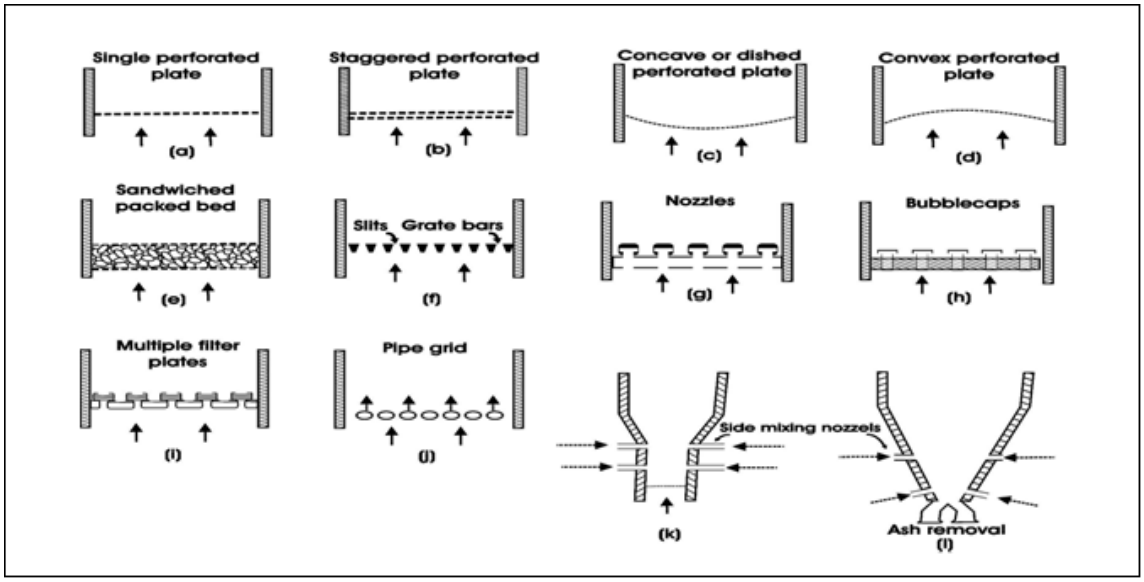

Fig. 4.2: Various types of grids and distributor plates

Table: 4.1: Basic design parameters of gas distributor plate

Parameter	Value
Fluidization Velocity (m/s)	0.66 m/s
Particle density (Kg/m^3)	1500
Gas density (Kg/m^3)	2.596
Mean particle size (m)	0.0022
Bed porosity at minimum fluidization (ε_{mf})	0.5
Bed zone diameter (m)	0.145

The design of distributor plates comprises of following steps.

Step 1: Determination of pressure drop across the bed and the distributor plates.

I. Pressure drop across the reactor bed, P_b : When gas is introduced at the bottom of the fixed bed, gas flows through the particles interstitial space. The bed pressure drops increase linearly until the gas velocity exceeds the minimum fluidizing velocity. The pressure drop across the bed can be calculated from equation (3.1) as,

$$\Delta P_b = \frac{M_{Bed} g}{A_r} \tag{4.7}$$

$$\Delta P_b = \frac{2 \times 9.81}{0.01651}$$

$$\Delta P_b = 1188.37 Pa$$

II. Pressure drop across the gas distributor, ΔP_d : Distributors should have a sufficient pressure drop, ΔP_d to achieve equal flows over the entire cross section of the bed and it is related calculated from bed pressure drop, ΔP_b

$$\Delta P_d = (0.2 - 0.4)\Delta P_b \tag{4.8}$$

$$\Delta P_d = 0.3\Delta P_b$$

$$\Delta P_d = 0.3 \times 11188.37 Pa$$

$$\Delta P_d = 356.5 \text{ Pa}$$

Step 2: Determination of velocity of the gas through the grid holes U_h using;

$$U_h = C_{d,h}\left(\frac{2\Delta P_d}{\rho_g}\right)^{1/2} \tag{4.9}$$

$$U_h = 0.77 \times \left(\frac{2 \times 356.5}{2.596}\right)^{1/2}, \text{ where } C_{d,h} = 0.77$$

$$U_h = 12.76 \text{ m/s}$$

Step 3: Determine the volumetric gas flow rate at the conditions below the grid. Assume that the temperature of the gas below the grid is the same as in the bed. Assume constant mass flow rate through the system;

$$Q_{gas} = U_o \times \frac{\pi}{4} D_d{}^2 \tag{4.10}$$

$$Q_{gas} = 0.665 \times \frac{\pi}{4} \times 0.145^2$$

$$Q_{gas} = 0.0109935\ \mathrm{m^3/s}$$

Step 4: Determine the number of grid holes, N required. The gas flow rate across the grid hole is given by:

$$Q_{gas} = N \frac{d_h{}^2}{4} U_h \ ,$$

Solving for, N,

$$N = \frac{4 \times Q_{gas}}{U_h \times \pi \times d_h{}^2} \tag{4.11}$$

$$N = \frac{4 \times 0.0109935}{12.76 \times \pi \times d_h{}^2}$$

$$N = \frac{1.0969 \times 10^{-3}}{d_h{}^2}$$

Step 5: Determine the hole density, N_d

$$N_d = \frac{4 \times N}{\pi D_d{}^2} \tag{4.12}$$

$$N_d = \frac{4 \times 1.09697 \times 10^{-3}}{\pi \times 0.145^2 \times d_h{}^2}$$

$$N_d = \frac{0.06643}{d_h{}^2}$$

Step 6: Determine the hole pitch arrangement either in triangular or rectangular

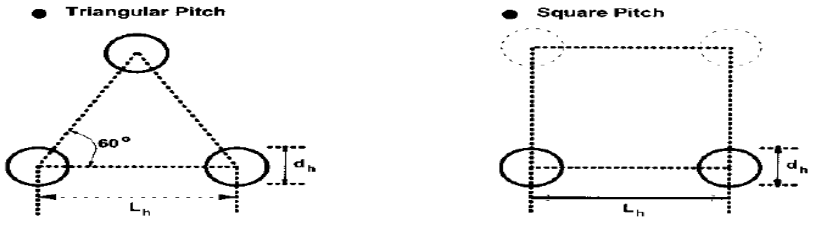

Fig. 4.3: Triangular and Square hole pitch arrangements

For triangular pitch arrangement, L_h is given as

$$L_h = \frac{1}{\sqrt{N_d \sin 60^0}} \tag{4.13}$$

For rectangular pitch arrangement, L_h is given as

$$L_h = \frac{1}{\sqrt{N_d}} \tag{4.14}$$

Table 4.2: Various Combinations of N, and d_h , satisfying the pressure drop requirements

d_h (m)	Number of holes, N	Hole density, N_d (per m^2)	Hole pitch arrangement (Triangular pitch), L_h(m)
0.0015	487.5	29524	0.00625
0.0022	226	13725	0.0092
0.0025	158	9564	0.0109

For this design I have used a 2.2 mm hole diameter. The distributor plate will have a total number of 226 holes arranged in a triangular pitch drilled at distance of 9.2 mm from each other.

4.4 Plenum

The purpose of the plenum is to collect the gas from compressor and to pass it equally into the reactor through the nozzles in the distributor plate. There are many configurations of plenum types depending on the type of suspension needed. If the gas–solid or gas–liquid suspension needs to be introduced into the plenum, as for example in a polyethylene reactor and some FCC regenerators, it is preferable to introduce the suspension at the lowest point of the plenum (Fig. 4.4 a, d, e) to minimize the accumulation of solids or liquids in the regions inaccessible to re-entrainment.

For two-phase systems, it is preferable to have some sort of deflection device (Fig. 4.4 d, e, and f) between the outlet of the supply pipe and the grid to prevent the solids from preferentially passing through the middle of the grid due to their high momentum. This preferential bypassing of solids causes mal-distribution of gases. In addition, the configurations of Fig. 4.4 e, f is preferable over the configurations of Figs. 4.4 a, d.

I have used the vertical type plenum configuration made up of a frustum of cone from a 2mm thick mild steel sheet. The height of the frustum is 75 mm, with 145 mm bigger diameter and 30 mm smaller diameter. Compressed air is fed into the plenum with the 20 mm diameter GI pipe fitted at

the center of the 60 mm diameter of the frustum. This plenum is welded at extreme bottom of the reactor to form a leak proof space between the distributor plate and the cone.

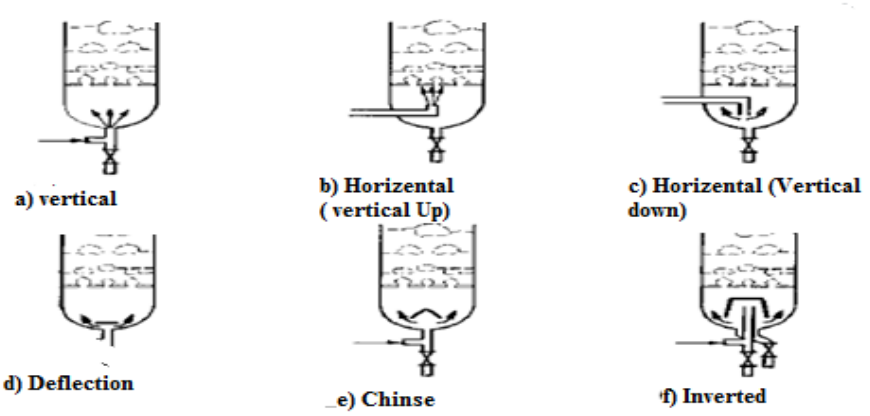

Fig. 4.4: Types of plenum configurations

4.5 Designing the Heating System

The fluidized bed fast pyrolysis reactor requires substantial flows of the fluidizing gas to achieve fluidization of silica sands and biomass for rapid heat transfer. Continuous supply of pre-heated gas at the reaction temperature is essential for a sustainable fast pyrolysis reaction. In the gas preheating chamber, the carrier gas which enters the system through the gas plenum is rapidly heated from room temperature up to the reaction temperature before entering the reactor.

The preheated gas enters the fluidized bed reactor through single perforated gas distributors. The fluidizing sand particles are rapidly heated in the reactor by the gas. With the bed expansion and rapid mixing of the fluidization, these solid particles spread heat uniformly in the reactor.

The biomass particles are then introduced into the dense phase of the fluidized bed reactor in order to gain solid-solid conductive heat transfer from sand, which assists to achieve rapid fast pyrolysis reaction. The pyrolysis reaction, with endothermic nature, rapidly absorbs heat from the reactor to break the chemical chains and decompose the biomass particles.

Consequently, auxiliary heat should be supplied to the reactor to prevent the temperature to drop below the reaction temperature; otherwise, the pyrolysis reaction will stop until the reactor temperature increase again above the reaction temperature. For steady reaction, therefore, the reactor is equipped with external heater to supply auxiliary heat in order to maintain the reactor temperature within the desired range.

Rapid heat transfer is achieved from the heated reactor wall to the fluidizing solids and eventually to the biomass particles which continuously fed into the reactor. The reactor temperature is then closely regulated by the control system to balance heat consumed and the auxiliary heat supplied so that continuous pyrolysis reaction is sustained throughout the desired operation duration. The heating system consists of electrical resistors wrapped around cylinders. These electrical resistors provide the necessary heat for endothermic reactions of pyrolysis. Additional insulation material was also added along the surface to decrease heat losses. The basic design parameters of the gas pre-heating chamber are given in table 4.3.

Table 4.3: Design data for Gas pre-heating chamber

Gas properties	
Working gas	Compressed air at 5 bar
Maximum inlet gas flow rate	250 l/min (specified)
Gas properties at inlet temperature, T_{n1} = 40℃	
(due to friction and heat transfer)	
Gas density, ρ_g	6.4126 kg/m^3
Specific heat capacity, C_p	1.02486 kJ/kgK
Dynamic viscosity, μ_g	1.85×10^{-5} kg/ms
Thermal conductivity, k_g	0.02682 W/mk
Prandtl number, Pr	0.708
Gas properties at exit, T_{n2} = 500℃	
Gas density, ρ_g	2.5965 kg/m^3
Specific heat capacity, C_p	1.0958 kJ/kgK
Dynamic viscosity, μ_g	3.597×10^{-5} kg/ms
Thermal conductivity, k_g	0.05609 W/mk
Prandtl number, Pr	0.703
❖ **Average Temperature in the pre-heating chamber, $T_{n\ avg}$**	
$T_{n,avg} = (T_{n2} + T_{n1}) / 2$	
$= (500 + 40) / 2$	
$= 270$ ℃	

Gas properties at average temperature, $T_{n\ avg}$ = 270℃	
Gas density, ρ_g	3.6964 kg/m^3
Specific heat capacity, C_p	1.06035 kJ/kgK
Dynamic viscosity, μ_g	2.725 $\times 10^{-5}$ kg/ms
Thermal conductivity, k_g	0.04145 W/mk
Prandtl number, Pr	0.697
Pre-heater geometrical dimensions	
Type	Fluidized bed
Material	Mild steel
Inner Diameter, Di	0.145 m
Outer diameter, Do	0.149 m
Thermal conductivity, k_s	43.0 W/m℃
Specific heat capacity, Cps	0.473 kJ/kg℃
Melting point, TM	1498.89 ℃
External insulation material	Gypsum
Density, ρ_{ins}	32 kg/m3
Thermal conductivity, k_{ins}	0.03 W/m℃
Thickness, t_{ins}	10 mm

4.5.1 Heating Power Requirement

- **Calculate heating energy required to increase the temperatures of air from room temperature to reaction temperature.**

The heating capacity of the gas preheating chamber is designed based on the power required to heat the fluidizing gas from room temperature to the reaction temperature. The mass flow rate of the gas is constant throughout the gas preheating chamber. Therefore, it can be calculated as the product of

the volumetric flow rate, Q_{n1}, and the gas density, ρ_{n1}, at inlet point where the temperature is 40℃. For the maximum gas flow rate allowable at the inlet point is 250 l/min (0.004167 m^3/s), the corresponding mass flow rate is,

$$m_n = \rho_{n1} \times Q_{n1} \tag{4.15}$$

$$m_n = 6.4126 \times 0.004167$$

$$m_n = 0.02672\,\text{kg/s}$$

By neglecting heat loss to the atmosphere, the heating energy required, q, can be estimated by using the gas properties given in Appendix, at average temperature in gas preheating chamber, $T_{n,\,avg}$ = 270 ℃, with the following equation,

$$q = m_n \times C_{pn,avg}\,(T_{n2} - T_{n1)} \tag{4.16}$$

$$q = 0.0267 \times 1060.35(500 - 40)$$

$$q = 13032\ \text{W}$$

4.5.2 Heating Unit of the Gas Pre-Heating Chamber

The power source of the gas pre-heating chamber is electrical heater. An electric heater is an electrical appliance that converts electrical energy into heat. The heating element inside every electric heater is simply an electrical resistor, and works on the principle of Joule heating; an electric current through a resistor converts electrical energy into heat energy. This electrical power is converted to heat energy using an electric resistance wire inserted on the backside of the grooved cylindrical pre-heater shelled by gypsum. Mathematically the power dissipated in an electric resistance wire can be expressed as:

$$P = VI = \frac{V^2}{R} \tag{4.17}$$

Where: V -the voltage (potential difference) from the supply line and R -resistance of the heating coil /wire/, I- nominal current.

The resistance coil materials in general used for electrical resistance heating are commonly made of Nickel-Chromium alloys. The resistance of the coil is directly proportional to its length and inversely proportional to its area, that is:

$$R \propto \frac{L}{A} = R = \rho_r \frac{L}{A} \tag{4.18}$$

Where ρ_r = resistivity is the proportional constant
From the power equation:

$$P = VI = \frac{V^2}{R} = \frac{(IR)^2}{R} = I^2 R = \frac{I^2 \rho_r L}{A} \tag{4.19}$$

As we see from the above equation, the power consumption is directly proportional to the length of the resistance wire. The stretched length of the resistance coil generally varies from 10 m to 12 m depending on the power needed. According to the calculation the minimum power required to heat the gas is around 12 kW. Due to this four resistors having a resistance of 15 Ohm each were winding around the pre-heater. The four resistors are connected in parallel to a 220 V one phase power supply. The detailed constructional characteristics of the electrical resistors used are shown below in table 4.4.

Table 4.4: Construction characteristics of electrical resistors

Wire diameter	1mm
Outer Diameter	6 mm
Stretched length	1200 mm
Nominal Power	3000 (each)
Voltage	220 V
Current	29.5 A
Maximum operating temperature	500 ^{0}c

a)

b)

Figure 4.5: Electrical heating coil samples when (un stretched and (b) stretched

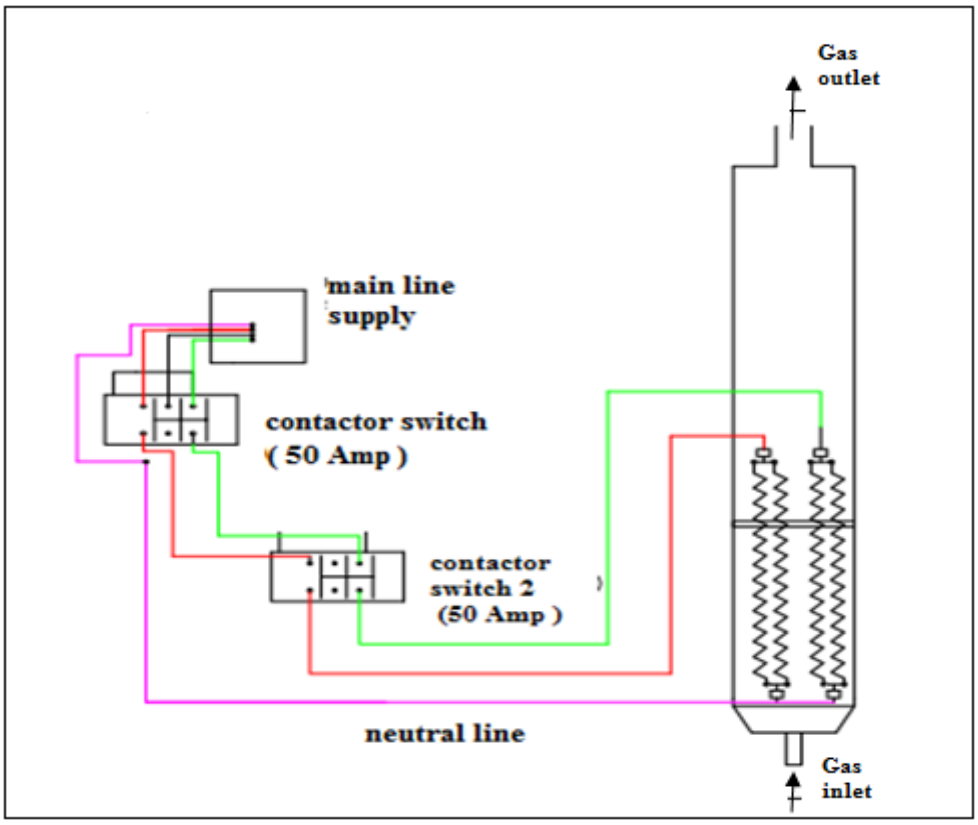

Fig 4.6 Electrical layout of 12 kW heaters installed to reactor and gas pre-heating chamber

- **Estimating overall heat transfer coefficient for gas preheating *chamber***

The overall heat transfer coefficient of the gas was evaluated from the flow regime of the gas in the gas preheating chamber by taking gas properties at average temperature, $T_{n,avg}$ = (40 +500)/2 = 270℃ . The average gas velocity is thus,

$$U_o = \frac{Q_{n,avg}}{A} \tag{4.20}$$

$$U_o = \frac{4 \times 0.0109935}{\pi \times 0.145^2}$$

$$U_o = 0.66 \text{ m/s}$$

From the properties of the gas, the Reynolds number of gas flow at the out let is,

$$R_{ed} = \frac{\rho_g \times U_o \times D_i}{\mu_g} \tag{4.21}$$

$$R_{ed} = \frac{3.694 \times 0.66 \times 0.145}{2.75 \times 10^{-5}} \qquad R_{ed} = 12967.08 > 2500$$

Since, turbulent flow is encountered; Nusselt number of the flow can be calculated by using the following equation.

$$N_{ud} = \frac{h_i D_i}{k} \tag{4.22}$$

$$N_{ud} = 0.023\, R_{ed}^{\ 0.28}\, \mathrm{Pr}^{n} \tag{4.23}$$

Where (n =0.4, for heating of gas)

$$N_{ud} = 0.023 \times 12967.08^{0.8} \times 0.697^{0.4}$$

$$N_{ud} = 38.84$$

Thus, the heat transfer coefficient of the gas inside the gas preheating chamber, h_i, is obtained by solving equation 13, where

$$N_{ud} = \frac{h_i D_i}{k}$$

$$h_i = \frac{38.84 \times 0.04145}{0.145} = 11.10 \frac{W}{m^2 k}$$

This value is considerably low to meet the rapid heat transfer requirement. However, heat transfer coefficient for gas heating is low since it is relying solely to convective heat transfer mechanism. The heat transfer coefficient can be significantly improved by using a fluidized bed gas preheating chamber rather than an empty gas preheating chamber. With rapid mixing of silica sand in the fluidized, bed heat is transmitted rapidly from heated wall to silica sands and from silica sands to carrier gas.

Therefore, the heating mechanisms in the chamber is changed towards solid-solid and solid-gas convective heat transfer.With the combination of conductive and convective heat transfer mechanisms of the fluidized bed gas preheating chamber, the overall heat transfer coefficient can be significantly improved.

As suggested by Botterill (1975), the gas convective heat transfer contribution to the fluidized bed can be estimated using the experimental correlation developed by Baskarov and Suprun in 1972. The heat h_{gc} , can be estimated using following transfer coefficient of the fluidized bed, equation,

$$h_{gc} = \frac{0.0175\, Ar^{0.46}\, \mathrm{Pr}^{0.33}\, k}{d_p} \tag{4.24}$$

The Archimedes number, Ar, is given by,

$$A_r = \frac{\rho_g \times {d_p}^3 \times (\rho_p - \rho_g) \times g}{{\mu_g}^2}$$

$$A_r = \frac{3.694 \times (450 \times 10^{-6})^3 \times (1500 - 3.694) \times 9.81}{(2.725 \times 10^{-5})^2}$$

$$A_r = 6654.12$$

Nusselt's number of the fluidized bed heat transfer when the working velocity is higher than minimum fluidizing velocity is given by two equations as follows,

$$N_{u,gc} = \frac{h_{gc} \times d_p}{k} \tag{4.25}$$

$$N_{u,gc} = 0.0175\, Ar^{0.46}\, \mathrm{Pr}^{0.33} \tag{4.26}$$

By solving equations (5.25) and (5.26) the fluidized bed heat transfer coefficient, $h_{gc,}$ can be obtained by,

$$\frac{h_{gc} \times d_p}{k} = 0.0175 Ar^{0.46}\, \mathrm{Pr}^{0.33}$$

$$h_{gc} = \frac{0.0175 Ar^{0.46}\, \mathrm{Pr}^{0.33}\, k}{d_p}$$

$$h_{gc} = \frac{0.0175 \times 296760^{0.46} \times 0.693^{0.33} \times 0.04145}{2.2 \times 10^{-3}}$$

$$h_{gc} = 33.37\ \mathrm{W/m^2K}$$

Therefore, it was found that more than 80% times improvement of heat transfer co-efficient can be achieved by using fluidized gas preheating chamber with 33.37 W/m^{2}K compared to the heating of gas in empty cylinder with 1.95 W/m^{2}K.

The overall heat transfer coefficient of gas preheating chamber, can be determined with following equation,

$$U_o = \frac{1}{\frac{A_o \ln\left(D_{ro}/D_{ri}\right)}{2\pi k_s L} + \frac{1}{f h_{gc}}} \tag{4.27}$$

In this gas preheating chamber with three passes, f is assumed as 3 according to the correlation suggested by Gupta (1986).

$$U_o = \frac{1}{\frac{\pi D_{or} L \ln\left(D_{ro}/D_{ri}\right)}{2\pi k_s L} + \frac{1}{3h_{gc}}} \tag{4.28}$$

$$U_o = \frac{1}{\frac{D_{or} \ln\left(D_{ro}/D_{ri}\right)}{2k_s} + \frac{1}{3h_{gc}}} \tag{4.29}$$

$$U_o = \frac{1}{\frac{0.149 \ln\left(0.149/0.145\right)}{2\times 36} + \frac{1}{3\times 33.7}} = 100.5 \text{ W/m}^2$$

- **Estimate the maximum wall temperature of gas preheating chamber**

The carrier gas entering the gas preheating chamber as cold gas is heated as it moves along the chamber from bottom to top through 3 vertical passes. Heat is transferred from the heater to the gas through the cylindrical vessel due to the temperature gradient created from the heater to the heated wall and eventually to the carrier gas. Therefore, the wall temperature at a specific point along the chamber, T w=x, is always higher than the fluidizing gas temperature at this point, T n=x. The temperature different is depending on the heating density and heat transfer coefficient of the system.

Consider that this system is designed to increase the carrier gas temperature to 500 °C before it leaves the chamber. Therefore, it is required to calculate the wall temperature at this point in order to ensure the maximum wall temperature required to create the temperature gradient is not exceeding the service temperature of the material.

From the energy balance from the heater to the gas,

$$q = U_o A_o \left(T_{w=x} - T_{n=x}\right) \tag{4.30}$$

Rearrange equation, the wall temperature corresponding to the gas temperature is obtained. The minimum heat required, q, is 13000 W correspond to a heating length, L, of 0.55 m. Therefore, by taking the consideration of actual fabrication, a three stage heaters with total 1300 W is installed to the gas preheating chamber with the 0.55 m in length.

$$T_{w=x} = \frac{q}{U_o A_o} + T_{n=x} \tag{4.31}$$

$$T_{w=x} = \frac{13000W}{100.5 \times \pi \times 0.149 \times 0.55} + T_{n=x}$$

$$T_{w=x} = 502.43 + T_{n=x}$$

It is found that the wall temperature is 502.43℃ above the gas temperature to achieve the temperature gradient required for heat transfer from the heater to the carrier gas.

4.6 The Feed Hopper

The feed hopper is used as the storage for the biomass feedstock. In order to provide a good mixing and to prevent blocking, a rotating screw is employed. There are two primary and distinct types of flow of solids in hoppers, mass flow and funnel flow. In mass flow all of the material in the hopper is in motion, though not necessarily all with the same velocity. In funnel flow only a core of material in the center above the hopper outlet is in motion while material next to the walls is stationary (stagnant). A wedge type hopper is selected due to its more consistent of flow, reduction of reduction of radial segregation over conical hopper.

4.7 Designing the Screw Feeder

In any process the taking of a feed stock at atmospheric pressure and passing it into a pressurized rector imposes complexity and loss of efficiency. A screw feeder is a dependable, controllable low rate feeder and is a good option for this purpose, because it offers one directional feed with variable feed rate. A screw feeder is mounted directly under opening of the hopper. The feed stock in the silo rests on a part of the screw, and the screw flights are filled completely. The flow rate of a screw

feeder depends on a number of interlinked factors such as; geometry of the screw, rotating speed, inclination, geometry of the feed hopper and tube and flowablity of the feed material.

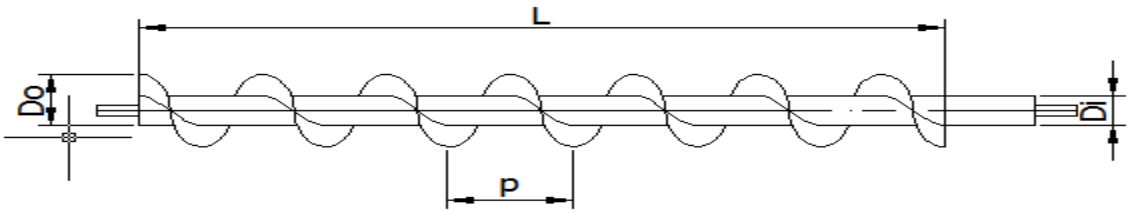

Fig 4.7: Single flight-standard pitch type screw feeder

For this design I have used a screw thread having a constant flight diameter, constant diameter of the central screw shaft core, and constant pitch.

Table 4.5. Design parameters and range of screw feeder

Parameters	Dimension	Design range
Nominal screw diameter, D(mm)	52.5	28.8 – 76.2
Core shaft diameter, D_i (mm)	22.5	12.34 – 32.657
Screw pitch, p (mm)	1.15 D	0.7 D – 1.5 D Single Flight-Standard Pitch type, where conveyor flights are frequently required for smooth conveying and discharge of common materials.
Screw rotation per minute, n	120 RPM	60 – 125 RPM
Conveyor Length, L (mm)	393	Fixed

The mass conveying capacity of a screw conveyor can be determined using the method given by British Standard BS 4409. In operation of a screw conveyor with specific diameter, D, the volumetric feed rate of the bulk solids, Q_V is known as the product of the working section of the screw conveyor, A, and the linear speed of material movement, v. The working section, A, and linear speed, v, can be respectively expressed as,

$$A = \lambda\left(\frac{\pi}{4}D^2\right) \tag{4.32}$$

$$v = p\frac{n}{60} \tag{4.33}$$

Where:

D = nominal screw diameter (m)

p = screw pitch (m)

n = screw rotation per minute (rpm)

λ = trough filling coefficient (dimension less), a value of 0.3 for coffee husk

Thus, the volumetric feed rate can be determined by working out as follows,

Volumetric feed rate of coffee husk is estimated as,

$$Q_V = A \times v \tag{4.34}$$

$$Q_V = \frac{\lambda \pi D^2 pn}{240} \tag{4.35}$$

Considered that the volumetric feed rate is more commonly expressed in m^3/h, thus, to covert the unit into m^3/h, the equation is multiplied by 3600, thus,

$$Q_V = 15\lambda \pi D^2 pn \tag{4.36}$$

In the operation involving with bulk solid such as coffee husk, feeding capacity is more often expressed in mass feed rate rather than volumetric feed rate. The screw conveyor capacity, Q_M at a specific shaft speed, n, can be determined by multiplying its volumetric feed rate with bulk density of coffee husk, ρ_b, thus,

$$Q_M = \rho_b \times Q_V \tag{4.37}$$

$$Q_M = 15\rho_b \lambda \pi D^2 pn \tag{4.38}$$

By inserting the design data and variables into Equation (4.32), the feeding rate of coffee husk with screw diameter of 0.0525 m at shaft speed 25 rpm is,

$$Q_M = 15 \times 196 \times 0.3 \times \pi \times 0.0525^2 \times 1.15 \times 0.0525 \times 25$$

$$Q_M = 11.53 \text{ kg/h}$$

The fillet height, h, of the screw is expressed as,

$$h = \frac{D - D_i}{2} \qquad 4.39$$

$$h = \frac{0.0525 - 0.0225}{2}$$

$h = 0.015$ m`

4.8 Designing the Cyclone

Cyclone separators are widely used as a collection device in bubbling fluidized bed systems to separate the unburned fuel from the condensable gases. Cyclone employs a centrifugal force to separate particulates from a gas stream. It is a relatively an inexpensive collector both in construction and operating costs.

The basic separation principle of cyclone is relatively simple. Particles enter the cyclone with the flowing gas. The gas stream enters tangentially at the top of the barrel and travels downward into the cone forming an outer vortex. The increasing gas velocity in the outer vortex results in a centrifugal force on the particles separating them from the gas stream. When the gas reaches the bottom of the cone, an inner vortex is created reversing direction and exiting out the top as clean gas while the particulates fall into the dust collection chamber attached to the bottom of the cyclone.

There are four major parts to a cyclone: the inlet, the cyclone body, gas outlet, and cone. Each part affects the overall efficiency of the cyclone.

- **Cyclone Inlet**

The cyclone inlet accelerates the gas in the cyclone to attain the required tangential velocity. The shape of the inlet assists the transformation of the incoming gas from a linear flow to a circular vortex pattern. The gas is then accelerated and combined with the already rotating gas in the cyclone. The pressure drop is increased, and more power is required to move the gas through the system. Inlet length and width are also important. As the inlet is made smaller, the inlet velocity increases. This gives higher removal efficiency at the expense of added pressure drop. A poorly designed inlet will create turbulence, which will ultimately decelerate the tangential gas velocity and in turn lead to the development of the flow eddies at the inlet. So the pressure drop will increase substantially and collection efficiency will decrease.

- **Cyclone Body and Cone**

The removal efficiency of a cyclone for a given particle size depends on cyclone dimensions. The diameter of the cyclone has a large effect on the pressure drop for a given volumetric flow rate. The overall length determines the number of turns of the vortex; as the number of turns increase, the removal efficiency increases.

The motion of a gas in a cyclone is not simple. Two vortices are formed – one descending and the other ascending. The descending vortex often is called the main vortex. For a properly designed cyclone, the vortex will change direction at the bottom of the cone and start ascending. This ascending vortex is smaller in radius with faster tangential velocities than the descending vortex.

The cone primarily serves as a mechanism for removing particulate matter from the walls of the cyclone and sending it to the hopper. However, the vortex formed in a cyclone sometimes deviates from the vertical axis. Because of this, it has been found that bottom of the cone should have a diameter of at least ~ ¼ th of the cyclone diameter. Otherwise, the outer vortex may touch the cone wall entraining already captured particles in the ascending vortex.

- **Dust Discharge System**

If the discharge bin is immediately below the cone and nothing is added to the bottom of the cone to arrest the vortex, the vortex will extend into the discharge bin. Dust can be re-entrained from the hopper into the vortex. If leaks exist in the bin, dust can be sucked back up into the cyclone. In general, any kind of ash removal system is attached to the bottom of the cone to avoid particulate re-entrainment.

4.8.1 Sizing the Cyclone

Design of the cyclone for bubbling fluidized bed reactor requires the establishment of a specific gas flow rate and inlet gas velocity, V_g of the cyclone. Classical cyclone design equations of Lappel and Shephered (1951) were used for determining of the cyclone geometric specifications as sown in Fig 4.6.

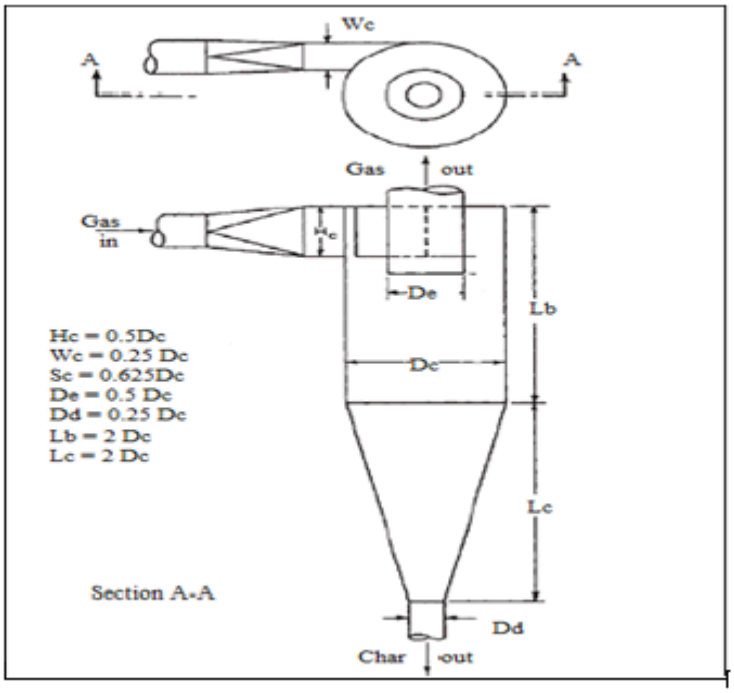

Figure 4.8: Standard Cyclone Dimensions (Pell, 1997)

In operating conditions, compressed gas enters the plenum at 20°C with flow rate of 250 l/min (0.0041667 m^3/s), and leaves the reactor at 500°C. Consider the constant mass flow rate throughout the system,

$$m_0 = m_c \tag{4.40}$$

In the flow with constant mass flow, volumetric flow rate of two points in a system can be calculated by the following equation,

$$\rho_{g,0} \times Q_{g,0} = \rho_{g,c} \times Q_{g,c} \tag{4.41}$$

Thus, the gas flow rate in the cyclone, $Q_{g,c}$ is

$$Q_{g,c} = \frac{\rho_{g,0} \times Q_{g,0}}{\rho_{g,c}}$$

$$Q_{g,c} = \frac{12.79 \times 0.0041667}{4.85}$$

$$Q_{g,c} = 0.0109935\ m^3/s$$

According to Lappel (1991), gas flow rate of the cyclone is determined from the width, W_c and height, H_c of the cyclone inlet;

$$Q_{g,c} = V_g \times A_{c,inlet} \tag{4.42}$$

Where:

$$A_{c,inlet} = H_c \times W_c$$

Substitute the relation of cyclone inlet width and height with cyclone diameter, D_c from fig 4.6,

$$A_{c,inlet} = 0.5D_c \times 0.25D_c = 0.125\,D_c^{\,2}$$

Substitute $A_{c,inlet}$ in Equation (5.36)

$$Q_{g,c} = V_g \times 0.125\,D_c^{\,2}$$

Solving for, D_c

$$D_c = \sqrt{\frac{8 \times Q_{g,c}}{V_g}} \tag{4.43}$$

$$D_c = \sqrt{\frac{8 \times 0.0109935}{4.5}}$$

$$D_c = 139.8mm$$

From Fig. 4.6, the other geometrical dimensions of the cyclone could be determined as follows,

$H_c = 0.5 \times 139.8 = 69.9mm$ $\quad$ $W_c = 0.25 \times 139.8 = 34.95mm$

$S_c = 0.625 \times 139.8 = 87.375mm$ $\quad$ $D_e = 0.5 \times 139.8 = 69.9mm$

$D_d = 0.25 \times 139.8 = 34.95mm$ $\quad$ $L_b = 2 \times 139.8 = 279.6mm$

$L_c = 2 \times 139.8 = 279.6mm$

4.8.2 Number of Effective Turns, N_e

The number of effective turns in a cyclone is the number of revolutions the gas spins while passing through the cyclone outer vortex. A higher number of turns of the air stream result in a higher collection efficiency. The Lapple model for N_e calculation is as follows:

$$N_e = \frac{1}{H_c}\left(L_b + \frac{L_c}{2}\right) \tag{4.44}$$

$$N_e = \frac{1}{69.9}\left(279.6 + \frac{279.6}{2}\right)$$

$$N_e = 6$$

The gas residence time in the outer vortex, Δt

$$\Delta t = path\ length\ /speed \tag{4.45}$$

$$\Delta t = \frac{\pi D_c N_e}{V_g}$$

$$\Delta t = \frac{\pi \times 0.1398 \times 6}{4.5}$$

$$\Delta t = 0.586 \text{ Sec}$$

4.8.3 Cut size or Cut Diameter, d_{50}

The cut-point of a cyclone is the aerodynamic equivalent diameter (AED) of the particle collected with 50% efficiency. As the cut-point diameter increases, the collection efficiency decreases. The particles sizes larger than the cut size were collected by cyclone more than 50%. The Lapple cut-point model was developed based upon force balance theory.

The Lapple model for cut-point (d_{50}) is based on the performance of cyclone with the ratio of d_p/d_{50}>10 as shown in Figure 4.7.

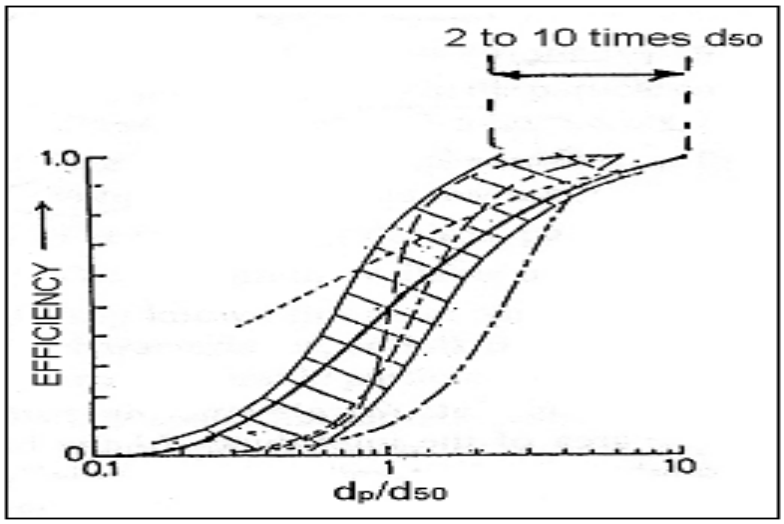

Fig 4.9: Cyclone fractional efficiency curves (Zenz, 1999)

.

Calculating the cut size using equation is as follows,

$$d_{p50} = \left[\frac{9\mu_g W_c}{2\pi N_e (\rho_{char} - \rho_g) V_g} \right]^{1/2} \tag{4.46}$$

`

$$d_{p50} = \left[\frac{9 \times 3.599 \times 10^{-5} \times 0.03495}{2\pi \times 6 \times (117 - 4.85) \times 4.5}\right]^{1/2}$$

$$d_{p50} = 0.00000244\,m$$

$$d_{p50} = 0.244\,\mu m$$

Where $\mu_g =$ viscosity of the gas (kg/ms)

$N_e =$ Effective number of turns

$V_g =$ Velocity of gas inlet (m/s)

$\rho_p =$ Density of particles (kg/m^3)

$W_c =$ Width of cyclone inlet (m)

Thus, $d_p/d_{50} > 10$, based on the calculation results, the char particles larger than 2.44μm could be efficiently separated from the vapors stream in the cyclone.

4.8.4 Cyclone Collection Efficiency

In general, cyclone collection efficiency varies with the char particle density and particle size, the area of the cyclone inlet velocity, cyclone body length, number of gas stream revolutions and ratio of cyclone body diameter to out let diameter. The collection efficiency varies inversely as the gas density, gas out let diameter, gas inlet duct width and inlet area increases. The collection efficiency of the cyclone depends on various factors.

The cyclone efficiency will increase when various factors increased such as,

- Size of the particles
- Density of the particles
- Velocity of the gas
- Length of the cyclone body
- Number of turns and smoothness of cyclone wall

The cyclone efficiency will decrease when some factors increase;

- Viscosity of gas
- Cyclone diameter
- Gas out let diameter
- Area of gas inlet

The overall collection efficiency, η_T of the cyclone is determined by:

$$\eta_T = \sum m_i \eta_i \qquad (4.47)$$

4.9 Condensation System

In fast pyrolysis system, rapid condensation of pyrolysis vapors is a decisive stage for bio-oil production. The time and temperature profile between the formation of pyrolysis vapors and condensation will influence the composition and quality of the bio-oil products. Secondary cracking reactions will take place to further decompose the valuable liquid components when the pyrolysis vapors remain in high temperature. The longer the vapors remain at high temperatures, the greater the extent of secondary cracking reactions. Therefore, freezing of these reaction are essential to recover the liquid components in the vapours.

Condensation of liquid components occurs when the vapors are cooled below its saturation temperature, such as when it comes into contact with a cold surface (Gupta, 1986). Due to the diversify nature of various chemical compounds in pyrolysis vapors, the bio-oils condense over a wide range of temperature. As the pyrolysis vapors rapidly cool down in the condenser, heavier chemical compounds with higher saturation temperatures will condense before those lighter chemical compounds.

Some organic and gaseous components in the vapors have the saturation temperatures lower than room temperature. These components are considered as non-condensable gases, which could not settle in condenser, and thus, they will be released to atmosphere through the exhaust pipe.

CHAPTER FIVE

MANUFACTURING PROCEDURE AND PRODUCTION COST

5.1 Manufacturing Procedure

The manufacturing process was performed using the design and the production drawings. Considering the practical aspects like the availability of raw material in the market, the cost of manufacturing, ease of the manufacturing process, skill of technician and machines in the workshop and taking into consideration other necessary factors.

The components of the system that were manufactured are listed below;

- The reaction chamber
- Plenum
- Gas preheating chamber
- Distributor plate
- Feed hopper
- Cyclone body
- Cyclone cone
- Cyclone inlet
- Supporting legs (frame)

The other components are selected and purchased based on the design analysis from the local market considering their availability and cost.

To manufacture these components we have used the following machines and tools in the workshop.

i. Sheet metal cutting or shearing machine
ii. Bending machine
iii. Drilling machine
iv. Lathe machine
v. Arc welding machine
vi. Rolling machine
vii. Power hack saw
viii. Grinding machine

ix. Metering and marking tools (e.g. Center punch, scriber)

- **Reactor (reaction chamber)**

The reaction chamber was a cylindrical vessel having 149 mm external diameter and 1500 mm length; and it is a place where rapid thermal decomposition of feed stock takes place. Make the development of the cylinder by calculating its circumference using, C = πD_{ro} = $\pi \times 149\ mm = 468.09\ mm$, where, D_{ro} is reactor outer diameter.

Material: milled steel

Procedures:

i. Prepare a 2 mm thick milled steel plate.
ii. Measure and mark the development of the cylinder (1500 mm x 468.09 mm) on the plate using meter and scriber for dimension measurement and for marking respectively.
iii. Then, cut the plate along the marking lines carefully using cutting machine.
iv. Roll the developed cut plate in a rolling machine along its circumference.
v. Weld evenly the sides of the rolled cylinder and make sure that the welding quality is good to prevent the problem of leakage.
vi. Draw a circle with a diameter of 149 mm using divider and cut out the circle using circle cutter machine. Draw another 57 mm diameter circle and bore it on the 149 mm diameter disc which is served as gas out let.
vii. Finally, cover the upper base of the cylinder by the 149 mm diameter cut plate and then weld finely.

- **Gas pre-heating chamber**

It is a cylindrical type pre-heating chamber where the fluidizing gas is pre-heated before entering the reaction chamber. It has an outer diameter of 149 mm and 500 mm length. It has the same manufacturing procedures with that of reaction chamber.

Material: milled steel

Procedures:

i. Make the development of the cylinder by calculating its circumference using, C = πD_{pro} = $\pi \times 149\ mm = 468.09\ mm$, where, D_{pro} is gas pre-heater outer diameter.

ii. Prepare a 2 mm thick milled steel plate.
iii. Measure and mark the development of the cylinder (500 mm x 468.09 mm) on the plate using meter and scriber for dimension measurement and for marking respectively.
iv. Then, cut the plate along the marking lines carefully using cutting machine.
v. Roll the developed cut plate in a rolling machine along its circumference.
vi. Weld evenly the sides of the rolled cylinder and make sure that the welding quality is good to prevent the problem of leakage.

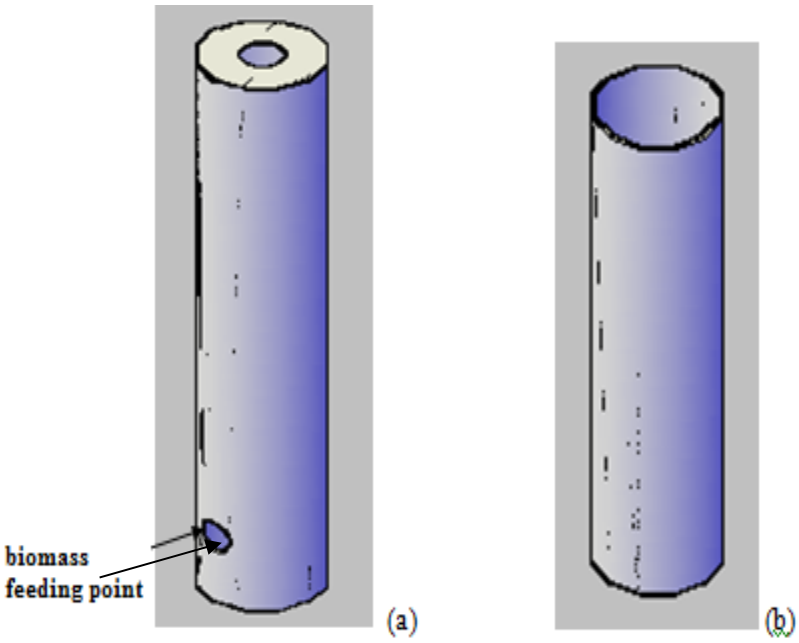

Fig 5.1 Reaction chamber (a) and gas pre-heating chamber (b)

- **Plenum**

It is a frustum of cone with nozzle at its base used to collect the fluidizing gas and pass it to the distributor plate.

Material: milled steel

Procedures:

i. Lay out the development of the frustum of cone. To do this, first calculate the hypotenuse (let Z) of the right full cone (which is 115.2 mm). The calculated value of the hypotenuse of the frustum is (let Y) 98.2 mm. The development of a right full cone, is simply a sector whose radius is equal

to the hypotenuse of the cone and whose arc length is equal to the circumference of the base of the cone.

The subtended angle of the cone is $\theta = \left(\frac{r}{z}\right) \times 360^0 = \left(\frac{74.5}{115.2}\right) \times 360^o = 232.2^0$

ii. Prepare 2 mm thickness milled steel
iii. Using a center punch, mark a point at available distance to find the center point (let O).
iv. With center at point O, draw two lines at a subtended angle 232.2°.
v. With center at point O, draw a circle at radius of, r = Z= 115.2 to find the circumference of the cone until it reaches the two lines.
vi. Again with center at point O, draw a circle at radius of, r = Y= 98.2 mm to find the circumference of the frustum cone.
vii. Carefully cut the development of the right full cone from the plate using cutting machine.
viii. Then, to make the cone frustum, cut the arc made by Y = 98.2 mm at a height of 12.9 mm.
ix. Finally, either manually using hammer or machine roll the cone and then weld the sides finely.

- **Gas Distributor Plate**

The gas plate was manufactured from a 2 mm thick milled steel plate having a diameter of 149 mm. The purpose of the gas distributor plate is to evenly distribute the fluidizing gas from gas pre-heating chamber to reaction chamber. The distributor plate has 226 nozzles (holes) arranged in a triangular pitch. The distance and the angle between the holes is 9.2 mm and 60°.

Material: milled steel

Procedures:

i. Prepare a 2 mm thickness milled steel.
ii. Using center punch marks a point anywhere in the plate, and then punches it by hammer that was used as a center point of the distributor plate.
iii. Use a divider to make a circle. Place one end of the divider at the center and the other end at radius, r = 74.5 mm. Then, rotate the divider clock wise or counter clock wise to make a full circle.
iv. Carefully cut out the circle from the plate using a circle cutter machine or plate cutting machine.

v. Divide the circle equally in to six parts or every 60°.
vi. Measure a distance of 9.2 mm along the 60° lines, then mark and punch using center punch to find the center of the holes. Continue this action until 226 numbers of holes.
vii. Finally, drill the 226 nozzles (holes) with a 2.2 mm drill bit diameter in a drilling machine.

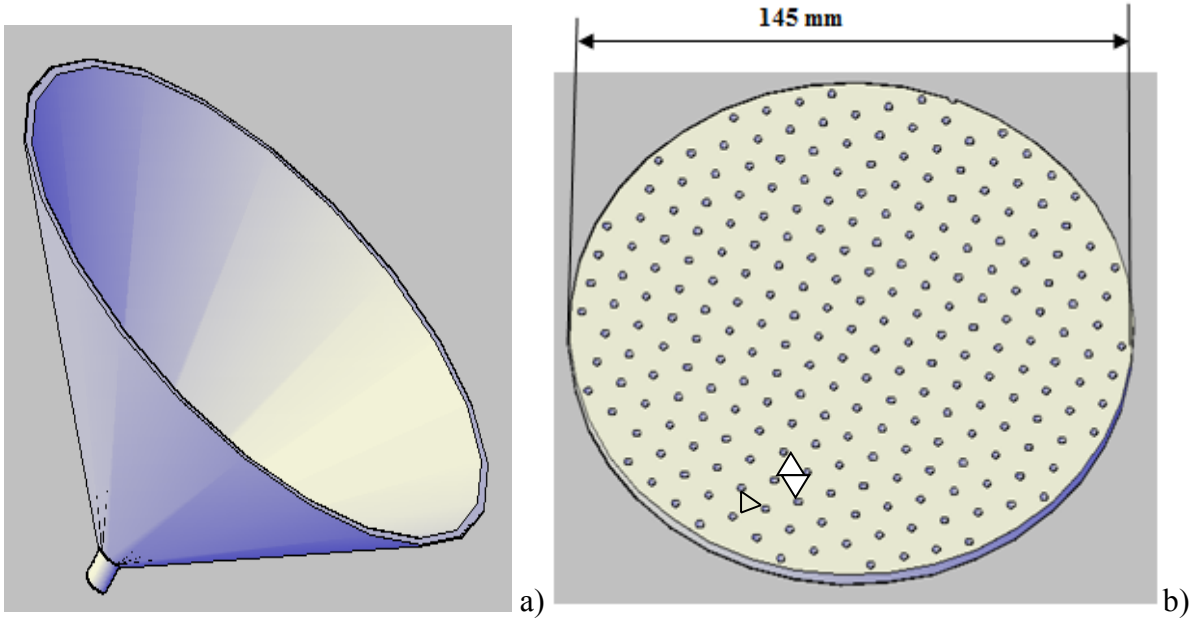

Fig 5.2 Plenum (a) and Gas distributor plate (b)

- **Cyclone body**

The cyclone body is always having a cylindrical shape. According to the design, the inner diameter and length of the cylinder (body) is 139.8 mm and 279.6 mm respectively. Make the development of the cylinder by calculating its circumference using, C = $\pi D_{oo} = \pi \times 143.8\,mm = 441.76\,mm$, where, D_{oo} is cyclone outer diameter.

Material: milled steel

Procedures:

i. Prepare a 2 mm thick milled steel plate.
ii. Measure and mark the development of the cylinder (279.6 mm x 441.76 mm) on the plate using meter and scriber for dimension measurement and for marking respectively.
iii. Then, cut the plate along the marking lines carefully using cutting machine.
iv. Roll the developed cut plate in a rolling machine along its circumference.

v. Weld evenly the sides of the rolled cylinder and make sure that the welding quality is good to prevent the problem of leakage.

viii. Draw a circle with a diameter of 143.8 mm using divider and cut out the circle using circle cutter machine. Draw another 73.9 mm diameter circle and bore it on the 143.8 mm diameter disc which is served as gas out let.

ix. Finally, cover the upper base of the cylinder by the 143.8 mm diameter cut plate and then weld finely to overcome leakage problem.

- **Cyclone Cone**

The cyclone cone primarily serves as a mechanism for removing particulate matter from the walls of the cyclone and sending it to the char (dust) collector. It is a frustum type cone made up of 2 mm thick milled steel. From the design calculation the outer diameter and length of the cone is 143.8 mm and 279.6mm. The outer diameter of the frustum is 38.94 mm.

Material: milled steel

Procedures:

Lay out the development of the frustum of cone. To do this, first calculate the hypotenuse (let Z) of the right full cone (which is 390.14 mm). The calculated value of the hypotenuse of the frustum is (let Y) 105.67 mm. The development of a right full cone, is simply a sector whose radius is equal to the hypotenuse of the cone and whose arc length is equal to the circumference of the base of the cone.

i. The subtended angle of the cone is $\theta = \left(\frac{r}{z}\right) \times 360^0 = \left(\frac{71.9}{390.12}\right) \times 360^o = 66.34^0$

ii. Prepare 2 mm thickness milled steel

iii. Using a center punch, mark a point at available distance to find the center point (let O).

iv. With center at point O, draw two lines at a subtended angle 66.34°.

v. With center at point O, draw a circle at radius of, r = Z= 390.14 to find the circumference of the cone until it reaches the two lines.

vi. Again with center at point O, draw a circle at radius of, r = Y= 105.67 mm to find the circumference of the frustum cone.

vii. Carefully cut the development of the right full cone from the plate using cutting machine.

viii. Then, to make the cone frustum, cut the arc made by Y = 105.67mm at a length of 104 mm.

ix. Finally, either manually using hammer or machine roll the cone and then weld the sides finely.

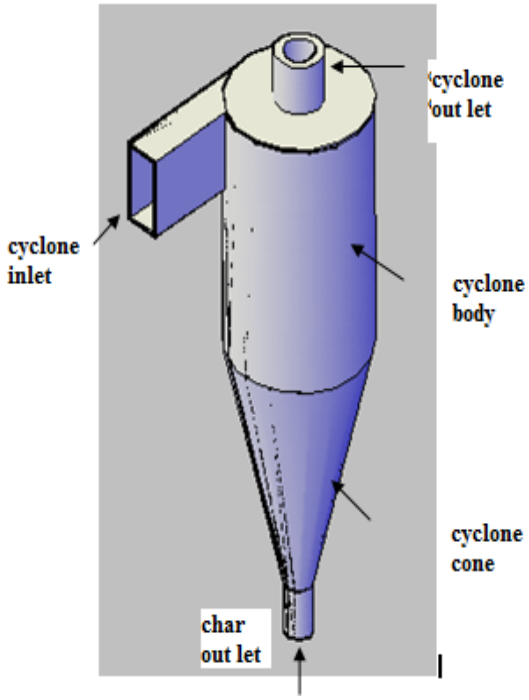

Fig 5.3 cyclone separator

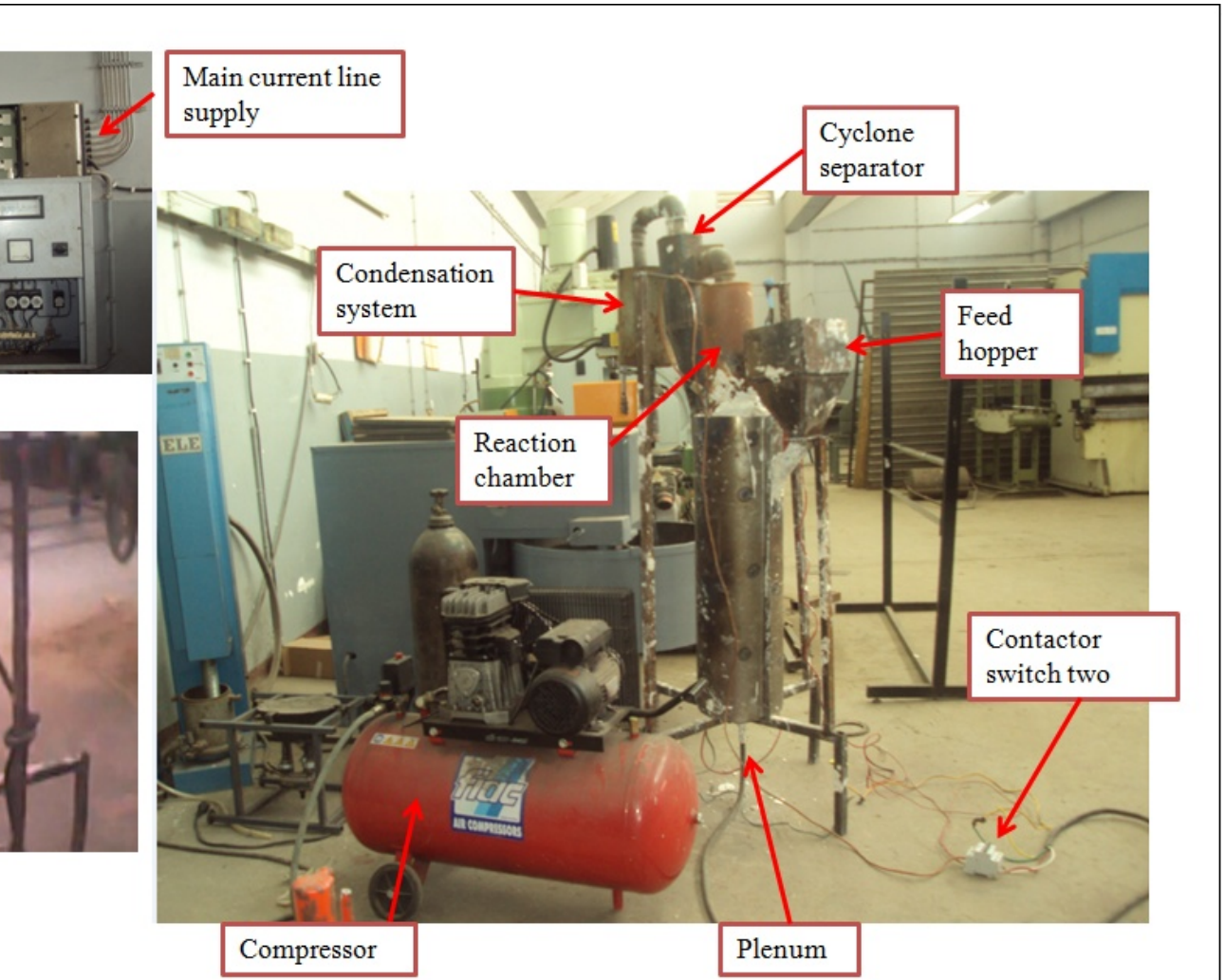
Main current line supply
Cyclone separator
Condensation system
Feed hopper
Reaction chamber
Contactor switch two
Compressor
Plenum

5.2 Production Cost

The production cost of the system is a function of equipment cost, labor cost, machine cost and time cost. In case of unbalancing marketing system in our country, for this condition I can't estimate the approach value of the construction cost. Then I attempt to describe the general way of the construction and material description unit and quantity and also some appropriate current cost.

- **Equipments Costs**

The equipment costs are cost of auxiliary equipments such as material costs, piping, insulation, electrical heater costs for nearly all equipment used in the manufacturing process. During construction of this fast pyrolysis system, I have used different materials for its auxiliary parts. Most of the reactor parts were manufactured from 2 mm thick mild steel plate; these parts includes reaction chamber, plenum and gas distributor plate, gas preheating chamber, cyclone separator, feed hopper and chilled water storage (condenser). To estimate the total equipments cost, it is necessary to know the cost of each material that were used in the manufacturing process and are provided in table 5.1.

- **Labor cost**

The system requires two skilled labors for cutting, rolling, grinding, welding, drilling, assembly, system installation and insulating. These processes took around 20 days. The price of the skilled labors for 8 hrs working per day was estimated to be 70 birr. Therefore,

Total labor cost = 2 workers*70 $birr/day$ *20 day= 2800 birr

- **Machine cost**

Welding, cutting, grinding, rolling and drilling machines are widely used for the work. The machine cost estimated for the above purposes were around 500 birr.

The production cost is the sum of all sub costs

Production cost =Material cost + Labor cost + Machine cost

Production cost = 3816.225 birr + 2800 birr + 1500 birr = 8116.225 birr

Table: 5.1: General description of equipment costs

No	Part Description	Material	Unit	Quantity	Price	
					Unit Price (Birr)	Total Price (Birr)
1	Feed hopper, Reactor, distributor plate, plenum, gas pre-heater. Cyclone and chilled water storage	Mild Steel, 2 mm thickness	2m x1m	2	650	1300
2	Gas inlet and out let line	G1 pipe	2.5 inch	1	400	400
		Elbow	2.5 inch	3	69.50	208.50
	Electrode	Arc	Φ=2.5mm	4 sets	60	240
	Frame (Stand)	20 x20 RHS	m	12 m	21	250
3	Heating system	Electrical Resistors	15 Ohm	5	86.20	431
	Insulation	Gypsum	kg	15	7	105
	Single phase Connectors	----------	--------	4	10	40
	Three phase Breaker	----------	50 A	1	500	500
	Electrical wire cables	Copper (Φ = 8mm)	m	20	8	160
Total Equipment Cost Contingency (5 %) **Grand Total Cost (Birr)**						3,634.50 1,817.25 **5,451.75**

CHAPTER SIX

FAST PYROLYSIS EXPERMENTAL SETUP

6.1 Introduction

A variety of organic solid wastes and agricultural biomass can be used as the feedstock for fast pyrolysis process. Coffee husk was selected as the primary feedstock for the system that has been developed. It is a preferred raw material among Ethiopia's biomass not only for its availability but also for its high contents of lingo-celluse compositions.

A bubbling fluidized bed rector was designed and developed in which heat is transferred to the pyrolysing biomass particles from the hot gases by convection and radiation. For conducting effective pyrolysis test, it was necessary to know the fuel characteristics, materials to be used and the operational procedures.

6.2 Equipments Required

The equipments required for testing of the fast pyrolysis are very sensitive ones. The equipments that are necessary for the different purposes are:

- Digital stopwatch, used to record the time of each of the different activities (i.e. reactor heating time, vapor residence time) during the tests.
- Gas analyzer equipment (Testo 350M/XL-testo 454, 110.230 V AC 50/60 Hz) to measure CO, H_2 , CH_4 , CO_2 and H_2O
- Digital thermometer indicator (range: 50℃ – 800℃) or a model of K-thermocouple thermometer for measuring reactor wall temperature.
- Gas Chromatography Mass Spectrum (GC-MS) Analysis in order to identify the individual compounds in the pyrolitic oil.

6.3 Test Procedures

- **Preparation of Feed Stock**

The biomass particles have to be processed into a uniform sizes to counter their poor thermal conductivity. Finer biomass particles in uniform sizes improve fluidization behavior and heat transfer co-efficient in a fluidized bed reactor in which the reactions are dictated by the vigorous

upward flowing and solid mixing actions. Then it should be dried and sized before loading into the reaction chamber.

The coffee husks used in this test were sun-dried for days with sizes ranging from 2 to 4 mm. The main characteristics of the coffee husk used as fuel in the experiments carried out in the pyrolysis reactor are presented in Table 6.1.

Table: 6.1 Composition of Solid Coffee Husk [30]

Elemental composition % wt (dry ash free)		**Proximate analysis % wt (air dry)**	
Carbon (C)	46.51	Volatile matter	76.6
Hydrogen (H)	6.77	Fixed carbon	15.5
Nitrogen (N)	0.43	Moisture content	7.22
Oxygen (O)	46.20	Ash content	0.68
Sulphur (S)	0.09		
Bulk density (kg/m^3)	136	LHV (MJ/kg)	16

- **Description of Operational Procedures**

The fast pyrolysis reactor set-up comprises the followings components, a feed vessel (hopper) with a chute pipe which replaces the screw feeder for feeding the coffee husk to the bottom of the reactor, fluidized bed reactor, gas pre-heater, solid –gas cyclone separator, liquid condenser and liquid collectors. Prior to each experiment, it is necessary to examine these systems are in a good condition. The following procedures are performed to prepare the system to be efficiently operated so that the data can be collected accurately.

I. Initially fill the compressor to its maximum capacity (10 bars) and connect its exhaust pipe to the entrance of the plenum.

II. Turned on the main power supply at the switch board. Then, switch on contactor switch 2 which supplies current to the electrical resistors.

III. Add iced or chilled water to the condenser vessel.

IV. When the temperature of the reactor reached in the range of 800 - 1000℃, turned on the compressor, adjust and slightly increase the flow rate. The temperature of the reactor wall and gas was measured by a thermocouple within the bed and the results were recorded at every minute.

V. When the temperature of the gas reaches 350 ℃ – 500 ℃ introduce the feed stock (coffee husk) to the hopper, and then was loaded by gravity at the bottom of the reactor. Heat is transferred to the coffee husk particles from the pre-heated fluidizing gas and bed material by convection and radiation respectively. The bed particles have an average sieve size of 2.16 mm. The coffee husk was then pyrolysed inside the externally heated 145 mm diameter and 1.2 m high milled steel fluidized bed reactor system to produce gases, water and condensable vapors.

VI. The occurring of pyrolysis reaction is detected when the color of the exhaust gas changed from light-gray smoke to thick white smoke. The vapor residence time is recorded as the time required from the start of feeding to the time of the gas color changed.

VII. The operation is carried out according to the operation time required. After that the system is turned off and cooled down by switching off the contactors switch 1 and 2 as shown in figure 4.6.

VIII. When the system is cooled down, the vapors and the gases were then passed through a water-cooled condenser. The liquid oil and the solid char were collected separately and the gas with the non-condensable vapors was flared. Then, the bio-oils are weighted, recorded and carefully kept in well sealed glass containers under room temperature. The char was separated from the condensable vapors and gases by means of cyclone separator. Chars are collected from the char collector and are also weighted and recorded before they are stored in sealed container.

IX. The bio-oils and char are calculated as the weight percents to the feed stock consumed. On the other hand, the gas yield is calculated as the difference of 100%. The gas composition is also measured by using gas chromatography.

CHAPTERTER SEVEN

RESULTS AND DISCUSSIONS

This section of this thesis discusses the experimental results obtained and the discussion of the results obtained.

7.1 Temperature Variation and Measurement on the gas pre-heating chamber wall

The gas pre-heating chamber was heated by four electrical resistors. Each two heaters were connected in parallel to give 6 kW each; the reactor wall temperature had increased gradually but the increasing rate was higher during initial heat up. The experimental test was conducted using K-type thermocouple on 12/10/2011, and the temperature readings were recorded in the computer.

Table: 7.1 Temperature readings obtained on the gas pre-heating chamber wall

Time	Temperature (°C)
09:04 AM	18.51
09:06 AM	95.5
09:08 AM	117.92
09:10 AM	186.18
09:13 AM	222.73
09:15 AM	282.05
09:17 AM	329.04
09:19 AM	347.63
09:21 AM	406.52
09:23 AM	453.76
09:25 AM	491.42
09:27 AM	532.50
09:29 AM	585.16
09:31 AM	630

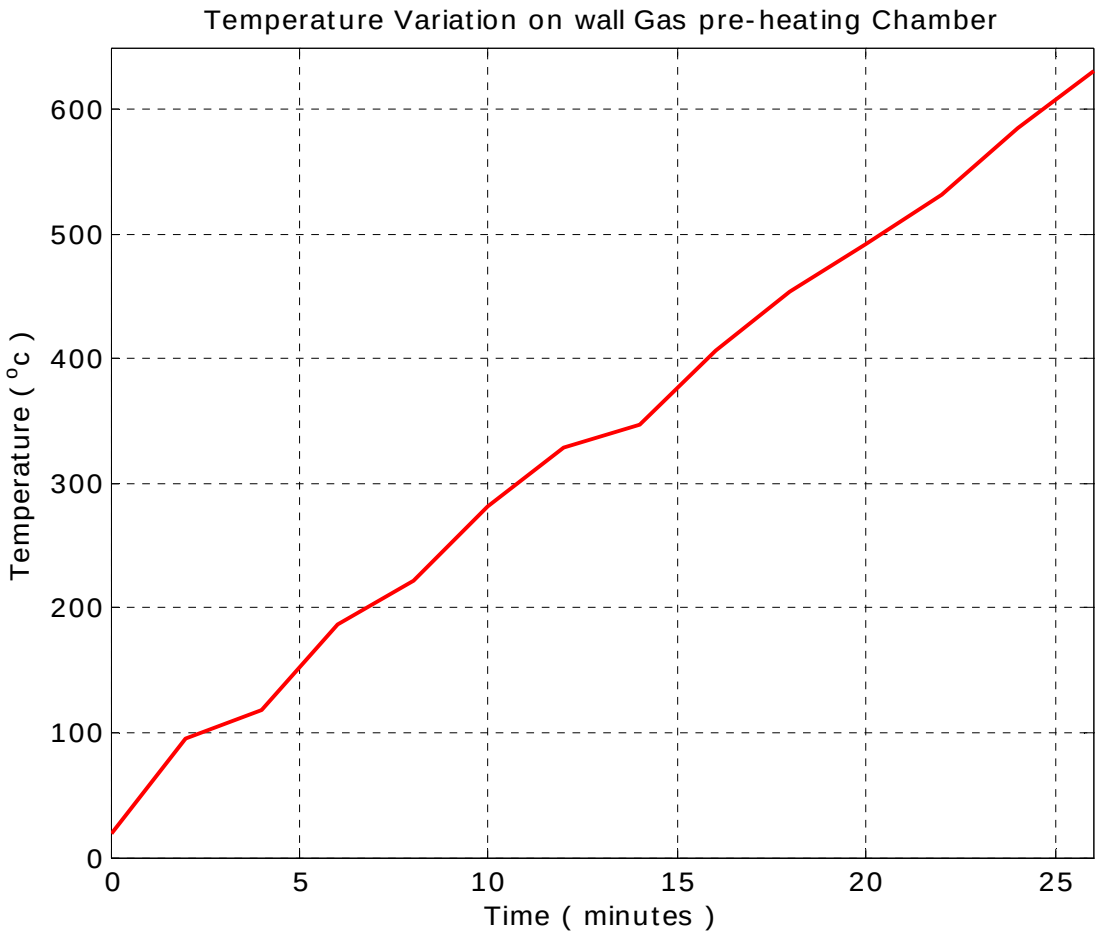

Figure 7.1: Temperature variation on gas pre-heating chamber wall

As shown from Figure 7.1, before power is supplied to the heaters, the gas pre-heating chamber temperature was 18.56℃. When power is given to the heaters, the wall temperature immediately rises to 95.5℃ within 2 minutes. As it was described in the figure the gas pre-heating chamber needs 27 minutes to reach 630℃.

7.2 Temperature Variation and Measurement of the Fluidizing Gas

The temperature of the fluidizing gas was measured by infrared thermo-meter after attain the reaction wall temperature. The fluidizing gas was introduced to the entrance of the plenum when the reactor wall temperature reached 630℃. To get the optimum temperature of the fluidizing gas, the compressor should be operated continuously. But the compressor used was not optimum for this application since it drops its pressure immediately; hence a temperature of 100.5 ℃ was obtained after 10 minutes. But this gas temperature is not enough to pyrolyze the biomass particles to the required reaction temperature.

Table : 7.2 Temperature readings obtained for the fluidizing gas

Time (min)	0	2	4	6	8	10
Temp (°C)	18.53	34.23	50.5	66.7	83.56	100.5

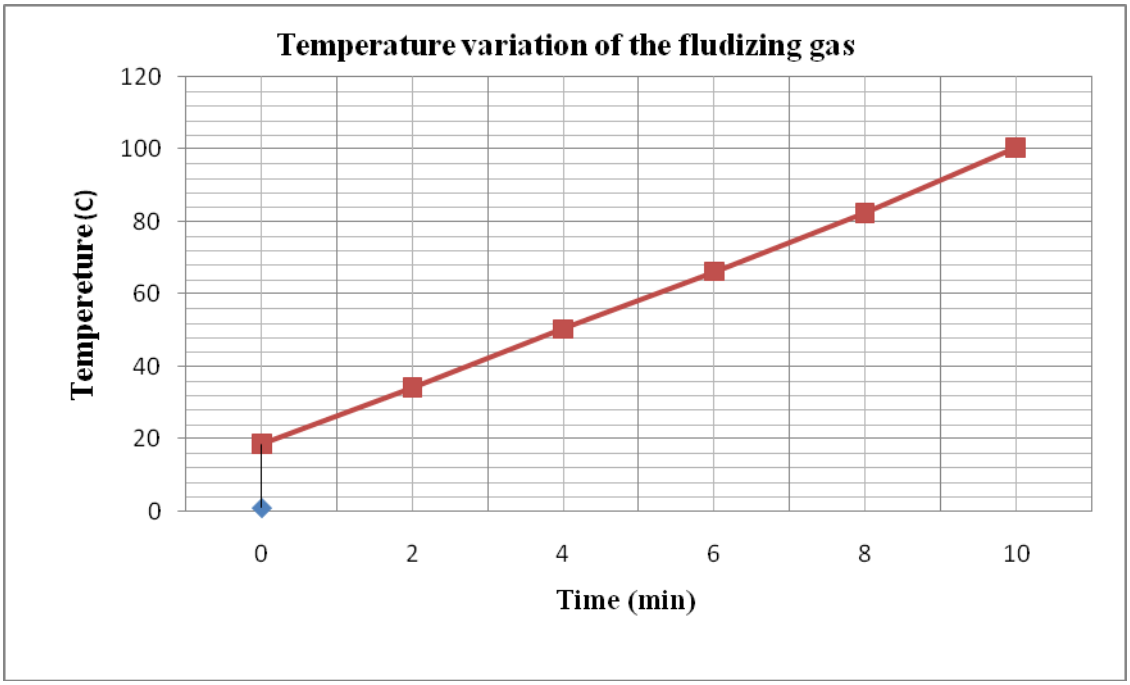

Figure 7.2: Temperature variation of the fluidizing gas

CHAPTER EIGHT

CONCLUSION AND RECOMMENDATION

8.1 Conclusions

As explained earlier the objectives of this thesis are to design, manufacture and perform experimental analysis on fast pyrolysis system.. The following points are given as concluding remarks.

- The use of biomass as a renewable source of energy has been stimulated strongly by governments during the last decennia for a number of different reasons, the main ones being:
  - The desired reduction of green house gas emissions to the atmosphere;
  - The threat of depletion of traditional fossil fuels;
  - National policies to secure the energy supply by diversification of the resources.

- To replace fossil fuels in the production of heat, power, transportation fuels, and chemicals, various biomass conversion routes are possible. Apart from the physical (pressing of seeds or fruits) and biochemical (anaerobic digestion, fermentation) ones, they all start with biomass combustion and

- The principle of fast pyrolysis is rapid heating of relatively small biomass particles (< 2 mm) to approximately 500℃ in absence of oxygen. Like in slow pyrolysis, the biomass is decomposed to three products, viz. charcoal, condensable vapors and permanent gases. However, the product distribution is completely different in a sense that the production of condensable vapors is maximized at fast-pyrolysis conditions.

- The fluidizing gas temperature in the experiment was measured but due to the problem of a continuous air supply compressor (pressure inside the compressor drops immediately) , the test was conducted until a temperature of 100 ℃. But, the minimum gas temperature required to perform fast pyrolysis reaction of the biomass is approximately 300 – 500℃.

8.2 Recommendation for Future Work

In this paper, a fast pyrolysis system has been developed. Extensive research works are necessary to enhance this technology and develop the applications of its products, in order to improve the competitiveness of fast pyrolysis technology.

Therefore, the following additions should be made in the future work.

- A continuous pressurized air supply should be searched or imported and the test has to be completed.
- The condensation system should be continuously supplied from water tanker using pump
- Provision of a screw feeder in the hopper for continuous fuel feeding system.
- It is also recommended that the energy consumption can be reduced by using the combustion of external fuel to replace electrical heating devices.

REFERENCES

[1] Ani.F.N. (2006), **Fast Pyrolysis of Bio-resources in to Energy and other Applications***:* Seminar on Energy from Biomass. Selangor: FRIM

[2] Bridgwater, A.V. and Bridge, S.A. (1991), **A Review of Biomass Pyrolysis and Pyrolysis Technologies.**

[3]. Brammer, J.G. and Bridgwater. A.V. (1999**), Drying Technologies for an Integrated Gasification Bio-energy Plant***:* Renewable and Sustainable Energy Reviews.

[4]. Bridgwater, A.V., and Grassi, G. (2000), ***Biomass Pyrolysis Liquids Upgrading and Utilizations,*** Elsevier Applied Science press, London and New York.

[5]. Bridgwater, A.V. Ed. (2001), ***Progress in Thermochemical Biomass Conversion***. Oxford: Blackwell Science.

[6]. Bridgwater A.V. (1994), ***Thermo Chemical Processing of Biomass***, Butter Worth England.

[7]. Bridgewater, A.V.S. and J.Piskorz, (2002), ***Fast Pyrolysis of Biomass.*** *Hand Book Volume2.*

[8]. Bridgwater, A.V., and Peacock, G.V.C. (2000), ***Fast Pyrolysis Process for Biomass***. Renewable and Sustainable Energy Reviews, 4:1-73

[9]. Demirbar, (2007), **Progress of recent trends in bio-fuels and, Progress in Energy and Combustion, Science.**

[10]. Diebold, J. (1991), **Development of Pyrolysis Reactor Concepts in USA**.

[11]. Dynamotive. (1999), *Biotherm TM:* **A System for Continuous Quality, Fast Pyrolysis Bio-Oil.** California, Oakland: Fourth Biomass Conference of the Americas.

[12]. Geldart, D. (1984), **Gas Fluidization Technology**. Chichester: John Wiley and Sons.

[13]. Gercel, H.F. (2002a), ***The Production and Evaluation of Bio-oils from the Pyrolysis of Sunflower-Oil Cake,*** Journal of Biomass and Bio-energy*, 23*: 307-314.

[14]. Grassi, G. Eds, **Biomass Pyrolysis Liquids Upgrading and Utilization**, London: Elsevier Applied Science.

[15]. Graham, R.G., Bergougnou, M.A, Mok, L.K.S., and De Lasa, H.I. (1985), ***Fast Pyrolysis (Ultra Pyrolysis) of Biomass Using Solid Heat Carrier***.

[16]. Howard, J.R.; and Hilge (1989), Adam, ***Fluidized Bed Technology Principles and Application***, Mc Milan Publishing, New York.

[17]. Holman A.; Alan J., ***Conductive and Radiative Heat transfer***, Macmillan Publishing Company.

[18]. Jonas A. England, ***Numerical Modeling and Prediction of Bubbling Fluidized Beds***, master Thesis , Virginia Poly Technique Institute and State University, April 2011

[19]. Kunni Levenspiel and Octave (1994), ***Hand Book of Fluidization Engineering***, Addison-Wesley Publishing Company.

[20]. Lim Xin Yi, (2008), ***Development and Characterization of Continuous Fast Pyrolysis of Oil Palm Shell for Bio-Oil Production***, Thesis of Master Science; Faculty of Mechanical Engineering, University Technology Malaysia.

[21] Li, J., Wu, L., and Yang, Z. (2008), ***Analysis and Upgrading of Bio-Petroleum from Biomass by Direct Deoxy-liquefaction***, Journal of Analytical and Applied Pyrolysis, 81. 199 - 204.

[22] Mohamad Azri Bin Sukiran, (2008), ***Pyrolysis of Empty Oil Palm Fruit Bunches Using the Quartz Fluidized - Fixed Bed Reactor,*** *Dissertation of Master Science*; Faculty of Science University of Malaya, Kuala Lumpur.

[23] Michael Siddoway, ***Measurement of Bubble Behavior and Heat transfer in a Fluidized Bed having Horizontal Heat Exchange Tubes***; Bsc.Thesis , Institute for Combustion and Energy Studies The University of Utah, May 2006

[24] Overend, R.P., Milne, T.A., and Mudge, L.K. Eds. (1985), ***Fundamentals of Thermo-chemical Biomass Conversion***. London: Elsevier Applied Science.

[25] Scott, D.S., and Piskorz, J. (1984), ***The Continuous Flash Pyrolysis of Biomass***; *Canadian Journal of Chemical Engineering*. 62(3): 404-412.

[26] Sharma, R.K. (2004), ***Characterization of Chars from Pyrolysis of Lignin***, *Journal of Fuel, 83*. 1469-1482

[27] Wyman, C.E. (Editor). (1996), ***Handbook on Bio-ethanol: Production and Utilization***. Washington: Taylor and Francis, University of Arkansas, Division of Agriculture.

[28] Wen-Ching Yang; ***Hand book of fluidization and fluid particle systems***, Siemens Westinghouse Power Corporation Pittsburgh, Pennsylvania, U.S.A.

[29] Zanzi Vigouroux, R. (2001***), Pyrolysis of Biomass: Rapid Pyrolysis at High Temperature and Slow Pyrolysis for Activated Carbon Preparation***; *Dissertation of Master Science*, Royal Institute of Technology, Stockholm.

[30] www.hindawi.com/journals/jc/2011/303168/

APPENDICES: I

APPENDICES A: Estimation of Fluidization Behaviors

A1: Design Parameters

The production of bio-oil from coffee was modeled using various assumptions. The table below summarizes the key design parameters used.

Table A1: Basic design parameters

Parameter	Value
1. Feed Stock	
Type	Coffee husk
Moisture content (%)	11.4
Particle size (μm), Average sieve size	450
Apparent density (kg / m^3)	136
2. Pyrolysis Design	
2.1. Reactor	
Pyrolysis reactor type	Bubbling fluidized bed
Geometrical shape	Cylindrical
Inner diameter, D_B (m)	0.145
Input pressure (bar)	5
Retension time (s)	1 – 6
Feed Rate, I_v (Kg / h)	
Pyrolysis bed Temperature,T_b (k)	500
3. Fluidizing Gas	
Fluidizing medium	Compressed Air
Density, ρ_g at 500 k and 5 bar (Kg /m^3)	2.569
Kinematic Viscosity, μ_g, at bed temperature (kg/ms)	3.599x10^{-5}
4. **Bed Material**	
Type	Silica sand (spherical)
Bed height, m	0.10
Particle size diameter (d_p), mm	(Average d_p = 2.2)

Density d_p, (kg / m^3) Bulk density, (kg/m^3)	1500 0.5 x 1500 = 750
Spericity (φ)	0.8
Void fraction (ε)	0.5

Appendix A-2: Thermo-physical properties of the fluidizing gas at operating pressure and temperature

A-2$_1$:- Calculating density of the gas, ρ_g

To calculate density of the compressed gas inside the compressor the ideal gas law should apply. That is,

$$PV = mRT$$

Dividing both sides by, V yields,

$$\frac{PV}{V} = \frac{mRT}{V} \quad \text{Where,} \frac{m}{V} = \rho_g$$

Therefore;

$$P = \rho_g RT$$

Solving for ρ_g,

$$\rho_g = \frac{P}{RT}, \text{ where, } P = P_{atm} + P_{guage}$$

$$\rho_g = \frac{P_{atm} + P_{guage}}{RT}$$

Where:

P = Absolute pressure (Pa)

P_{atm} = Atmospheric pressure at ambient temperature, (for Addis Ababa the Atmospheric pressure at ambient temperature of 20 ^oC is 76053.225 Pa).

P_{guage} = Guage pressure (5 bar, for this case)

R = Universal gas constant (287 J/kg k, for air)

T = Gas Temperature (K)

A-2$_2$: Calculating of the kinematic viscosity, μ_g specific heat capacity, C_p, thermal conductivity, k_g, and Prandtl number, Pr of the gas

From thermo-physical properties of compressed air given in table by, the kinematic viscosity, specific heat capacity and thermal conductivity of the gas at the operating pressure (P_{abs} = 5.7605bar) and temperature was calculated as follows.

Pabs (bar)	T (K)	μ_g (x 10^{-4} kg/ms)	$C_{p,g}$ (Kj/kgK	k_g (W/mK)
5	*260*	*0.165*	*1.015*	*0.0234*
5.76053	*260*	$\mu_{g,1}$	$C_{p1,g}$	$k_{g,1}$
10	*260*	*0.166*	*1.026*	*0.0237*

Interpolating the above table to find the value of $\mu_{g,1}$ at P=5.765 and T=260K

$$\frac{10-5}{5.76053-5}=\frac{0.166-0.165}{X-0.166}$$

$$(10-5)\times(\mu_{g_1}-0.166)=(5.76053-5)\times(0.166-0.165)$$

$$\mu_{g1}=0.165152\times10^{-4}\ \text{Kg/ms}$$

Interpolating the above table to find the value of $C_{p,g1}$ at P=5.765 and T=260K

$$\frac{10-5}{5.76053-5}=\frac{1.026-1.015}{C_{p,g1}-1.015}$$

$$6.57436\times(C_{p,g1}-1.015)=0.011$$

$$C_{p,g1}=1.01667\ \text{KJ/kgK}$$

Interpolating the above table to find the value of k_{g1} at P=5.765 and T=260K

$$\frac{10-5}{5.76053-5}=\frac{0.0237-0.0234}{k_{g1}-0.0234}$$

$$6.57436\times(k_{g1}-0.0234)=0.0003$$

$$k_{g1}=0.023446 \text{ W/mK}$$

By interpolating:

The value of μ_{2g} at P=5.765 and T=800K

$$\frac{10-5}{5.76053-5}=\frac{0.370-0.370}{\mu_{2g}-0.370}$$

$(10-5)\times(\mu_{2g}-0.370)=(5.76053-5)\times(0.370-0.370)$, Solving for μ_{2g},

$$\mu_{2g}=0.370\times10^{-4} \text{ kg m/s.}$$

The value of $C_{p,g1}$ at P=5.765 and T=800 K

$$\frac{10-5}{5.76053-5}=\frac{1.100-1.100}{C_{p,g2}-1.100}$$

$$6.57436\times(C_{p,g2}-1.100)=0$$

$$C_{p,g2}=1.100 \text{ KJ/kgK}$$

The value of K_{g1} at P=5.765 and T=800 K

$$\frac{10-5}{5.76053-5}=\frac{0.0579-0.0578}{k_{g2}-0.0578}$$

$$6.57436\times(k_{g2}-0.0578)=0.0001$$

$$k_{g2}=0.05781 \text{ W/mK}$$

Now the gas kinematic viscocity, specific heat capacity and thermal conductivity At P= 5.76053 bar and temperature T_i, could be find using the following relations.

At P= 5.76053 bar and T =800K,

Pabs (bar)	T (K)	μ_g (x 10^{-4} kg/ms)	$C_{p,g}$ (Kj/kgK	k (W/mK)
5.76053	*260*	*0.165152*	*1.01667*	*0.023446*
5.76053	T_i	μ_g	$C_{p,g}$	k_g
5.76053	*800*	*0.370*	*1.100*	*0.05781*

By interpolating:

The value of μ_g at P=5.765 and T = T_i,

$$\frac{800-260}{T_i-260}=\frac{0.370-0.165152}{\mu_g-0.165152}$$

$$(800-260)\times(\mu_g-0.165152)=(T_i-260)\times(0.370-0.165152)$$

$$\mu_g=\left[0.00037935\ T_i+0.0665215\right]\times 10^{-4}\ kg/ms$$

The value of $C_{p,g}$ at P=5.765 and T=T_i,

$$\frac{800-260}{T_i-260}=\frac{1.100-1.01667}{C_{p,g}-1.01667}$$

$$(800-260)\times(C_{p,g}-1.01667)=(T_i-260)\times(1.100-1.01667)$$

$$C_{p,g}=\left[0.000154312\times T_i+0.9765596\right]\ \text{KJ/kg K}$$

The value of k_g at P=5.765 and T= T_i

$$\frac{800-260}{T_i-260}=\frac{0.05781-0.023446}{k_g-0.023446}$$

$$540(k_g-0.023446)=0.034364(T_i-260)$$

$$k_g=(0.000063637\times T_i+0.0069)\ \text{W/m K}$$

The Prandtl number of the gas is related to its kinematic viscosity, specific heat capacity and thermal conductivity as follows. It was calculated using the following formula,

$$P_r = \frac{\mu_g \times C_{p,g}}{k_g}$$

The following table summarizes the values of the thermo-physical properties of the gas at absolute pressure of 5.76053 bar gas temperature temperatures, T_i

Gas Temperature T_i , K	Density, ρ_g, (kg/m^3)	Kinematic Viscocity,μ_g, (kg/ms)	Specific Heat Capacity, C_{pg}, (KJ/kgK)	Thermal Conductivity, k_g, (W/mk)	Prandtel number, Pr
0	7.352	1.711×10^{-5}	1.0187	0.0243	0.7138
50	6.21	1.899×10^{-5}	1.0264	0.0275	0.7068
100	5.38	2.088×10^{-5}	1.0341	0.0306	0.7022
150	4.74	2.277×10^{-5}	1.0418	0.0338	0.6993
200	4.24	2.466×10^{-5}	1.0495	0.0370	0.6977
250	3.84	2.655×10^{-5}	1.0573	0.0402	0.6971
300	3.50	2.844×10^{-5}	1.0650	0.0434	0.6972
350	3.22	3.032×10^{-5}	1.0727	0.0465	0.6980
400	2.98	3.221×10^{-5}	1.0804	0.0497	0.6992
450	2.77	3.41×10^{-5}	1.0881	0.0529	0.7009
500	2.596	3.599×10^{-5}	1.0958	0.0561	0.7029

APPENDIX B: Mat Lab Code

```
%% Mat lab program for effect particle diameter on minimum fluidization
velocity %%%%%

clear all
clc
Patm=76053.225;      % Atmospheric pressure (Pa)
Pgua=5*10^5;         % Gauge pressure (Pa)
P=Patm+Pgua;         % Absolute pressure (Pa)
R=287;               % Universal gas constant (J/kgK)
Tg= 773;             % gas temperature (K)
roh_g=P/(R*Tg);      % gas density (kg/m^3)
g=9.81;              % gravity deu to acceleration (m/s^2)
roh_p=1500;          % particle density of sillica sand (kg/m^3)
mu_g=3.599e-5;       % kinematic viscocity of gas (kg/ms)
dp=[216:50:650]*10^-5;  % average particle diameter of sand (m)
 for i=1:9
  Ar(i)=(roh_g*g*dp(i)^3*(roh_p-roh_g))/(mu_g)^2;
  umf(i)=(mu_g)/(roh_g*dp(i))*(sqrt(1135.7+0.0408*Ar(i))-33.7);
end
plot(dp,umf,'k*-'); grid on
xlabel('Mean Particle Size,dp(m)')
ylabel('Minimum Fludizing Velocity,Umf(m/s)')
legend('Umf of sand particles at 500^0c')
pause
clf

%%%% Mat lab program for effect of gas temperature to minimum fluidizing
velocity   %%%%%%

clear all
clc
g=9.81;                 % gravity deu to acceleration (m/s^2)
roh_p=1500;             % particle density (kg/m^3)
dp_1=0.00216;           % Mean particle diameter (m)
dp_2=0.003;             % Mean particle diameter (m)
dp_3=0.0045;            % Mean particle diameter (m)
Patm=76053.225;         % Atmospheric pressure (Pa)
Pgua=5*10^5;            % Gauge pressure (Pa)
P=Patm+Pgua;            % Absolute pressure (Pa)
R=287;                  % Universal gas constant (J/kgK)
Tg=[0:50:500]+273;      % gas temperature (K)
for i=1:11;
Y=R*Tg(i);
roh_g(i)=P/Y;           % Gas density (kg/m³)
mue_g(i)=(0.00037768*Tg(i)+0.067955)*10^-4;

Ar_1(i)=(roh_g(i)*g*dp_1^3*(roh_p-roh_g(i)))/(mue_g(i))^2;
Ar_2(i)=(roh_g(i)*g*dp_2^3*(roh_p-roh_g(i)))/(mue_g(i))^2;
Ar_3(i)=(roh_g(i)*g*dp_3^3*(roh_p-roh_g(i)))/(mue_g(i))^2;
umf_1(i)=(mue_g(i))/(roh_g(i)*dp_1)*(sqrt(1135.7+0.0408*Ar_1(i))-33.7);
umf_2(i)=(mue_g(i))/(roh_g(i)*dp_2)*(sqrt(1135.7+0.0408*Ar_2(i))-33.7);
umf_3(i)=(mue_g(i))/(roh_g(i)*dp_3)*(sqrt(1135.7+0.0408*Ar_3(i))-33.7);
end
```

```
plot(Tg,umf_1,'k*-',Tg,umf_2,'K-',Tg,umf_3,'ro--'); grid on
xlabel('Gas Temperature,T (K)')
ylabel('Minimum Fludizing Velocity,Umf(m/s)')
title('Influence   of   gas   trmperture,T   to   Minimum   Fludization
Velocity,umf')
legend('dp =0.00216 m','dp = 0.003 m','dp = 0.0045 m,')

% Ar= Archimedes number (dimension less)
% umf= Minimum fluidization velocity (m/s)

pause
clf

%%%%%%%%%%%%%%%%%%%%%%%%%%%%%%%%%%%%%%%%%%%%%%%%%%%%%%%%%%%%%%%%%%%%%%%%%%%%%%%%
%%%%%%%%%%%%%%%%%%%%%%%%

%% Main Program for Effect of Pressure on Minimum Fluidization Velocity
%%%%

clear all
clc
Patm=76053.225;
Pgua=5*10^5;
P=Patm+Pgua;
R=287;
Tg= 773;                % gas temperature (K)
roh_g=P/(R*Tg);         % gas density (kg/m^3)
g=9.81;                 % gravity deu to acceleration (m/s^2)
roh_p=1500;             % particle density of sillica sand (kg/m^3)
dp=220e-5;
Patm=76053.225;         % average particle diameter of silca sand (m)
 Pgua=[1:1:10]*10^5;
for i=1:10
   Pabs(i)=Patm+Pgua(i);
     Y=R*Tg;
     roh_g(i)=Pabs(i)/Y;
     mue_g(i)=(1.1e-6*Pgua(i)+0.035959)*10^-4;
     Ar(i)=(roh_g(i)*g*dp^3*(roh_p-roh_g(i)))/(mue_g(i))^2;
  umf(i)=(mue_g(i))/(roh_g(i)*dp)*(sqrt(1135.7+0.0408*Ar(i))-33.7);
end
plot(Pgua,umf,'k*-'); grid on
xlabel('Presssure,P(bar)')
ylabel('Minimum Fludizing Velocity,Umf(m/s)')
pause
clf

%%%%%%%%%%%%%%%%%%%%%%%%%%%%%%%%%%%%%%%%%%%%%%%%%%%%%%%%%%%%%%%%%%%%%%%%%%%%%%%%
%%%%%%%%%%%%%%%%%%%%%%%% Main Program for Effect of Gas Temperature on
Terminal Settling Velocity of the Particle Assuming Constant Particle
Diameter

clear all
clc
phi_1=0.8;              % sphercity of the particles
roh_p=1500;
g=9.81;                 % gravity deu to acceleration (m/s^2)
```

```
dp=220*10^-5;         %average particle diameter of sand (m
Patm=76053.225;
Pgua_1=5*10^5;
Pgua_2=10*10^5;
P1=Patm+Pgua_1;
P2=Patm+Pgua_2;
R=287;
T=[0:50:500]+273;     % gas temperature (K)
for i=1:11;
     Y(i)=R*T(i);
     roh_g1(i)=P1/Y(i)
     roh_g2(i)=P2/Y(i);
     mue_g1(i)=(0.00037768*T(i)+0.067955)*10^-4;
     mue_g2(i)=(0.00037926*T(i)+0.0675925)*10^-4;
     Ar1(i)=(roh_g1(i)*g*dp^3*(roh_p-roh_g1(i)))/(mue_g1(i))^2;
     Ar2(i)=(roh_g2(i)*g*dp^3*(roh_p-roh_g2(i)))/(mue_g2(i))^2;
     dp1(i)=Ar1(i)^0.33333
     dp2(i)=Ar2(i)^0.33333;
     y_1(i)=(2.335-1.744*phi_1)/dp1(i)^0.5;
     y_2(i)=(2.335-1.744*phi_1)/dp2(i)^0.5;
     x_1(i)=(18)/dp1(i)^2;
     x_2(i)=(18)/dp2(i)^2;
    ut_1(i)=(x_1(i)+y_1(i))^-1;
    ut_2(i)=(x_2(i)+y_2(i))^-1;
    Ut_1(i)=ut_1(i)*((mue_g1(i)*g*(roh_p-
roh_g1(i)))/(roh_g1(i)^2))^0.3333;
    Ut_2(i)=ut_2(i)*((mue_g2(i)*g*(roh_p-
roh_g2(i)))/(roh_g2(i)^2))^0.3333;
end
plot(T,Ut_1,'k*-',T,Ut_2,'r-o'); grid;
xlabel('Gas Temperature,T(K)')
ylabel('Terminal Settling Velocity,Ut(m/s)')
gtext('5 bar')
gtext('10 bar')
pause
clf

%%%%%%%%%%%%%%%%%%%%%%%%%%%%%%%%%%%%%%%%%%%%%%%%%%%%%%%%%%%%%%%%%%%%%%%%%%%%
%%%%%%%%%%%%%%%%%%%%%%%%
%%%%% Main Program for Effect of Pressure on Terminal Settling Velocity
of the Particle Assuming Constant Particle Diameter and gas Temperature
%%%%%%%%%%%%%%%%%%
%%
clear all
clc
phi_1=0.8;           % sphercity of the particles
roh_p=1500;
g=9.81;              % gravity deu to acceleration (m/s^2)
dp=220*10^-5;        %average particle diameter of silca sand (m
Patm=76053.225
R=287;
T=773;   % gas temperature (K)
Pgua=[1:1:10]*10^5;
for i=1:10;
    Pabs(i)=Patm+Pgua(i)
     Y=R*T;
```

```
     roh_g(i)=Pabs(i)/Y
     mue_g(i)=(1.1e-6*Pgua(i)+0.35959)*10^-4
     Ar1(i)=(roh_g(i)*g*dp^3*(roh_p-roh_g(i)))/(mue_g(i))^2;
     dp1(i)=Ar1(i)^0.33333;
     y_1(i)=(2.335-1.744*phi_1)/dp1(i)^0.5;
     x_1(i)=(18)/dp1(i)^2;
    ut_1(i)=(x_1(i)+y_1(i))^-1;
    Ut_1(i)=ut_1(i)*((mue_g(i)*g*(roh_p-roh_g(i)))/(roh_g(i)^2))^0.3333;
end
plot (Pgua,Ut_1,'k*-'); grid;
xlabel('Pressure,P(bar)')
ylabel('Terminal Settling Velocity,Ut(m/s)')
gtext ('500 ^oC ')


%%%%%%%%%%%%%% END OF PROGRAM %%%%%%%%%%%%%%
```

APPENDIX II

I. DETTAIL DRAWING

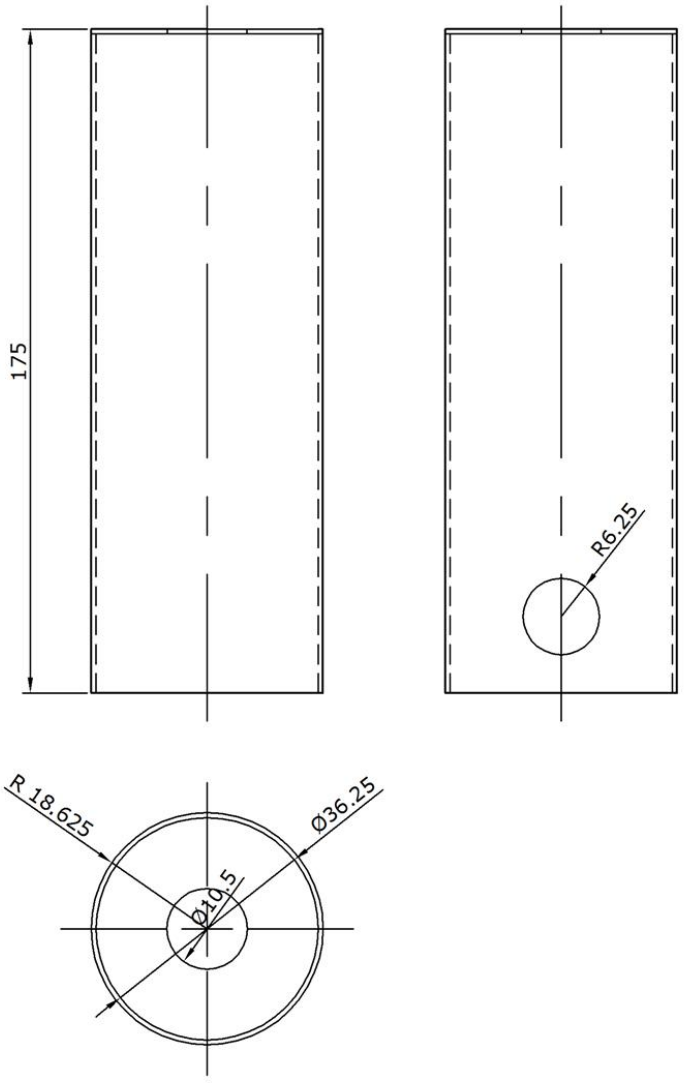

Note:-Dimensions are in Millimeter

DR.BY	TIGABU ABRHA	REACTIONC HAMBER			AAiT
DATE					
CHE. BY	SILESHI KORE				
DATE					
APPR.BY	Dr.Ing:-ABEBAYEHU A.	QUANTITY	SCALE	DR. NO	MATERIAL
DATE		ONE	1:4	1	MILD STEEL

ENERGY CENTER

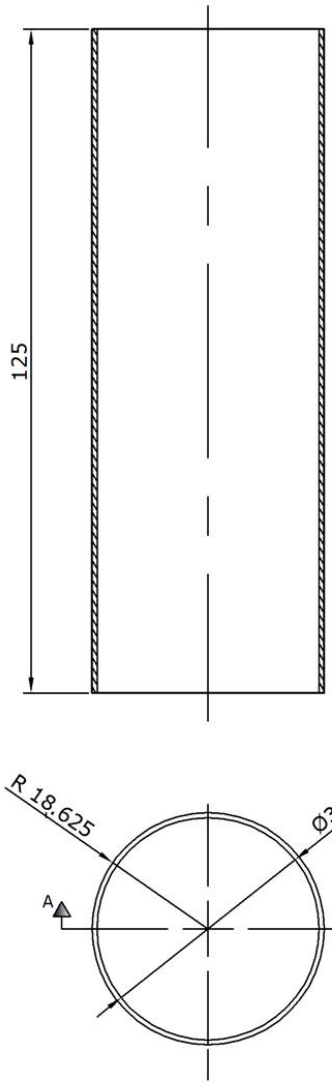

Note:-Dimensions are in Millimeter

DR.BY	TIGABU ABRHA	REACTIONC HAMBER			AAiT
DATE					
CHE. BY	SILESHI KORE				
DATE					
APPR.BY	Dr.Ing:-ABEBAYEHU A.	QUANTITY	SCALE	DR. NO	MATERIAL TYPE
DATE		ONE	1:4	1	MILD STEEL

ENERGY CENTER

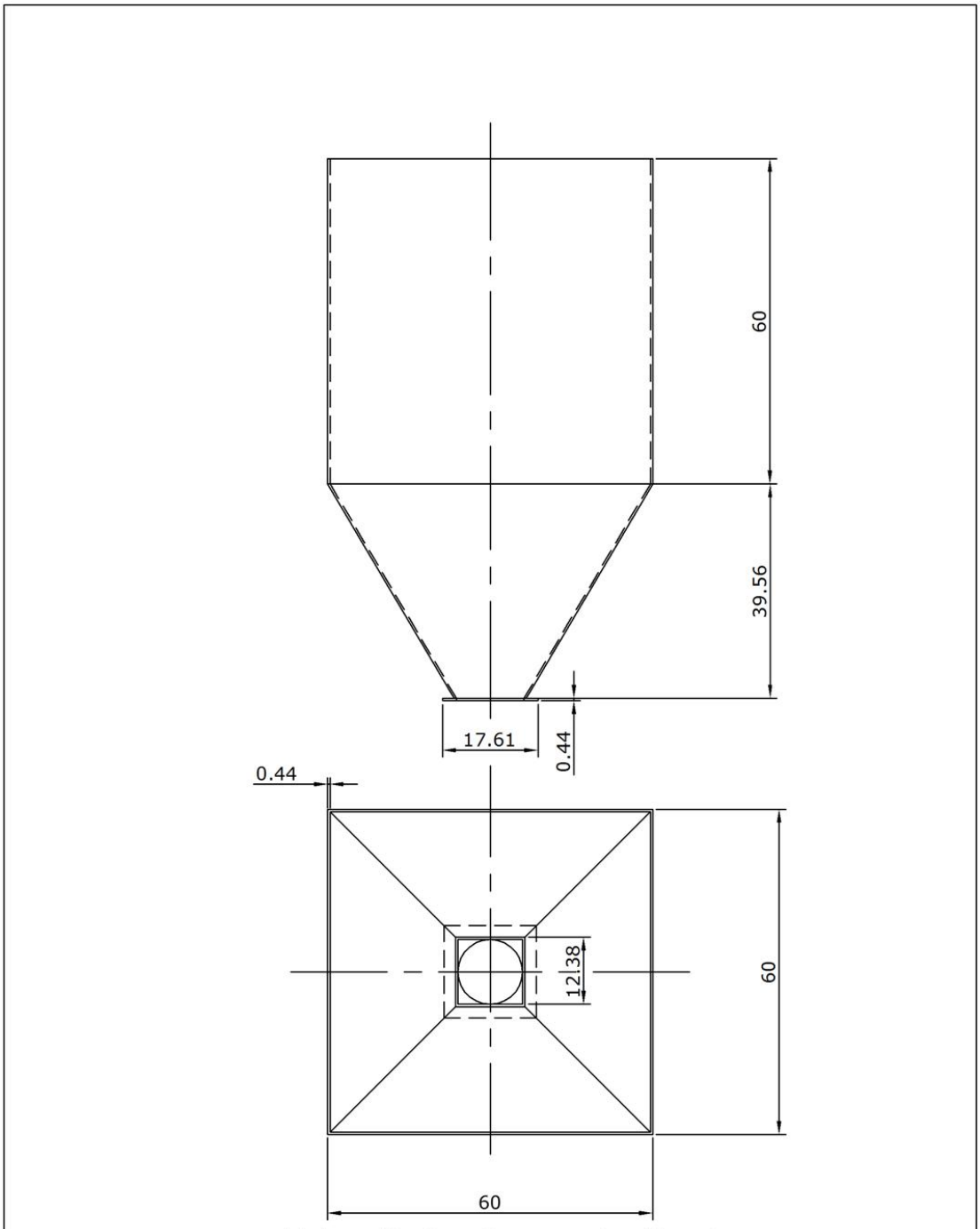

Note:- All dimensions are in milli meter

DR.BY	TIGABU ABRHA	HOPPER			AAiT
DATE					
CHE. BY	SILESHI KORE				
DATE					
APPR.BY	Dr.Ing:-ABEBAYEHU A.	QUANTITY	SCALE	DR. NO	MATERIAL TYPE
DATE		ONE	1:4.5	1	MILLED STEEL

ENERGY CENTER

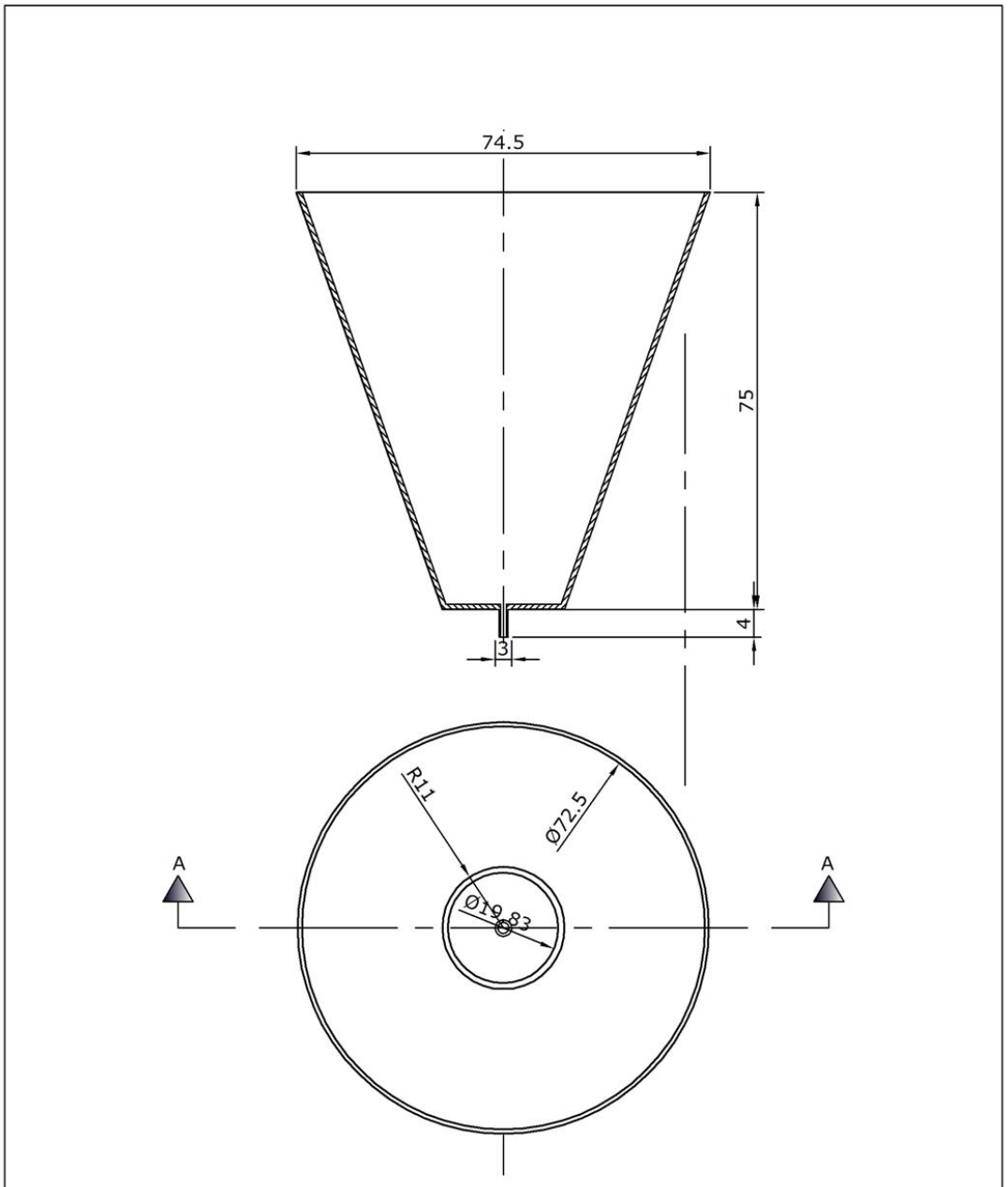

NOTE:- DIMENSIONS ARE IN MILLI METERS

DR.BY	TIGABU ABRHA	PLENUM			AAiT
DATE					
CHE. BY	SILESHI KORE				
DATE					
APPR.BY	Dr.Ing.ABEBAYEHU A.	QUANTITY	SCALE	DR. NO	MATERIAL TYPE
DATE		ONE	1:2		MILLED STEEL
ENERGY CENTER					

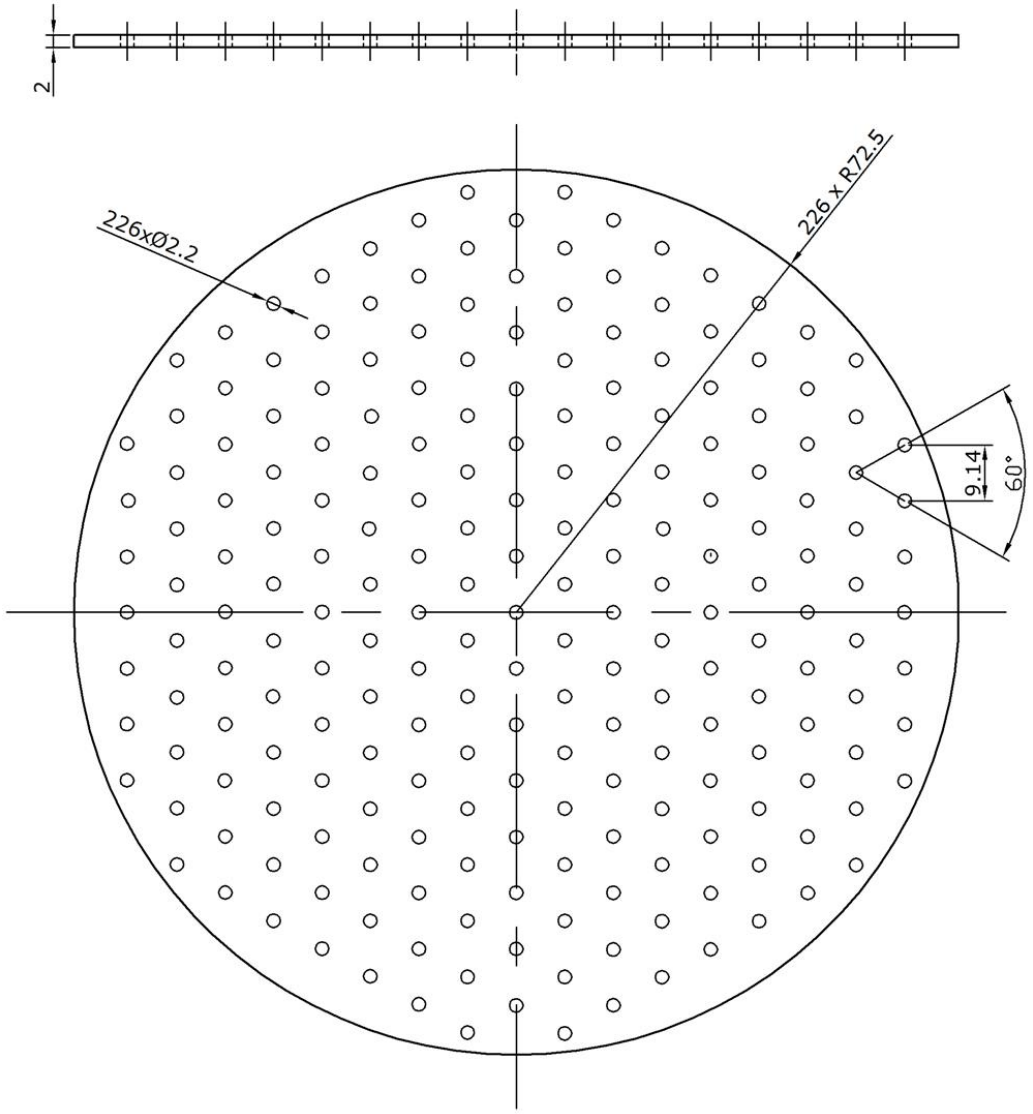

Note:- Dimensions are in Milli Meter

DR.BY	TIGABU ABRHA	DISTRIBUTOR PLATE			AAiT
DATE					
CHE. BY	SILESHI KORE				
DATE					
APPR.BY	Dr.Ing.ABEBAYEHU A.	QUANTITY	SCALE	R. NO	MATERIAL
DATE		ONE	1:1		MILLD STEEL

ENERGY CENTER

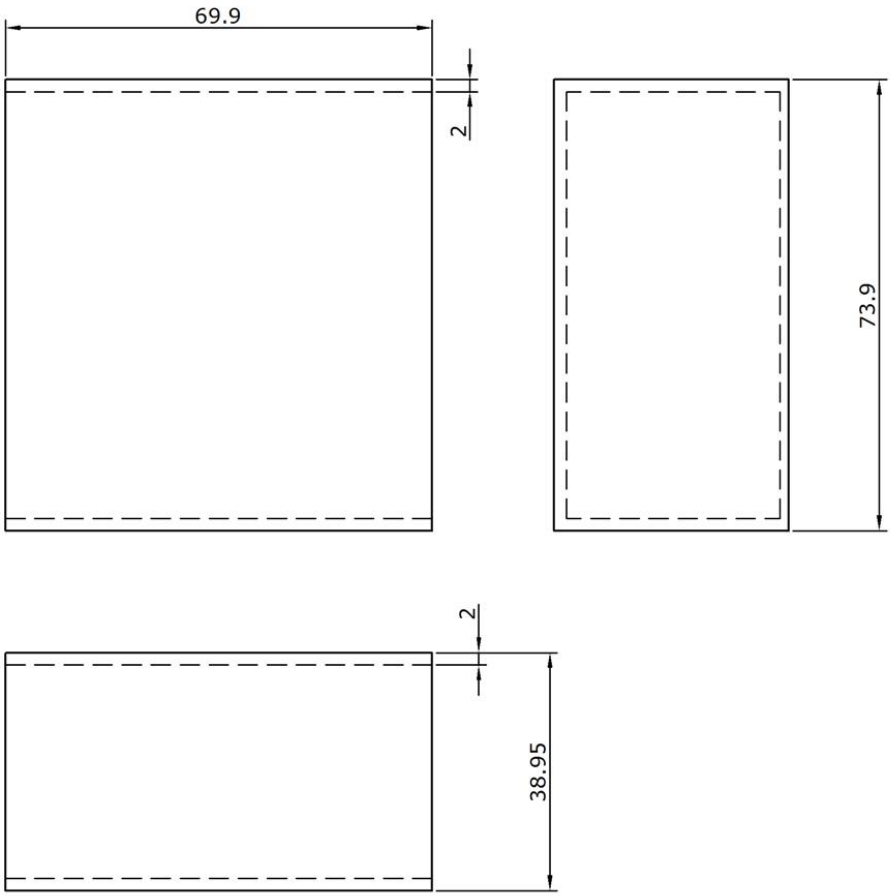

DR.BY	TIGABU ABRHA	CYCLONE INLET			AAiT
DATE					
CHE. BY	SILESHI KORE				
DATE					
APPR.BY	Dr.Ing.ABEBAYEHU A.	QUANTITY	SCALE	DR. NO	PROJECTON TYPE
DATE		1	1:1		FIRST ANGLE

ENERGY CENTER

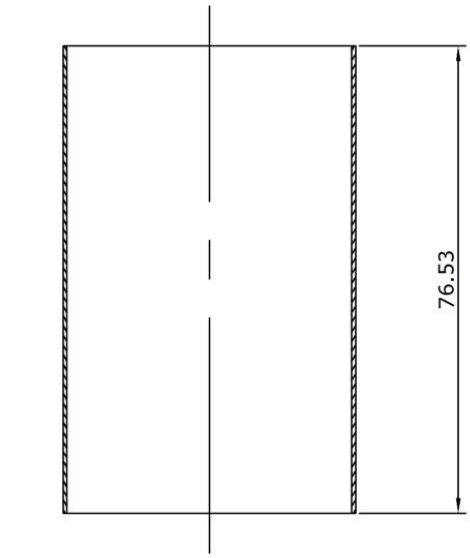

DR.BY	TIGABU ABRHA	CYCLONEBODY			AAiT
DATE					
CHE. BY	SILESHI KORE				
DATE					
APPR.BY	Dr.Ing.ABEBAYEHU A.	QUANTITY	SCALE	DR. NO	MATERIAL
DATE		ONE	1:3		MILD STEEL

ENERGY CENTER

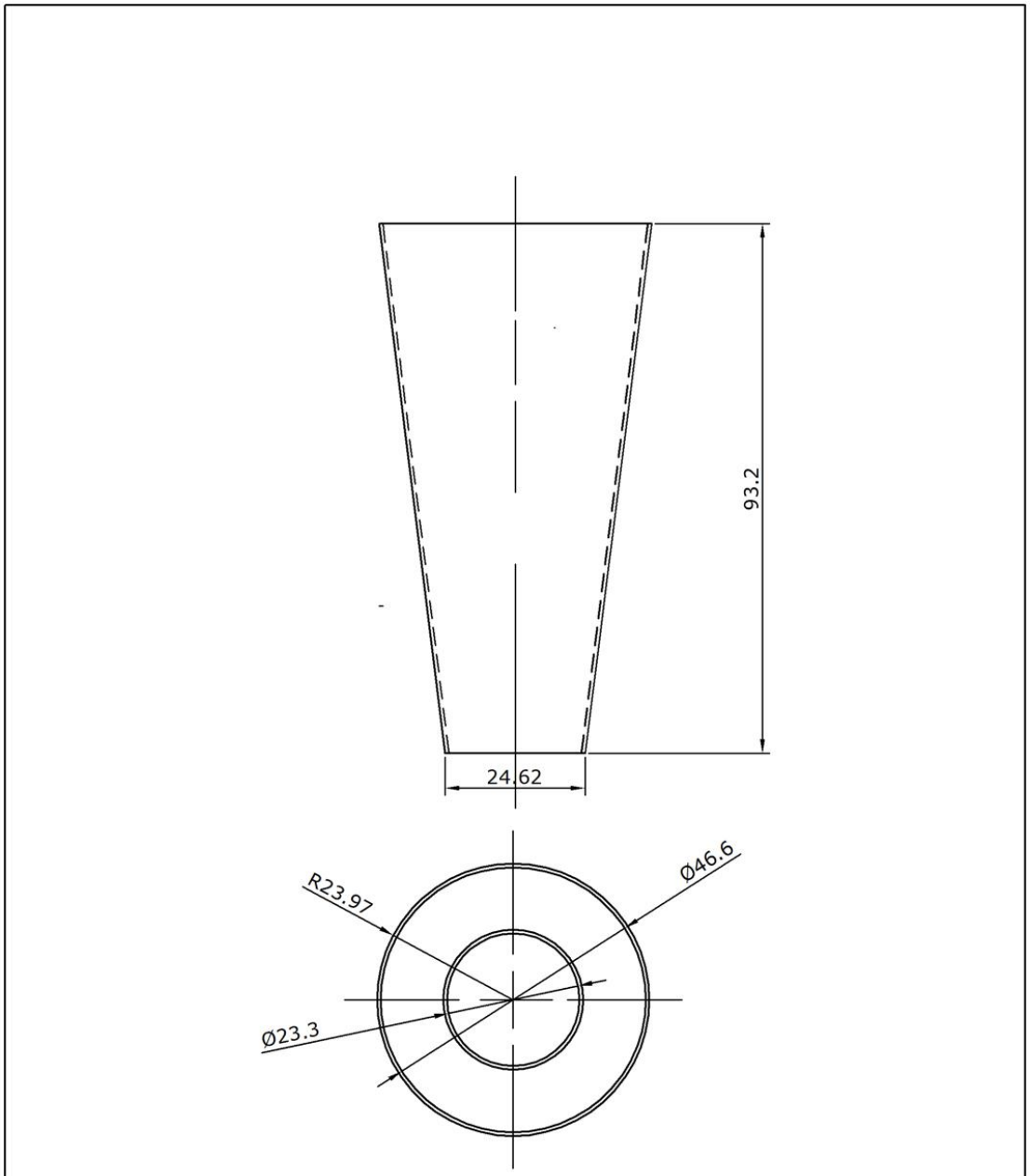

DR.BY	TIGABU ABRHA	CYCLONE CONE			AAiT
DATE					
CHE. BY	SILESHI KORE				
DATE					
APPR.BY	Dr.Ing.ABEBAYEHU A.	QUANTITY	SCALE	DR. NO	MATERIALE
DATE		ONE	1:3		MILD STEEL
ENERGY CENTER					

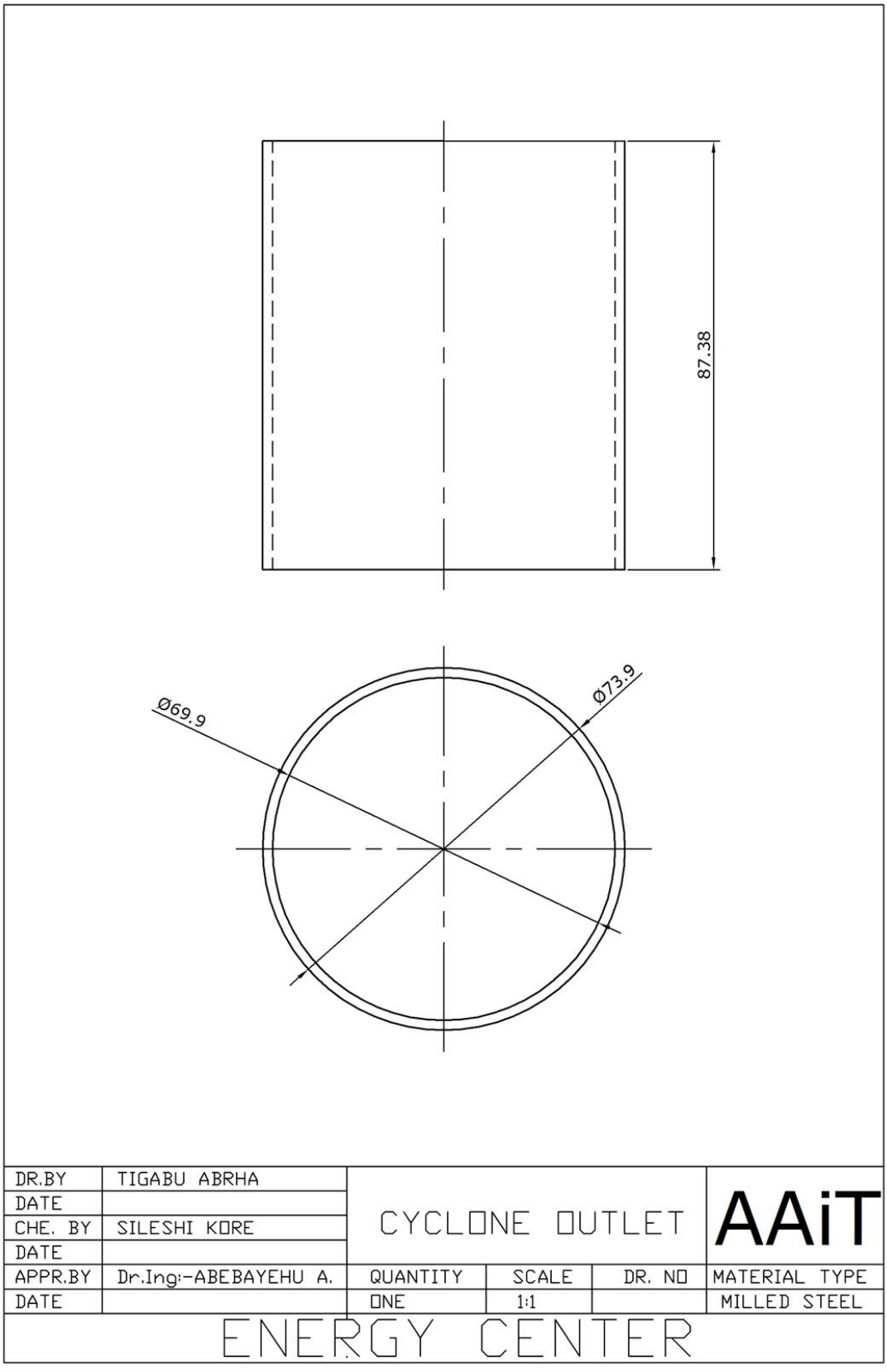

DR.BY	TIGABU ABRHA	CYCLONE OUTLET			AAiT
DATE					
CHE. BY	SILESHI KORE				
DATE					
APPR.BY	Dr.Ing:-ABEBAYEHU A.	QUANTITY	SCALE	DR. NO	MATERIAL TYPE
DATE		ONE	1:1		MILLED STEEL
ENERGY CENTER					